Effect of Processing Parameters on Reliability of VARTM/SCRIMP Composite Panels – Phase I

The AEWC Center

THE UNIVERSITY OF MAINE

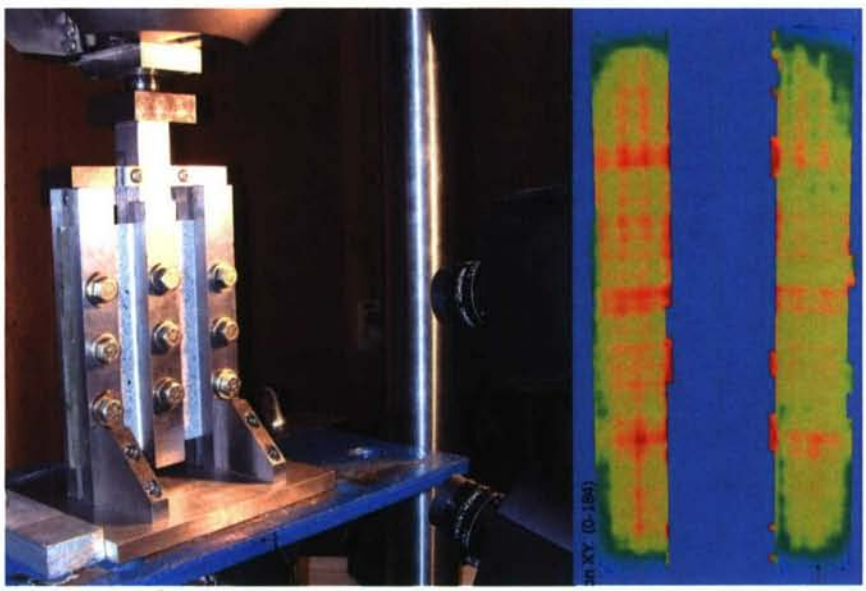

Report 08 – 01
Project 206

July 2007

Prepared by

Dr. Habib J. Dagher, P.E. Director AEWC

Dr. Roberto Lopez-Anido, P.E. , UMaine

Dr. Larry Thompson, P.E., Applied Thermal Sciences, Inc.

Fadi El-Chiti, UMaine

Ghassan Fayad, UMaine

Keith Berube, UMaine

Prepared for

Dr. Paul Hess, Office of Naval Research

Mr. Brian Jones, Naval Surface Warfare Center Carderock Division

Acknowledgements

This project was funded by by a grant from the Office of Naval Research (award number N00014-03-1-0542). We would like to thank the program sponsors Mr. Patrick Potter and Dr. Roshdy Barsoum at the Office of Naval Research for their support. Additionally, we greatly appreciate the support and guidance of our steering committee from the Naval Surface Warfare Center – Carderock Division members: Dr. Paul Hess, Mr. Scott Bartlett and Mr. Brian Jones.

Table of Contents

List of Figures

List of Tables

1. Project Summary

1.1. Introduction

In recent years, the U.S. Navy has shown increased interest in ship construction using advanced fiber-reinforced polymer (FRP) composites. This interest has been fueled by at least three issues: (1) the ability to design and affordably construct large composite parts has improved significantly over the past 25 years, assisted particularly by advances in resin-infusion processing and preformed reinforcements; (2) the Navy's continuing, expanding demand for vessels with dramatically reduced electronic and acoustic signatures; and (3) the Navy's initiative to reduce Total-Ownership-Cost (TOC), which requires mitigating the very high cost of corrosion/maintenance on metallic ships.

While FRP manufacturing processes have advanced, questions remain regarding the consistency of material properties for large composite parts. The state of the art for structural design of FRP composites essentially follows an Allowable-Stress-Design (ASD) methodology in which deterministic safety factors are applied to account for variability in mechanical-strength properties and uncertainties in loadings (Karbhari and Li, 2002). In contrast with this deterministic-based ASD, a Reliability-Based Design (RBD) methodology formally accounts for uncertainties in mechanical properties, processing parameters, environmental exposures, and loadings, thereby yielding more reliable FRP composite structures (Lopez-Anido and Karbhari, 2000; Bausano and Lesko, 2002). RBD methodologies have been adopted in structural design by most building codes in the US and abroad (MIL Handbook 17, 1998), such as the American Institute of Steel Construction Specifications, the American Association of State Highway and Transportation Officials LRFD Bridge Construction Specifications (AASHTO, 1998), the National Design Specifications for Wood Construction (AF&PA, 1996), and the EuroComp Design Code.

RBD and acceptance criteria are currently being developed by the U.S. Navy using Navy load and strength prediction methodologies (Ayyub et al, 1995; Hess et al, 1998; Hess and Beach, 2000). However, this work considers only traditional structural materials and systems and a limited range of structural-failure modes (Bruchman and Ayyub, 1995). Though limited, this effort represents a significant shift in composite design methodology and assessment of design acceptance and provides a framework used in this program (Hess and Beach, 2000). The structural risks associated with new FRP composite ship structures can be mitigated by characterizing the variability of composite material properties thus ensuring acceptable levels of safety.

Development of an RBD method for FRP composites Navy ship structures requires the following information:

1. Structural reliability analysis techniques suitable for FRP composite ship structures;

2. Statistical models of static and dynamic properties of FRP composite material properties for applicable marine composite manufacturing processes;
3. Statistical static and dynamic design properties for FRP composite connections;
4. Statistical properties of loadings; and
5. Structural reliability analyses of traditional steel Navy ship structures to form a benchmark for reliability calibration of new designs.

This program focuses on addressing the first and second tasks outlined above.

1.2. Phase I - Objectives

The objectives for work outlined in this report are as follows:

- Identify apparent material variability resulting from ASTM test procedures.
- Modify/recommend a series of coupon level test procedures that minimizes testing variability.
- Develop a probabilistic finite element tool to predict material variability.

1.3. Phase I – Material Testing Accomplishments

Panels from a commercial manufacturer, *Seemann Composites Inc.*, were obtained for the testing program. The panels were manufactured using a proprietary Seemann technology, known as Seemann composite resin infusion molding process (SCRIMP). The resin used was Derekane 8084 (Ashland, 2004)) and the fabric used was woven with Saint Gobain Vetrotex 324 style. The material system selection is consistent with other Navy sponsored programs. Three different fiber lay-ups were adopted: warps parallel, warps alternating, and pseudo-quasi-isotropic. Three different thicknesses were manufactured for each fiber lay-up: 25.4 mm (1 in) and 12.7 mm (0.5 in) used for structural testing, and 5.08 mm (0.2 in) witness panels used for coupon testing.

The test program used 576 mechanical property specimens, 192 additional specimens, 176 flexure specimens, and 126 physical property specimens for a total specimen count of 1070. The following outlines a list of the mechanical property tests.

Test	Standards Referenced
Tensile	ASTM D3039 (rectangular)
	ASTM D638 (dumbbell)
Compressive	ASTM D6641 (CLC fixture)
	SACMA SRM 1R (ASTM D695)
Shear	ASTM D4255 (3-Rail)
	ASTM D5379 (V-notch)
Flexure	Used to Develop ASTM D7264

1.4. Phase I – Shear Testing

The COV for the v-notch shear test was found to be as high as 30%, while the COV for the three-rail shear test was between 1.5% and 9%. Additionally, the gage area of the three rail shear specimens is representative of the weave pattern of the reinforcement fabric. Therefore the three-rail shear test is recommended.

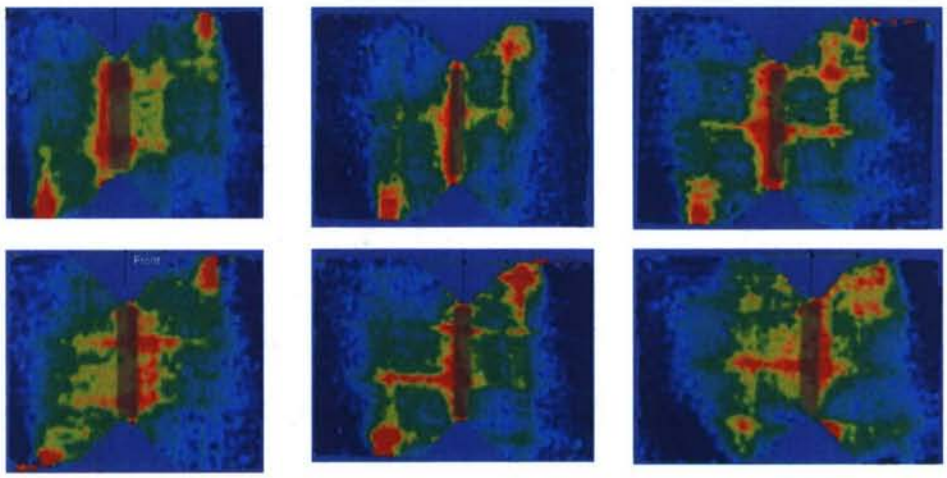

Figure 1.1 - Full-field strain measurement of the v-notch shear test revealed the sources of variability.

1.5. Phase I – Compression Testing

In the compression test, the COV was reduced by 50% when the modified D6641 (CLC) was used as compared to the D695 compression test. Full-field strain measurement of the D695 compression test indicated strain concentrations that were attributed to the higher COV in the results.

1.6. Phase I – Accomplishments: Tension Testing

An optimized geometry for tension coupon testing was developed for marine grade composites. The new geometry reduces specimen preparation time and forces more failures in the gage area.

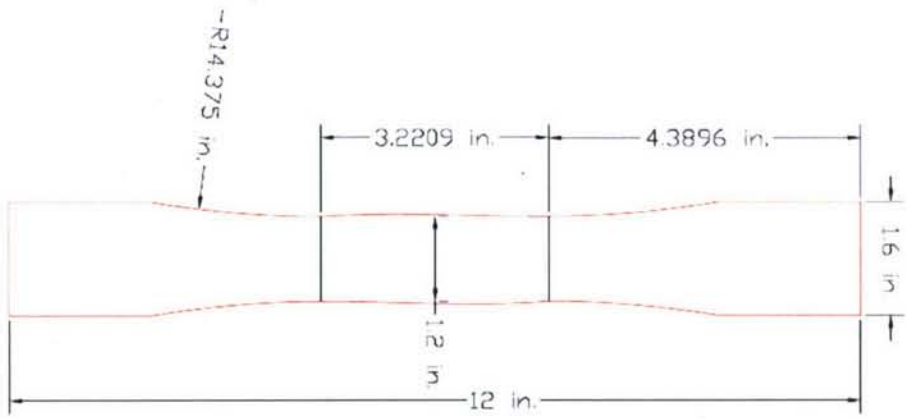

Figure 1.2 - Optimized Tensile Coupon

1.7. Phase I – Flexure testing

Flexural test results conducted in this study were incorporated into a new ASTM flexural test standard for composites:

Unlike Test Method D 6272, which allows loading at both one-third and one-half of the support span, in order to standardize geometry and simplify calculations this standard permits loading at only one-half the support span.

ASTM D7264/D7264M-06 Standard Test Method for Flexural Properties of Polymer Matrix Composite Materials

1.8. Phase I – Probabilistic FEA

A probabilistic finite element tool was developed that predicts tension coupon property variability using spatially correlated material properties. The purpose of this tool is to track the material variabilities from material coupon test data to component and structural tests. Figure 1.3 shows a tensile coupon with spatially varying material properties.

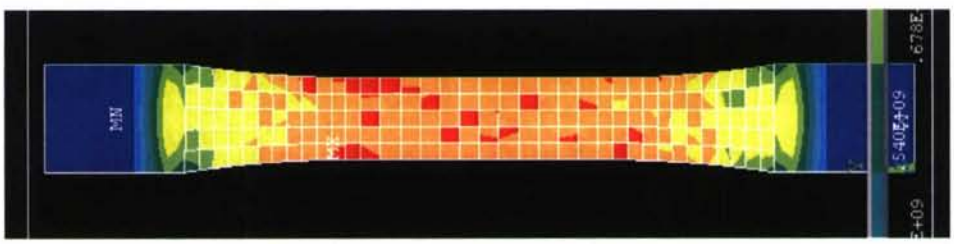

Figure 1.3 - Tensile coupon with spatially varying material properties

2. Program Details

2.1. Motivation and Objective

Variability in material properties obtained from experimental testing has three sources: material variability, fabrication variability, and testing variability. The material variability originates from the constituents of the material. The constituents of the polymer matrix composite (PMC) under study in this project is the polymer matrix and the reinforcing woven fabric. The material variability is influenced by the resin type affecting the matrix properties; and is influenced by the variation in the number of filaments per tow, fiber areal weight, fiber sizing, and tow spacing that affects the woven fabric properties.

The fabrication variability is influenced by: the fabrication method (e.g. hand lay-up, vacuum assisted resin transfer molding, etc.); repeatability of the fabrication method; resin promotion schedule; cure cycle; consolidation method (e.g. vacuum or pressure); thickness variations in the panel; fiber misalignment; fiber volume content; and panel cutting.

The testing variability depends on the experimental technique adopted from specimen configuration and test configuration. The testing variability is also influenced by the test coupon cutting tool, tabbing procedure – if needed, strain measurement system, loading frame including the load measuring device (i.e. load cell), specimen alignment, and operator expertise.

The variability calculated in the experimental results is a combination of all three sources. The equation that defines the relationship of the variance of the experimental results to the different sources of variability is depicted in equation (2.1).

$$Var = \sqrt{Var_M^2 + Var_F^2 + Var_T^2} \tag{2.1}$$

where:

Var = variance of the experimental results
Var_M = material variance
Var_F = fabrication variance
Var_T = testing variance

The standard test methods used to calculate the material properties of polymer matrix composites (PMCs) were originally designed for unidirectional laminates, cross ply laminates, and relatively light fabrics. These conventional standards exhibit significant variability in the experimental results when used to test marine grade composites, which are composed of a matrix of rubberized elastomer-modified vinyl ester resin and are reinforced with heavy tow woven fabric. The objective this project is to characterize the testing variability of the material properties caused by the adopted experimental methods.

The objectives of the project were achieved by optimizing the testing procedures used for obtaining mechanical properties: tension, compression, and shear; and, the use of a 3D-digital image correlation (DIC) system for measuring full-field strains and displacements. Two standard testing methods were used for calculating each material property. The advantages and disadvantages of each test were considered when recommending modifications in the testing procedure, thus helping reduce the testing variability of marine grade composites. In addition, the physical properties of the material were calculated in accordance with standard methods; the physical properties accompanied the mechanical properties, thereby supporting the modifications suggested by the recommendations.

The fiber dominated material properties were normalized to a nominal thickness and used to obtain the design allowables. Once the material properties were normalized, equivalent properties were obtained from different test methods and different panel fabrication batches were compared using statistical methods to quantify their difference. In addition, the experimental results were evaluated by comparing these values to a micromechanics model based on classical lamination theory.

A combined experimental and numerical evaluation of the conventional testing standard methods brought about recommendations that helped achieve the project's objective in reducing the variability of the experimental values caused by testing techniques and experimental preparation, testing variability.

2.2. Composite Material Evaluated

Panels from a commercial manufacturer, *Seemann Composites Inc.*, were obtained for the testing program. The panels were manufactured using vacuum assistant resin transfer molding process (VARTM) with the proprietary Seemann technology, known as Seemann composite resin infusion molding process (SCRIMP). The resin used was Derekane 8084 (Ashland, 2004)) and the fabric used was woven with Saint Gobain Vetrotex 324 style. The material system selection is consistent with other Navy sponsored programs. Three different fiber lay-ups were adopted: warps parallel, warps alternating, and pseudo-quasi-isotropic. Three different thicknesses were manufactured for each fiber lay-up: 25.4 mm (1 in) and 12.7 mm (0.5 in) used for structural testing, and 5.08 mm (0.2 in) witness panels used for coupon testing.

For the warp's parallel lay-up, each layer of fabric was laid in such a way that the fabric warps were all coincident with the x-axis. The nomenclature of this lay-up is $[0]_{nsf}$, where "[0]" indicates the orientation of each layer's warp direction, "n" stands for the number of fabric layers, "s" indicates the symmetry of the lay-up about the mid plane of the panel, and "f" designates that each layer is reinforced with a woven fabric. The warp's alternating lay-up was made with the warps of each layer alternating between zero and ninety degrees from the x-axis, yet keeping symmetry about the panel mid plane. Starting with zero degrees

orientation and ending with ninety degrees orientation at the plane of symmetry. The nomenclature of the this lay-up is $[0/90]_{nsf}$, where "[0/90]" corresponds to a set of two layers with alternating warp directions and "n" stands for the number of sets. The pseudo-quasi-isotropic lay-up was made with layers oriented at zero degrees, ninety degrees, and plus-minus forty five degrees.. The nomenclature of this lay-up is, $[0/\pm45/0]_{nsf}$, where "[0/±45/0]" corresponds to a set of four layers with different warp directions and "n" stands for the number of sets.

Two different fabrication batches were manufactured. The first fabrication batch simultaneously infused a 25.4 mm (1 in) thick panel and a 5.08 mm (0.2 in) thick panel, which acted as a witness panel for the 25.4 mm (1 in) thick panel. Similarly, the second fabrication batch simultaneously infused a 12.7 mm (0.5 in) thick panel and 5.08 mm (0.2 in) thick panel which acted as a witness panel for the 12.7 mm (0.5 in) thick panel. The intent of this fabrication arrangement was to insure the similarity of materials for coupon and component/structural level testing. In this way the material variability over a wide range of tests can be controlled and/or tracked.

The fiber reinforcement was woven roving with a weight per unit area of 814 kg/m^2 (24 oz/yd^2). The warp and fill directions have 55% and 45% respectively of the total fiber weight. The warp direction tows are spaced 5.1 mm (5 tows per inch) and in the fill direction 6.4 mm (4 tows per inch). A schematic representation of the woven fabric used is depicted in Figure 2.1. The pattern of the weave is presented in Figure 2.2 for both directions: warp and fill.

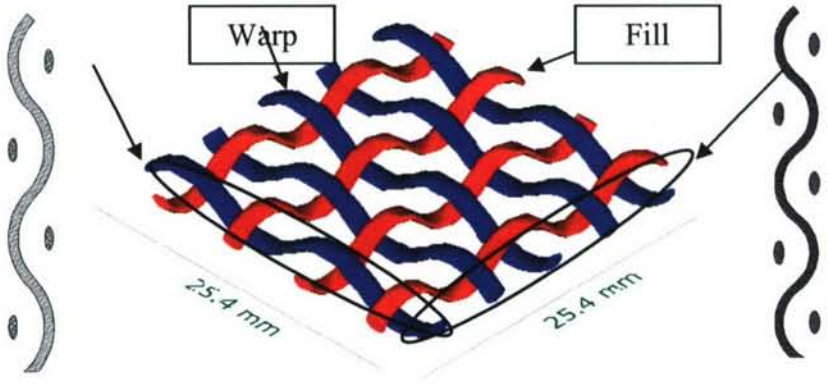

Figure 2.1: Weave Pattern Schematic

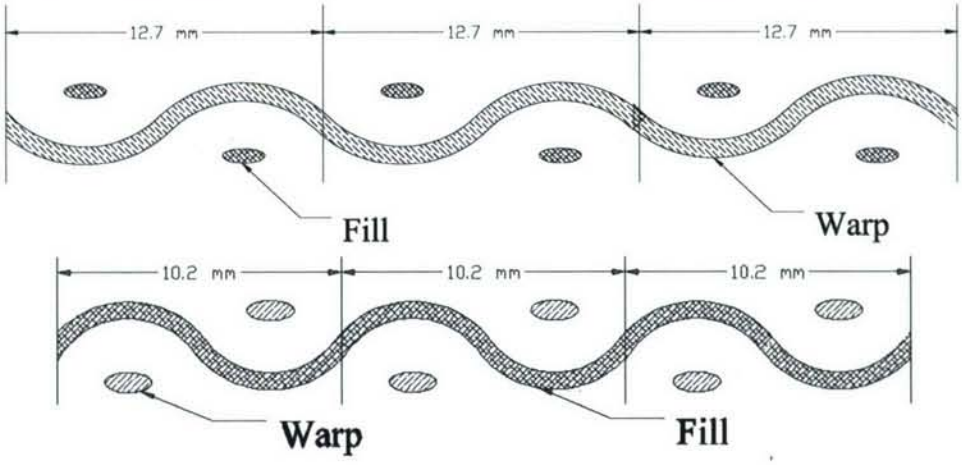

Figure 2.2: Fabric Weave Pattern in the Warp and Fill Direction

The shear tests were conducted on two sets of panels, manufactured using two different batches. The first batch was used to infuse a 25.4 mm (1 in) thick panel and simultaneously infuse a 5.08 mm (0.2 in) thick panel, which acted as a witness panel for the 25.4 mm (1 in) thick panel. Similarly, the second batch was used to infuse a 12.7 mm (0.5 in) thick panel and simultaneously infuse a 5.08 mm (0.2 in) thick panel which acted as a witness panel for the 12.7 mm (0.5 in) thick panel. For each batch, three fiber lay-ups were adopted: $[0]_{4sf}$, $[0/90]_{2sf}$, and $[0/\pm45/0]_{sf}$. Therefore, there were two panels for each fiber lay-up that had the same thickness but were infused with a different batch and at different environmental conditions. A set of 8 specimens was tested for each direction in each panel. Having a total of 6 witness panels, 12 sets of results were computed.

2.3. Inplane Shear Testing

2.3.1. Introduction

Shear properties of polymer matrix composite (PMC) reinforced with woven fabric were calculated using two American Society for Testing and Materials (ASTM) standard tests. This section reviews the literature which discusses obtaining the shear properties of PMC materials and the issues related to the testing process and specimen configuration.

Two ASTM standard shear tests were selected for evaluation under this program. The first was ASTM D4255 which is under the jurisdiction of ASTM Committee D30 on Composite Materials (ASTM D4255/D4255M, 2002). The second test method was ASTM D5379 which is also under the jurisdiction of ASTM Committee D30 on Composite Materials (ASTM D5379/D5379M, 1999). The main difference between the two test standards is the shape and size of the specimens.

The different techniques used to conduct the test are explained below. The specimen configuration used for each test, the specimen preparation, the process of collecting the data, and the analyzing techniques are briefly explained and compared to the recommendations of the standards. Any deviation from the standard is noted and justified.

Once the results from each test standard were collected, they were compared to one another. Statistical analysis was employed to make the comparison between the two sets of experimental results. Recommendations conclude the section and the advantages and disadvantages of each test method used in this study are stated.

2.3.2. Background

Several test methods have been used to obtain the shear properties of a fiber reinforced PMC. One of the main obstacles faced when these test methods were conducted was the inability to induce a uniform shear state. A standard guide for testing PMC materials supplied by ASTM recommended three test methods for calculating the in-plane shear properties of the composite material (ASTM D4762, 2004). The tests were: the v-notch specimen method ASTM D5379, the rail shear method ASTM D4255, and the tensile test of [±45] lay-up ASTM D3518 (ASTM D5379/D5379M, 1999; ASTM D3518/D3518M, 2001; ASTM D4255/D4255M, 2002). It was noted in the ASTM D4762 standard that the tensile test of [±45] laminate was limited to panels with [±45] fiber lay-up. As for the two standards selected for this study, it was noted that the v-notch specimen method was recommended where stress-strain data is required and that it gave accurate modulus measurements for laminates of the [0/90] family; while, it was noted that the three-rail method was a difficult test to run.

A theoretical and experimental analysis of the rail shear test method, presented by Whitney (Whitney, Stansbarger et al., 1971), stated that the most idealized means of measuring the in-plane shear properties of a material was by torquing a tubular specimen. But due to the difficulties that accompanied preparing tubular specimens, a flat specimen was preferred. Whitney concluded that a uniform shear stress state was produced in the gage section at a short distance away from the free edges, for rail specimens having the ratio of the specimen length to the gage section width less than or equal to ten.

A study was conducted to improve the measurement of strain between the notches of a v-notch shear specimen (Ifju, 1994). The study presented a new type of strain gage that covers the entire section between the notches and averages the shear strain across this section. The study concluded that a benefit of the strain gage was that it accounts for non-uniform and impure shear distributions. In addition, since the strain gage covers a large area, its use is an effective method to measure shear strains for laminated and textile composite materials.

Adams and Lewis studied the short beam shear method ASTM D2344, the v-notch shear method ASTM D5379, the axial tension of a [±45] laminate method ASTM D3518, and the two-rail shear test method ASTM D4255, to assess the different shear test methods (Adams and Lewis, 1997). The paper concluded that of the four ASTM shear test methods evaluated, the v-notch shear test method appeared to produce the best results. It was also observed in the paper that the rail shear test offered the possibility of a pure shear stress state similar to the v-notch shear test method.

Both the v-notch shear test method ASTM D5379 and the short beam shear test method ASTM D2344 were recommended as part of a testing program for material qualification of PMC material systems (Tomblin, Ng et al., 2001).

The v-notch shear test method ASTM D5379 was used to evaluate the shear material properties of a unidirectional hybrid composite. The study showed that the v-notch test method exhibits a limited region having a reasonable pure and uniform strain state between the notches. The paper stated that the v-notch test was effective for the evaluation of the shear modulus, but not for the shear strength of the hybrid composite (He, Chiang et al., 2002).

2.3.3. Shear Test in Accordance with ASTM D4255

Two procedures are presented in ASTM D4255: two-rail shear test and three-rail shear test. The three-rail shear test procedure was selected for the study and is addressed in this section. The three-rail shear test was selected over the two-rail shear test due to the balance that the three-rail test fixture provides on the specimen and since the off axis load of the two-rail method introduces small tensile load in the specimen during loading (ASTM D4255/D4255M, 2002).

The three-rail shear method utilizes a fixture made from three rails parallel to each other. The rails secure the specimen, a flat panel. The outside rails were supported by the fixture base and a compressive load was applied on the center rail. The applied load produced nearly pure shear in the two gage sections of the specimen. The three-rail shear fixture and a test specimen are shown in Figure 2.3.

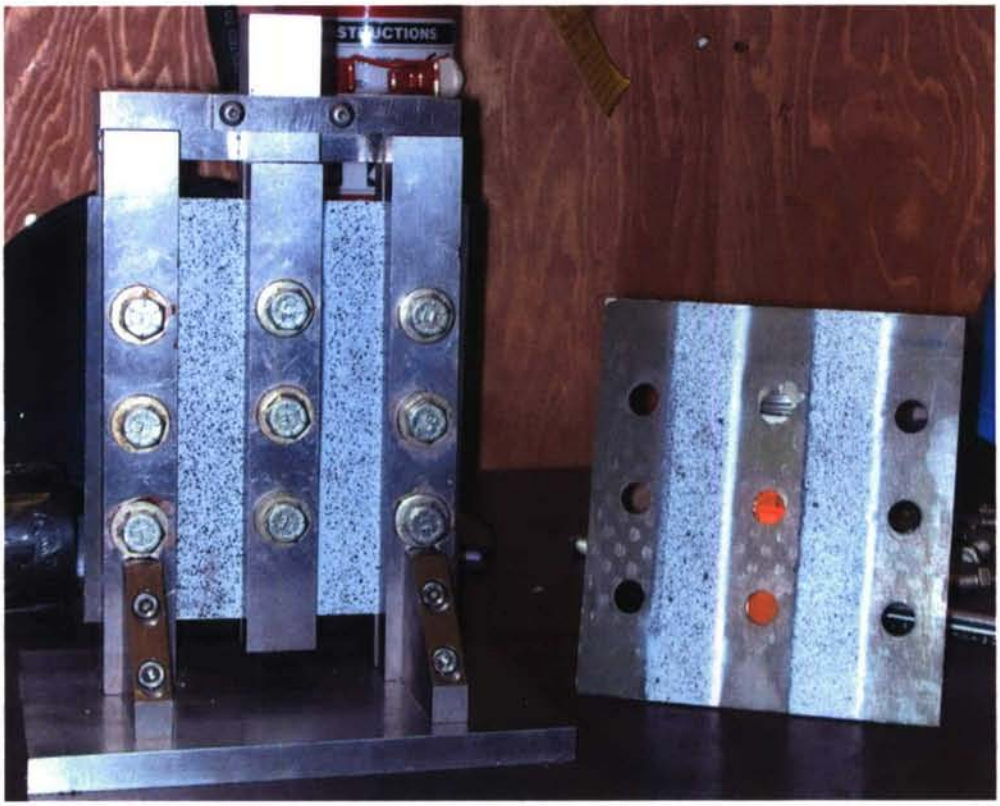

Figure 2.3: Three-Rail Shear Fixture with D4255 Specimen

The ASTM D4255 standard recommended the procedure to cut and prepare the specimens for testing. The following sections outline the procedure used to conduct the test in this study; the tools used to measure the specimen dimension, the strain measuring devices and the procedure to collect the data.

2.3.4. Specimen Preparation

The ASTM D4255 standard recommended that at least 5 specimens per test condition be tested (ASTM D4255/D4255M, 2002). For this study 8 specimens were tested per test condition. Extra specimens were needed to account for loss of data while testing or during data collection. Two sets of specimens were cut from each panel. One set in the x-direction, the laminate principal axis, and another set in the y-direction, orthogonal to the laminate principal axis. Although, ideally, there should be no difference in the shear properties of the PMC in these two directions, the two sets were selected to verify that assumption. The specimens were cut using a computer numerical control (CNC) water-abrasive jet machine.

The specimen configuration was in accordance with the recommendation in the standard. The specimen length was 152.4 mm (6 in) and the width was 136.53 mm (5.375 in). The specimen contained 9 holes with a diameter of 12.7 mm (0.5 in) each as depicted in the 2D-CAD drawing in Figure 2.4.

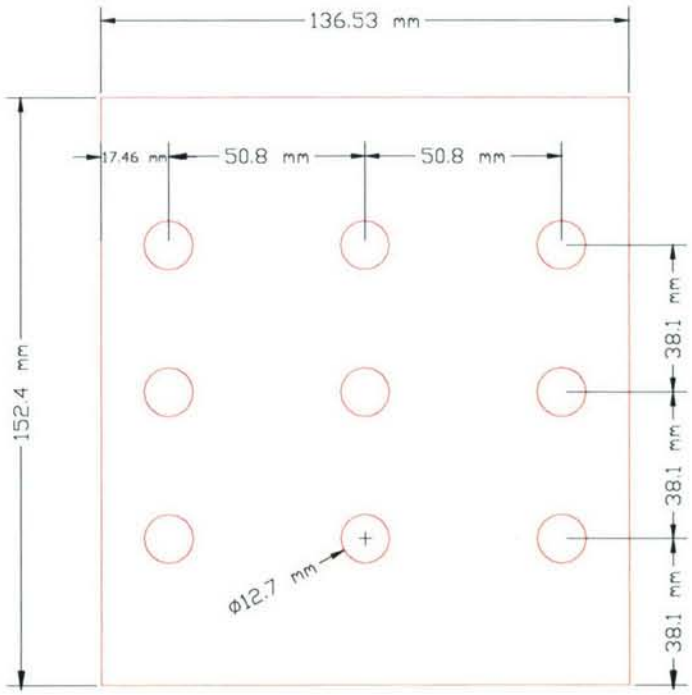

Figure 2.4: D4255 Specimen Configuration

The specimens were conditioned for 3 months at a temperature of 22 ± 3°C (71.6 ± 5°F) and 50 ± 3% relative humidity in accordance with procedure C of ASTM D5229 (ASTM D5229/D5229M, 2002) prior to testing.

The specimen thickness was measured using a 5 mm (0.19685 in) nominal diameter double-ball-interface micrometer at two random locations on each specimen gage length. The specimen length was measured at the same locations using a double-flat-anvil caliper. The measurements were recorded and the average area was later used in the computation of the material shear properties.

The standard recommended the use of four three-element strain gage rosettes for measuring the shear strain while the specimen was loaded. A 3-D digital image correlation (DIC) system was used to measure full-field strains of the gage section instead.

When the specimen was installed in the fixture, 9 grade eight steel bolts were used to clamp the specimen. Modifications to the commercially available fixture were necessary; the studs were drilled out leaving the required bolting pattern. The torquing force recommended by the standard was 94.9 N-m (70 lbf-ft). To simplify the torquing process a thread lubricant was used and the torque applied was 54.2 N-m (40 lbf-ft), which was the limiting torque before the bolts material yielded. To insure good clamping with every specimen, the bolts and nuts were replaced for every specimen.

2.3.5. Test Setup

After the specimen was installed in the fixture, the fixture was placed in the testing machine, a servo controlled hydraulic machine capable of controlling the velocity of the moving cross head. The testing machine specifications were in conformance with ASTM Practices E4 (ASTM E4, 2002). The load applied by the testing machine through a ball bearing was used to remove any bending forces on the specimen from imperfections in the frame and fixture. The three-rail fixture with a specimen installed in it is shown in Figure 2.5 during a test.

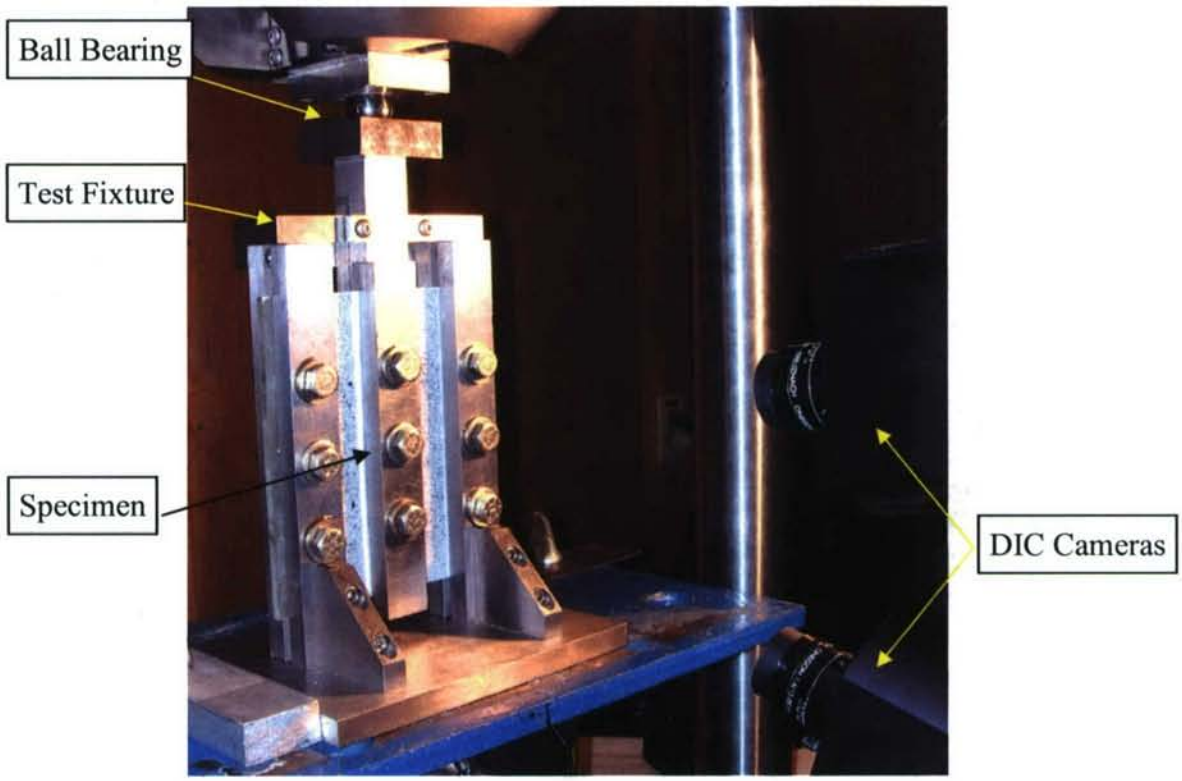

Figure 2.5: Testing of D4255, Three-Rail Shear, Specimen

The test was conducted at a load rate of 1.2 mm/min (0.047 in/min). At this rate, the test lasted between 5 minutes to 6 minutes. The load and strain data were collected at a rate of 1 hertz. The DIC system collected the data as a series of paired digital images that were later used to obtain full-field strains of the specimen. A typical full-field shear strain of a D4255 specimen is depicted in Figure 2.6.

Figure 2.6: Full-Field Shear Strain of a D4255 Specimen

The strains were exported from the DIC system by selecting two areas over the specimen gage lengths. The average shear strain from each area was exported. The gage areas are represented on the specimen gage length shown in Figure 2.6 as two faint rectangles in the foreground. The data exported had two strain values for each data point. The average of these values was used to represent the stress strain curve.

2.3.6. Shear Test in Accordance with ASTM D5379

The second test conducted in this study to obtain the material in-plane shear properties was the v-notched beam method described in ASTM D5379 (ASTM D5379/D5379M, 1999). In this method, the specimen was a rectangular flat strip with a centrally located v-notch; and a special fixture, referred to as Iosipescu shear test fixture, was utilized to transfer the loading to the specimen. The intent of the fixture and the specimen configuration was to produce pure shear strain in the material along the area between the notches of the specimen. A picture of a specimen installed in the fixture is shown in Figure 2.7. Any deviation from the ASTM standard is stated and justified.

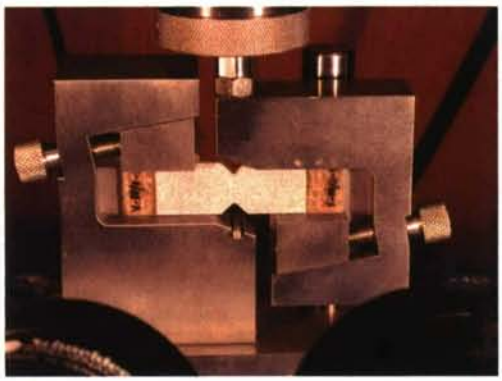

Figure 2.7: D5379 Specimen installed in the V-Notch Fixture

2.3.7. Specimen Preparation

The standard states that at least 5 specimens should be tested per testing condition. To account for specimen data that may be lost during the testing process or during the data analysis, 8 specimens for each direction were tested. Although the in-plane shear properties of the panels were ideally independent of the principal in-plane direction, the specimens were cut from the panels in two directions, x-direction and y-direction, and tested to verify this fact. The specimens were cut from the panels with a CNC water-abrasive jet machine.

The standard recommended a specimen configuration that was used with the Iosipescu test fixture. The standard recommendations were adhered to and the specimen configuration and dimensions used in this study are shown in Figure 2.8.

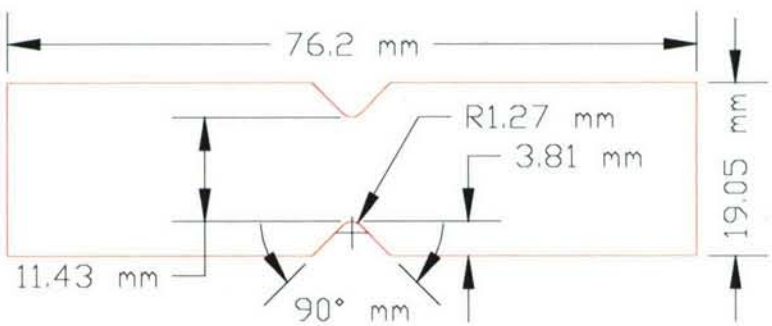

Figure 2.8: D5379 Specimen Configuration

The specimens were conditioned in accordance with procedure C of test method D5229 (ASTM D5229/D5229M, 2002). The specimens were stored in a conditioning chamber for 3 months at a temperature of 22 ± 3°C (71.6 ± 5°F) and 50 ± 3% relative humidity.

As recommended in the standard, the specimen thickness was measured with a 5 mm (0.19685 in) nominal diameter double-ball-interface micrometer at three random locations between the notches of the specimen which had a length of 11.43 mm (0.45 in). The length of the notched section was measured using an edge-end caliper. The measurements were recorded and the calculated average area was later used in the computation of the material in-plane shear properties.

The ASTM D5379 standard recommended the use of strain gages to measure the shear strain in the gage section. It was recommended that two strain gages be bonded between the notches at an angle of +45° and -45° to the loading axis. Instead of using strain gages, a 3-D DIC system which measures full-field strains was used.

2.3.8. Test Setup

The specimen was installed in the fixture and placed in the testing frame which was a hydraulic machine capable of controlling the velocity of the moving crosshead. The specifications of the testing machine were in conformance with ASTM Practices E4 (ASTM E4, 2002).

The test set-up is shown in Figure 2.9 as a test was in progress.

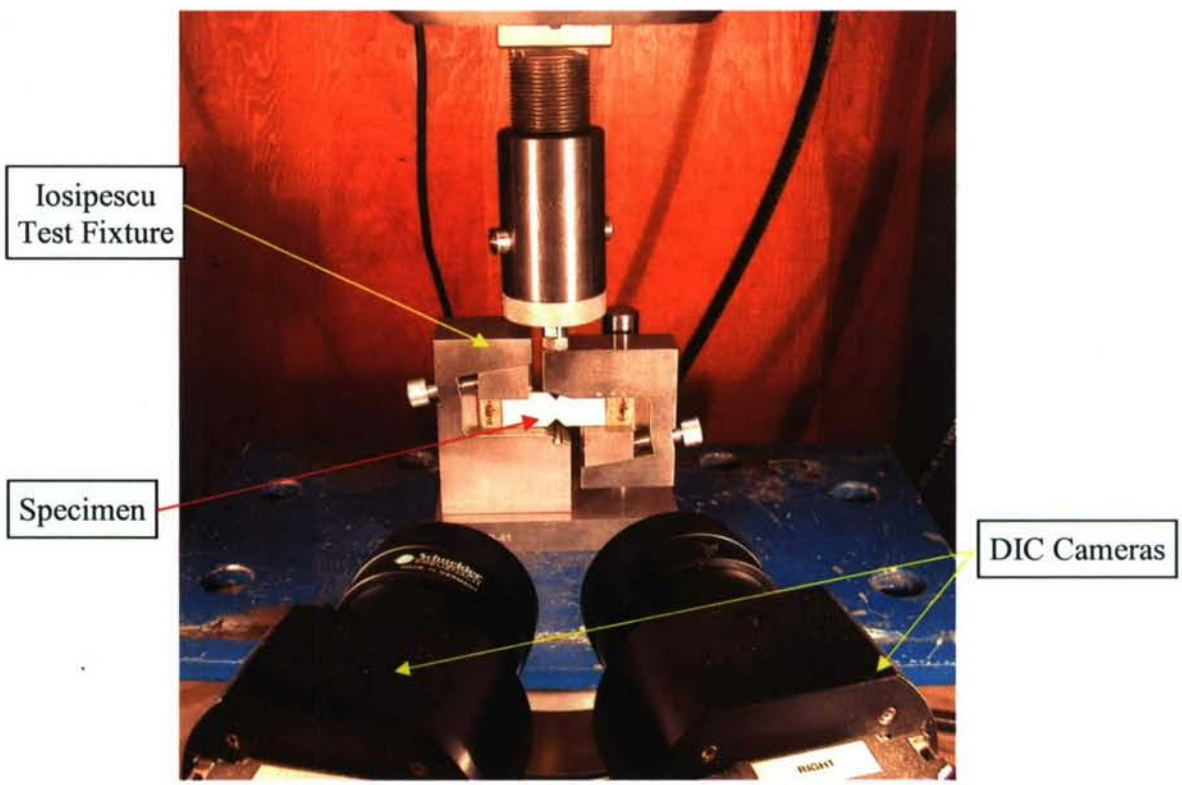

Figure 2.9: Testing of D5379, V-Notched Shear Specimen

The standard recommended selection of the test speed to cause failure within one to ten minutes. The load rate selected was 1.2 mm/min (0.047 in/min) that caused a failure after approximately three minutes of the test start. During the loading process, the data was collected at a rate of approximately one hertz. Every data point collected included the load and the full-field strains on the face of the specimen in the gage section as seen by the DIC system. A typical full-field shear strain captured by the DIC system for an ASTM D5379 v-notch shear specimen under load is shown in Figure 2.10.

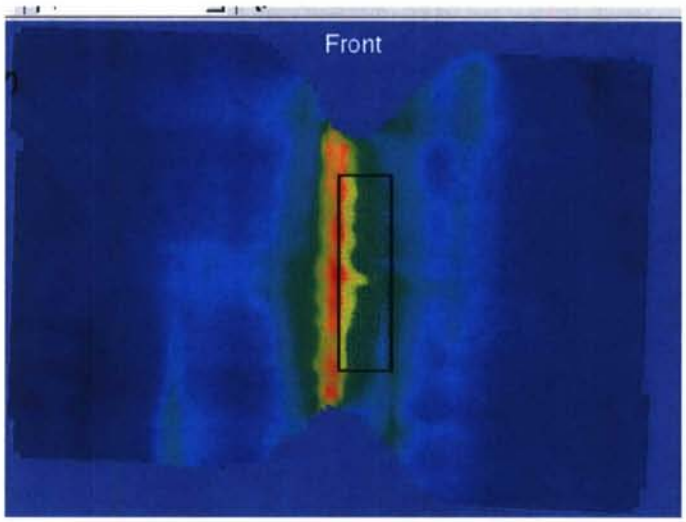

Figure 2.10: Full-Field Shear Strain of a D5379 Specimen

A faint rectangle in the foreground is depicted in Figure 2.10. This rectangle represented the area of full-field shear strain that was exported from the DIC system. The strain in this area was averaged and exported as one data point. In addition to the shear strain, each data point was accompanied with the value of the load carried by the specimen at that instant.

2.3.9. Stress-Strain Representation

Both standards recommended calculating the material shear modulus of elasticity by taking the chord of the curve over a range of 4000 micro-strain at the start of the curve, beginning in the range of approximately 2000 micro-strain. The shear strength was recommended to be calculated by taking the intersection of the curve with the 0.2% offset of the chord modulus calculated. Due to the extent of the non-linearity observed with the data, standard recommendations were not followed to calculate the material properties of the material tested in this study. Instead a hyperbolic tangent curve fit was used. The hyperbolic tangent curve fit is given in equation (2.2) (Barbero, 1998).

$$\tau_{12} = a \cdot \tanh\left(\gamma \cdot {}^{b}/_{a}\right) \tag{2.2}$$

where:

τ_{12} = shear stress, MPa (psi),
γ = shear angle, radians
a = asymptote of the curve, MPa (psi),
b = slope of the tangent of the curve at the base, MPa (psi).

Using equation (2.2) the elastic shear modulus was considered to be the value of b. The value of the asymptote of the curve was recommended in the reference to be used as the ultimate shear strength of the material. For this study, the stress-strain curve of the material exhibited an asymptote for the curve fit that had a large value. The failure of the material was detected in the curve by a flat region were the strain increased at a constant load. Therefore, the ultimate shear strength of the material was considered to be the point at which the strain increased and the load was constant or decreased. A typical stress-strain curve of a shear specimen with the hyperbolic tangent curve fit is depicted in Figure 2.11. The calculated value of the shear modulus of elasticity and shear ultimate strength of the stress-strain curve are presented in Figure 2.11.

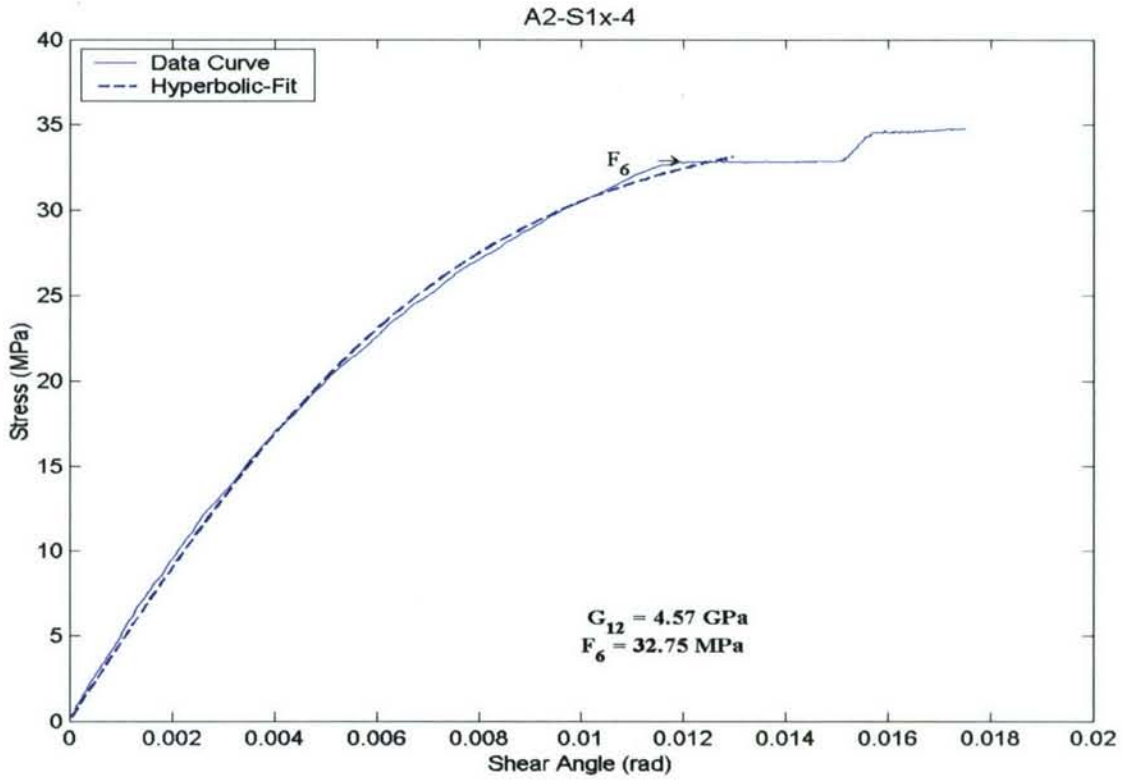

Figure 2.11: Typical Stress-Strain Shear Curve with Hyperbolic Tangent Curve Fit

2.3.10. Discussion of the Experimental Results

2.3.10.1. Shear Properties in Accordance with ASTM D4255

The shear modulus of elasticity was calculated by using the hyperbolic tangent fit curve given in equation (2.2) to model the stress-strain curve. The mean values of each set of specimens are presented in Figure 2.12. The chart has the standard deviation error bars and the coefficient of variation for each set. The chart was organized to compare the shear modulus values between the two batches tested for each fiber lay-up. As noted earlier, each panel had two orthogonal directions: x-direction and y-direction, where the x-direction is the laminate principal axis. Both directions are plotted in one chart to verify that the shear modulus was independent of the in-plane principal material axes.

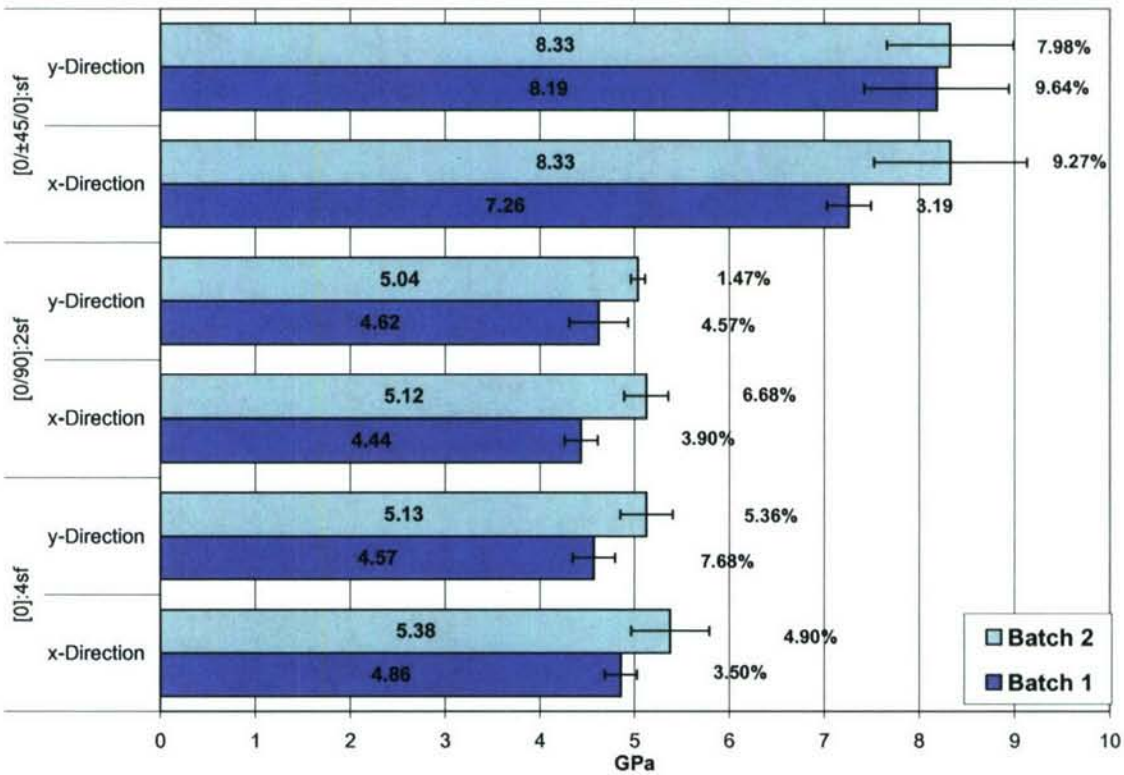

Figure 2.12: Shear Modulus of Elasticity (D4255)

The ultimate shear strength of the composite was determined as the flat region illustrated by an increase in the strain with a constant load or, in some cases, a drop in the load. This behavior was explained by the reorientation of the reinforcing fabric after the matrix fails. And in some cases, an increase in the load and strain continued after the flat region and then produced another flat region. This is a result of the fabric holding the load for a given amount until it started to reorient again. This behavior is

seen in Figure 2.11, which is a typical stress-strain curve of an ASTM D4255 three-rail shear specimen from batch 1.

The shear ultimate strengths of the PMC under study for batch 1 and for two fiber lay-ups only are shown in Figure 2.1.

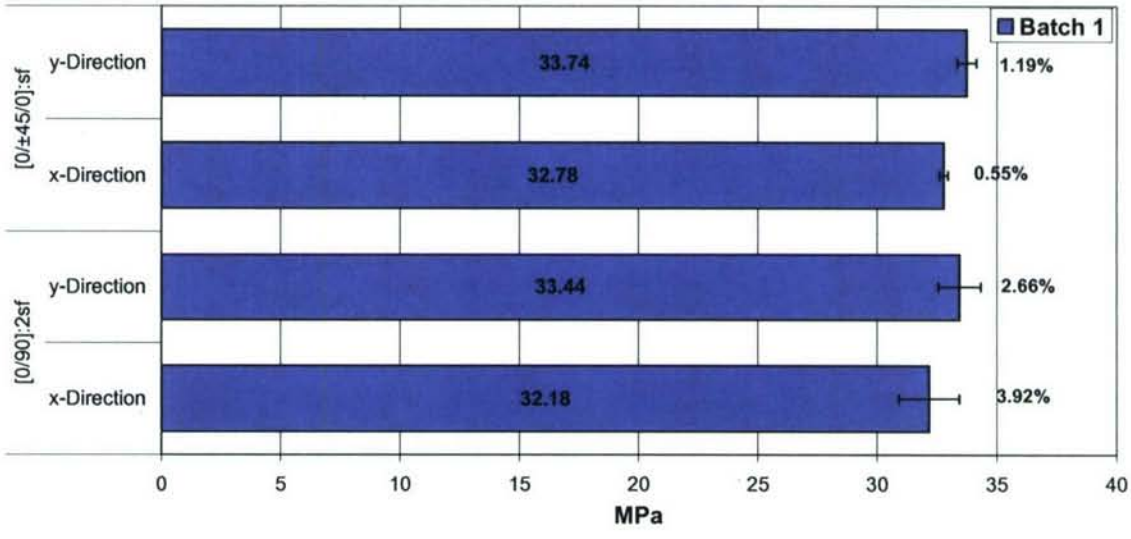

Figure 2.13: Shear Ultimate Strength (D4255 – Batch 1)

The shear ultimate strength for the $[0]_{4sf}$ fiber lay-up for batch 1 was not calculated due to testing errors. As for the ultimate shear strength for batch 2, the data was calculated but a premature failures were noticed in the specimens. The premature failure was detected in the stress-strain curve that depicted a small drop in the load at the early stages of loading. A stress strain curve for an ASTM D4255 specimen from batch 2 is represented in Figure 2.14. The shear ultimate strength for $[0]_{4sf}$ and $[0/90]_{2sf}$ fiber lay-ups ranged between approximately 19 GPa (2755.7 ksi) and 17.8 GPa (2581.7 ksi); while, the ultimate shear strength for $[0/\pm45/0]_{sf}$ fiber lay-up was approximately 45 GPa (6526.7 ksi).

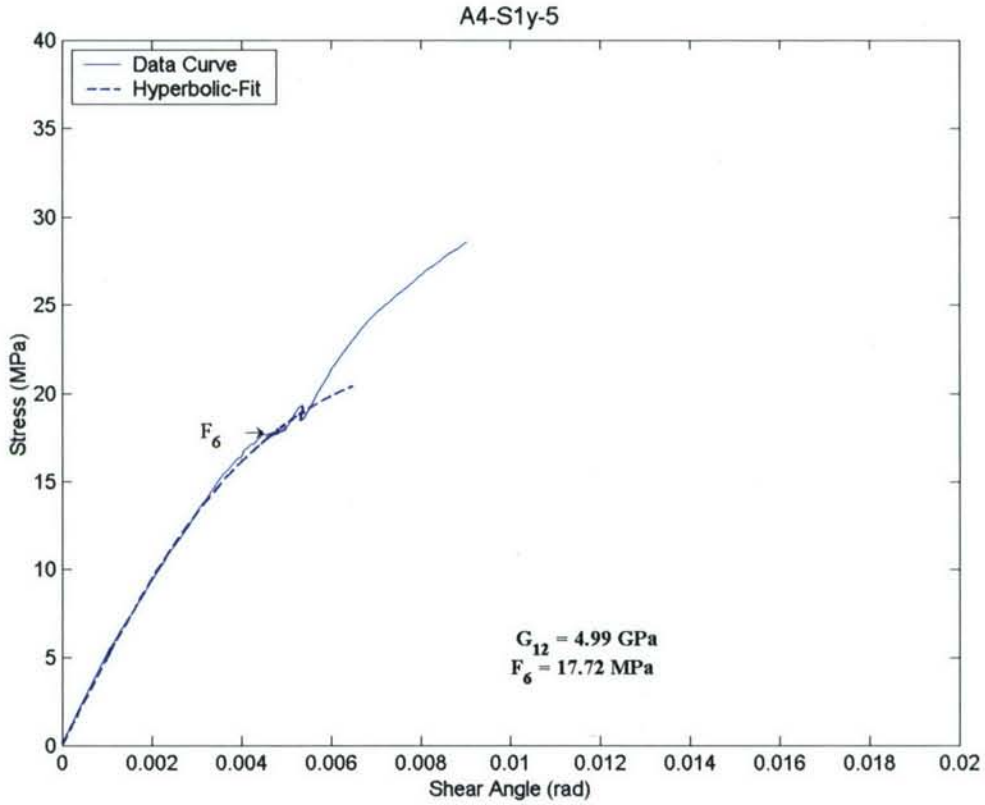

Figure 2.14: Premature Failure in an ASTM D4255 Batch 2 Specimen

2.3.10.2. Shear Properties in Accordance with ASTM D5379

The stress-strain curve for the v-notch specimens was obtained by considering the shear strain between the notches. An area between the notches was selected and the shear strain in that area was averaged and used with the cross-sectional area and the load carried by the specimen to build the stress-strain curve. It was noticed that the shear strain was not solely concentrated between the notches as was intended by the design of the test. A set of full-field shear strains are depicted in Figure 2.15; they represent the strain of all three lay-ups in the two directions tested: x-direction and y-direction.

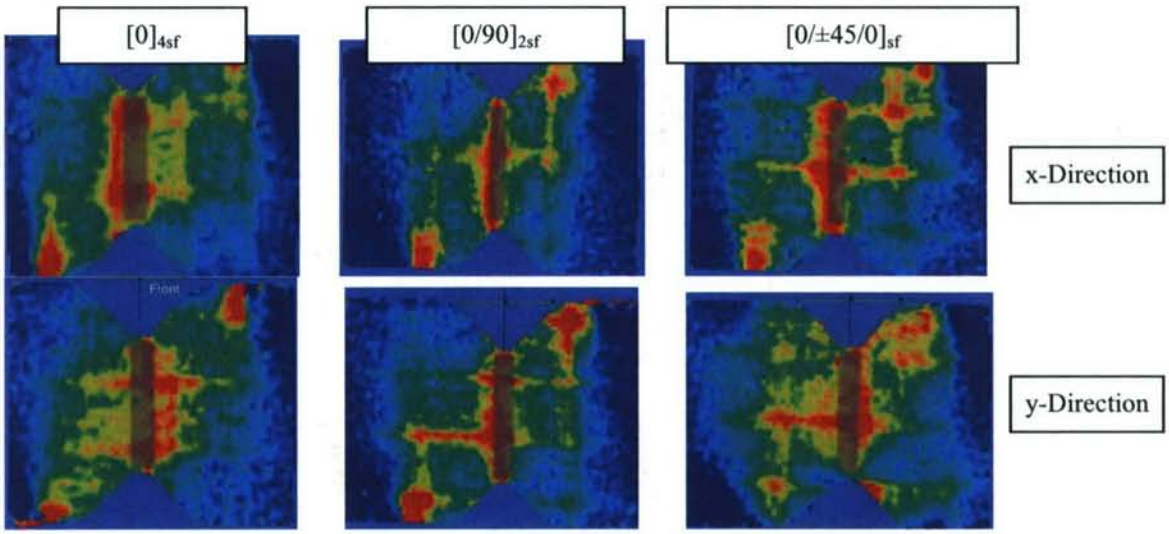

Figure 2.15: Full-Field Shear Strain Distribution in V-Notch Specimens

Due to the inconsistent strain concentrations observed in the full-field shear strain distributions captured by the DIC system (Figure 2.15), large variability was observed in the experimental results. The variability was a result of the distribution of the shear strain across the surface specimen. The material shear properties were calculated by considering the cross-sectional area and shear strain located between the notches as recommended by the ASTM standard. The results ranged between 2 GPa (290 ksi) to 3 GPa (435 ksi) for the specimens cut from batch 1 with a coefficient of variation of up to 30%.

Another factor that caused the variability in the experimental results was the coarseness of the fabric used. This type of fabric used had a tow spacing of 5.1 mm (5 tows per inch) in the warp direction and 6.35 mm (4 tows per inch) in the fill direction. This added to the variability of the results. The notch in the ASTM D5379 specimen in some cases was over a tow and in other instances was over a gap between two tows. The randomness of the notch placement with respect to the weave pattern caused large differences in the experimental results which was observed in the comparison of the values calculated from batch 1 and batch 2. The shear modulus of elasticity of the second batch ranged between 0.3 GPa (43.5 ksi) and 0.4 GPa (58 ksi), which was approximately one order of magnitude smaller than the values calculated from the specimens in the first batch. Similarly, the coefficient of variation of the results was up to 30% in some cases.

The ultimate shear strength could not be calculated for the ASTM D5379 test method. The stress-strain curve had no flat region or a drop in the load. A 0.2% offset value could have been used to obtain the ultimate shear strength as recommended in the standard (ASTM D5379/D5379M, 1999);

but, since there was large variability in the experimental results of the shear modulus of elasticity, the shear ultimate strength was not calculated.

2.3.11. Conclusion

The experimental results obtained were very dependent on the type of fabric used. The fabric used in this study was coarse and woven with relatively large tows. The ASTM test methods conducted did not relate the specimen configuration or gage section to the type of fabric used. When the ASTM D4255 test method was conducted, the results were comparable to test results found in the literature and the variability was less than 10%. On the other hand, when the ASTM D5379 test method was conducted, the results had coefficients of variability of up to 30% with very different results between batch 1 and batch 2 of the specimens. The gage section in the three rail shear test method was approximately 140 mm x 25.4 mm (5.51 in x 1 in), which was enough to cover a large area of the fabric reinforcing the PMC.

The fabric is represented properly when 3 tow patterns are included in the gage section; the edge patterns are affected by the boundary conditions, thus, leaving the middle pattern unaffected by outside conditions. The tow pattern of the fabric used repeated every 12.7 mm (0.5 in) in the warp direction and every 10.16 mm (0.4 in) in the fill direction.

The three rail shear test (ASTM D4255) performed better than the v-notch shear test (ASTM D5279). The main reason was the specimen configuration and the scale of the specimen compared to the fabric used. The specimen configuration and the gage section of the specimen should be correlated to the reinforcing fabric of the PMC. In the case where the PMC is reinforced with fibrous fibers (not tows) small gage sections would give acceptable results. In addition, failure was detected in the stress-strain curve of the three rail shear tests by a flat region in the curve or by a drop in the load, which was not found in the v-notch shear test.

2.4. Compression Testing

2.4.1. Introduction

For characterizing polymer matrix composites (PMC) with woven fabric reinforcement in compression, two test methods were selected. The first test method was ASTM D6641 and is under the jurisdiction of Committee D30 on Composite Materials; while the second test method selected was the Suppliers of Advanced Composite Materials Association (SACMA) SRM 1R test method (SACMA SRM 1R-94, 1994). The method was derived from ASTM D695 which is under the jurisdiction of Committee D20 on Plastics (ASTM D695, 1996). SACMA SRM 1R is used for determining the compression properties of reinforced plastics by end-loading. Conversely, the test method in accordance with D6641 is used to determine the compression properties of PMC by introducing combined end and shear loadings (ASTM D6641/D6641M, 2001).

A literature review cites different papers that characterize the compression properties of PMC; the findings of these papers are discussed and compared with the findings of the study presented in this section. The test methods used in this study are explained in the following sections and are referenced to the ASTM standard and SACMA recommended method. Any deviation from the standard are explained and justified. The specimen configuration used, the method to cut the specimens, and the specimen preparation before testing are explained. The test setup and instrumentation systems are presented; the problems with experimental methodology are stated and discussed.

Statistical analysis was conducted on the results of the test methods and the advantages and disadvantages of each test are discussed. A set of conclusions and recommendations are presented. The main recommendation is a modification of the compression test method combining the advantages of each test method. The modified test method was conducted and the experimental results were analyzed. The results from the test methods in accordance with the standards and the modified test method that were recommended from the study conducted on these tests were compared.

2.4.2. Background

Various compression tests are used to characterize the material properties of a composite material. These test methods have been modified and changed over time to improve the results calculated and reduce the uncertainty of the testing method. Recently, the ASTM D30 Committee devised a standard guide for testing PMC materials (ASTM D4762, 2004). For characterizing the composite material compressive properties, the guide recommended four ASTM standards: ASTM D6641, ASTM D695, ASTM D3410, and ASTM D5467 (ASTM D695, 1996; ASTM D6641/D6641M, 2001; ASTM D3410/D3410M, 2003; ASTM D5467/D5467M, 2004). ASTM D4762 recommends that the D695 test method is not recommended for continuous fiber composites and a modified version of the D695 test method was released as the SACMA SRM R1 test method (SACMA SRM 1R-94, 1994). However, ASTM 4722 recommends the use of ASTM D6641 instead.

Additionally, a report sponsored by the United States Department of Transportation recommended the SACMA SRM R1 for calculating the compressive properties of PMC reinforced with unidirectional tape or woven fabric (Tomblin, Ng et al., 2001). The report presented a qualification plan to help ensure the control of repeatable base material properties.

Wolfe compared the various test methods for compression testing (Wolfe and Weiner, 2004). The paper describes the test methods conducted on three types of PMC panels. It was concluded in the study that there was no difference in the compressive material properties between the SACMA SRM 1R test method and ASTM D6641 test method. In addition, the paper stated that ASTM D695

test method produced a lower material compressive strength than the other test methods.

Adams and Lewis studied the effect of the specimen gage length on the material compressive properties (Adams and Lewis, 1990). This study used two test methods: ASTM D3410 and SACMA SRM 1R. It concluded stating that the measured compressive strength of a high-strength, highly orthotropic composite material appeared to be independent of the slenderness ratio, the length ratio of the gage section to the minimum radius of gyration of the cross-sectional area.

Note that the literature reviewed did not illustrate the effect of the fabric used to reinforce the PMC on the type of test conducted. In addition, the scale of the woven fabric used was not related to the specimen configuration.

This section addresses two compression test methods that were used to characterize the compression material properties of PMC with woven fabric reinforcement. The compression test methods used are ASTM D6641 (ASTM D6641/D6641M, 2001) and SACMA SRM 1R (SACMA SRM 1R-94, 1994).

2.4.3. ASTM D6641Compression Test

This test method is used for determining the compressive strength and stiffness properties of PMC using a combined loading compression (CLC) fixture. The load is introduced into the specimen by combined end- and shear-loading (ASTM D6641/D6641M, 2001).

The following sections explain the specimen configuration, the apparatuses, and procedures used for conducting the compression test in accordance with ASTM D6641 in this study. Any deviation from the standard is stated and justified.

2.4.4. Specimen Preparation

The standard recommended testing at least 5 specimens for each testing condition. To account for data loss during testing or during the collection of experiment data, 8 specimens were used in the testing program for each testing condition. Two sets of specimens were cut from each panel. One set represented the x-direction, the laminate principal axis, and the other set represented the y-direction, orthogonal to the laminate principal axis. The cutting tool used to cut the specimens from the panels was a water-abrasive jet computer numerically controlled (CNC) machine.

The specimen configuration was selected according to the standard recommendations. The specimen length was 139.7 mm (5.5 in) and the specimen width was 19.05 mm (0.75 in). The specimen thickness was confined to be the same as the panel thickness. The panel thickness was approximately 5.08 mm (0.2 in), which resulted in a specimen thickness of 5.08 mm (0.2 in).

A 2D-CAD drawing of the specimen used in this test and the specimen dimensions are depicted in Figure 2.16.

Figure 2.16: D6641 Specimen Configuration

The specimen gage length was 12.7 mm (0.5 in) when placed in the fixture. The length of the gage section was checked to be sufficient to rule out the Euler column buckling of the specimen by the use of equation (2.2) that was recommended in the standard (ASTM D6641/D6641M, 2001).

$$h \geq \frac{l_g}{0.9069 \cdot \sqrt{\left(1 - \frac{1.2 \cdot F_c^e}{G_{xz}}\right) \cdot \left(\frac{E^f}{F_c^e}\right)}} \qquad (2.2)$$

where:

h = specimen thickness, mm (in),
l_g = length of gage section, mm (in),
F_c^e = expected ultimate compressive strength, MPa (psi),
E^f = expected flexural modulus, MPa (psi),
G_{xz} = through-the-thickness (inter-laminar) shear modulus, MPa (psi).

The expected ultimate compressive strength, expected flexural modulus, and the inter-laminar shear modulus were estimated from the literature on PMC with woven fabric reinforcement.

Prior to testing, the specimens were conditioned for 3 months at a temperature of 22 ± 3°C (71.6 ± 5°F) and 50 ± 3% relative humidity in accordance with procedure C of ASTM D5229 (ASTM D5229/D5229M, 2002)..

The specimen width and thickness were measured using a 5 mm (0.19685 in) nominal diameter double-ball-interface micrometer at three random locations along the gage length of the specimen which was 12.7 mm (0.5 in). The measurements were recorded and the average area was later used in the computation of the compression properties of the material.

Since the cutting tool introduced a slight taper in the specimens along the thickness, the ends of the specimens were machined square and flat. The taper

angle is approximately 2 or 3 degrees. Machining the specimen ends was necessary to prevent end crushing of the specimen while loading was applied.

As recommended by the standard, the loading was introduced to the specimen using a CLC fixture. The fixture transferred the compression load applied to the specimen into a combined end loading and shear loading. The fixture consisted of two metal blocks that were connected to each other by a pair of rails. The specimen ends were clamped in the metal blocks. The specimen was positioned in the fixture such that the specimen ends were flush with the metal blocks; and the unclamped region of the specimen represented the specimen gage length. A partially disassembled fixture with a specimen clamped in one metal block is represented in Figure 2.17.

Figure 2.17: D6641 CLC Fixture – Assembled and Disassembled

The circular recess in the center of the fixture is designed for using an extensometer to measure the strain of the specimen as the load is applied. For this study, a 3-D digital image correlation (DIC) system was used to measure the strains. Due to the design of the fixture, the cameras of the DIC system were able to view the edge of the specimen gage length when the gage length was 12.7 mm (0.5 in). Therefore, a speckle pattern was applied to the specimen surface (edge of the specimen) that would be facing the digital cameras.

2.4.5. Test Setup

The specimen was installed in the fixture by following the manufacturer's instructions. When the specimen was installed, the specimen ends were flush with the metal blocks as seen in Figure 2.17 and the gage length was not supported by the fixture. The four screws of each metal block were torqued in three approximately equal increments. As recommended by the standard, the required torque depends on the thickness of the specimen (ASTM D6641/D6641M, 2001). Several trials were required to reach an acceptable torque that was sufficient to prevent specimen end crushing without inducing stress concentrations that might lead to premature failures. A torque of 3.39 N-m (30 in-lb) was sufficient for the material used in this study with a specimen thickness of approximately 5.08 mm (0.2 in).

The CLC fixture was placed in the testing frame. The testing machine was a servo controlled hydraulic machine with the capability of controlling the velocity of the moving cross head. The testing machine specifications were in conformance with ASTM Practices E4 (ASTM E4, 2002). The load was applied by the testing machine through a ball bearing used to remove any bending forces on the specimen due to imperfections in the frame and fixture. The use of a ball bearing was recommended by ASTM D6641.

The test was conducted at a compressive load rate of 0.6 mm/min (0.0236 in/min) to failure of the specimen. Each test elapsed between four and a half minutes and five and a half minutes. During the loading process, the data was collected at a rate of approximately 1 hertz. Every data point collected included the load and the full-field strains on the specimen edge in the gage length as seen by the DIC system. A typical full-field strain in the direction of the load applied as captured by the DIC system of a D6641 compression specimen is shown in Figure2.18.

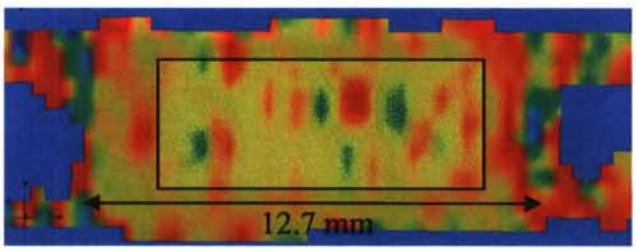

Figure2.18: Full-Field Strain of a D6641 Specimen

A faint rectangle in the foreground is depicted in Figure2.18. This rectangle represented the area that the full-field strains were exported from the DIC system. The strain in this area was averaged and exported as one data point. The strains exported for each data point were longitudinal strain, in the direction of the applied load and transverse strain, which was orthogonal to the longitudinal strain and through the specimen thickness.

2.4.6. SACMA SRM R1Compression Test

The compression test used in this study was in accordance with the SACMA SRM R1 recommended test method. The SACMA recommended test method was derived from ASTM D695 and covered the procedure for the determination of the compressive properties of oriented fiber-resin composites reinforced by continuous high modulus fibers (SACMA SRM 1R-94, 1994). The ASTM D695 standard test method for compressive properties of rigid plastics presented the method for determining mechanical properties of reinforced rigid plastics when loaded in compression (ASTM D695, 1996). Referring to the ASTM standard, the SACMA recommended test method described the procedure behind conducting the test and calculating the composite material properties: elastic compressive modulus, ultimate

compressive strength, and in-plane Poisson's ratio. Any deviation from the recommendation is noted in the following sections.

2.4.7. Specimen Preparation

Although the standard recommended the use of at least 5 specimens, 8 specimens were used for each testing condition, to accommodate the loss of specimens or data through the testing procedure. Each set represented either the x-direction or the y-direction of the panel. The x-direction was along the laminate principal axis, and the y-direction was orthogonal to the laminate principal axis. The cutting tool used to cut the specimens from the panels was a (CNC) water-abrasive jet.

The SACMA standard recommended a specimen length of 80.77 mm (3.18 in) and a width of 12.7 mm (0.5 in). The specimen thickness was recommended to be 3.05mm (0.12 in) but the panels were infused with 8 layers of fabric as reinforcement and the total laminate thickness was approximately 5.08 mm (0.2 in). Therefore, the specimen thickness was not in accordance with the recommendation in the standard and was 5.08 mm (0.2 in). The specimen dimensions are shown on a 2D-CAD drawing of the specimen in Figure 2.19.

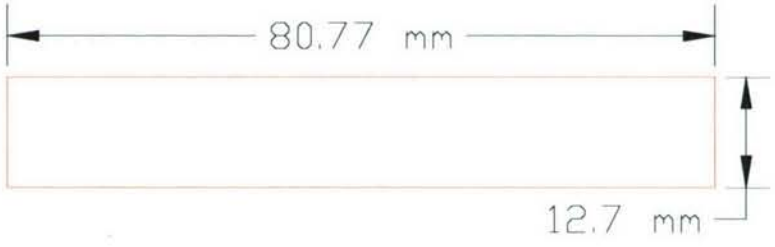

Figure 2.19: SACMA SRM 1R Specimen Configuration

The specimens were stored in a conditioning chamber for 3 months at a temperature of 22 ± 3°C (71.6 ± 5°F) and 50 ± 3% relative humidity. While testing the specimens, the testing room was climate controlled at room temperature (22°C) and relative humidity of 50%.

Two specimen types were recommended by the SACMA standard to measure the modulus of elasticity and the ultimate strength. An un-tabbed specimen was used to measure the modulus of elasticity and a tabbed specimen was used to measure the ultimate strength. This procedure was recommended due to the difficulty of using a strain measurement device on the tabbed specimens when loading to failure since the distance between the tabs is smaller than any conventional strain measuring device, approximately 4.75 mm (0.188 in). On the other hand, the un-tabbed specimen could not be loaded to failure since the ends of the specimen would crush. Since the 3-D DIC system was used to measure the strains as the specimen was loaded, the test was conducted with the use of one specimen to measure both properties: the modulus of elasticity and the ultimate strength.

In order to carry out the test to failure, a tabbed specimen was used. The tabbing material used was a cross-ply E-glass/epoxy composite known as G11 and used mainly for electric boards. The tabs had a length of 38.1 mm (1.5 in) and the same width as the specimen with a thickness of 1.575 mm (0.062 in). The tabs material and dimensions agreed with the recommendations of the standard.

To improve the bond of the tab to the specimen, an 80 grit sandpaper was used to roughen the surface where the tabs had to be bonded, and a degreaser was used to remove any residue of mold release from the panel manufacturing process and any dust particles. The tabs were bonded to the specimen with Plio-Grip 7770, a structural adhesive. The adhesive was mixed and applied in a climate controlled room with a temperature of 20°C and relative humidity of 50% to insure curing of the adhesive. The tabs were clamped and left 12 hours at the same temperature and relative humidity to cure. A 3D-CAD drawing represents a tabbed specimen in Figure 2.20.

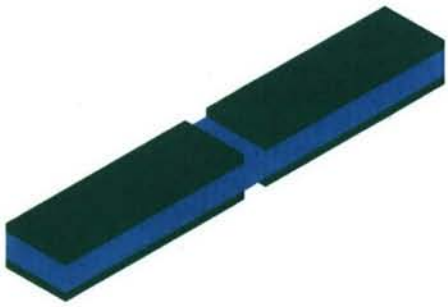

Figure 2.20: 3D-CAD Drawing of a SACMA SRM 1R Tabbed Specimen

After the specimens were tabbed, the ends of the specimens were machined parallel and square. In addition, to insure flat faces of the tabbed specimen, the faces of the specimen were also machined parallel and square. The process of preparing the specimen - tabbing and machining - was very time consuming.

The specimens' width and thickness were measured using a 5 mm (0.19685 in) nominal diameter double-ball-interface micrometer at three random locations along the specimen gage length which was 4.75 mm (0.188 in). The measurements were recorded and the average area was later used in the computation of the compression properties of the material.

A 3-D DIC system was used to measure the strain on the specimen surface as the load was applied. Similar to the previous compression test, in accordance to ASTM D6641, the cameras of the DIC system were able to view the specimen edge due to the design of the fixture used to hold the specimen

during loading. Therefore, a speckle pattern was applied on one edge of the specimen.

2.4.8. Test Setup

The specimen was installed in a test fixture that was supplied by Wyoming Test Fixtures Inc. The test fixture was made of two parallel V-grooved plates. The plates supported the specimen with little friction due to the grooves. The specimen was supported in such a way to resist buckling when the specimen was end loaded in a vertical plane (SACMA SRM 1R-94, 1994). The SACMA standard recommended mounting the specimen in the fixture by torquing the bolts to 0.7 – 0.1 N-m (6 – 10 in-lb), but the bolts were fixed by finger tight torquing which was in accordance with the ASTM D695 standard (ASTM D695, 1996). A disassembled fixture and a fixture with a specimen installed are pictured in Figure 2.21.

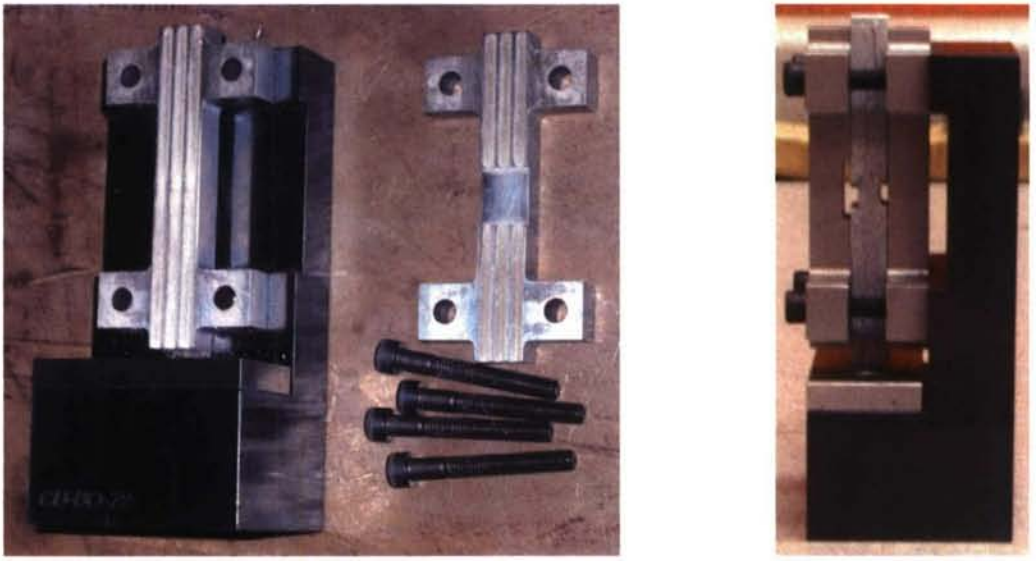

Figure 2.21: SACMA SRM R1 Fixture

The fixture was then placed in the testing machine such that the speckled edge was facing the DIC system cameras. The cameras were then calibrated to measure strain and displacement in the volume of space that the specimen was being tested.

The testing machine used was a servo hydraulic machine with the capability of controlling the velocity of the moving crosshead. The specifications of the testing machine were in conformance with ASTM Practices E4 (ASTM E4, 2002). The load was applied by the testing machine through a ball bearing used to remove any bending forces on the specimen from imperfections in the frame and fixture. The use of a ball bearing was recommended by ASTM D695. The test fixture with the specimen placed in the testing frame and loaded by the ball bearing with the cameras capturing images is shown in Figure 2.22.

Figure 2.22: Testing of a SACMA SRM 1R Specimen

The test was conducted at a compressive load rate of 0.6 mm/min (0.0236 in/min) to failure of the specimen. Each test lasted between approximately two minutes and three minutes. During the loading process, the data was collected at a rate of approximately 1 hertz. Every data point collected included the load and the full-field strains on the specimen edge in the gage length as seen by the DIC system. A typical full-field strain in the direction of the applied load during testing is shown in Figure 2.23.

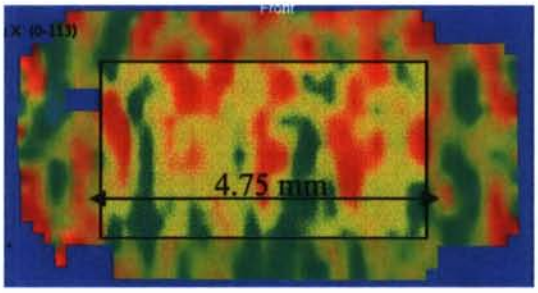

Figure 2.23: Full Field Strain of a SACMA SRM 1R Specimen

A faint rectangle in the foreground is depicted in Figure 2.23. This rectangle represented the area that the full-field strains were exported from the DIC system. The strain in this area was averaged and exported as one data point. The strains exported for each data point were the longitudinal strain, in the direction of the applied load, and the transverse strain, orthogonal to the longitudinal strain and through the specimen thickness.

2.4.9. Stress-Strain Representation

Using the data exported from the DIC system, the measured average area of the specimen and the applied load a stress-strain curve was formed for each specimen. The standard recommended calculating the compressive modulus of elasticity of the material by considering the stress-strain relation in a specific range. In this range, the chord of the curve was recommended to be used as the laminate compressive modulus. The strain range of 25% and 50% of the ultimate strain was recommended to be used.

It was noticed that the stress-strain curves were slightly nonlinear therefore, and more than one linear range was found. A bilinear representation of the stress-strain curve was adopted. The material was then classified to have an initial modulus of elasticity and a final modulus of elasticity.

Then two regions were selected from the stress-strain curve: the first region lay between 5% and 20% of the ultimate strain and the second region lay between 60% and 90% of the ultimate strain. For each region, the least square error approach was used to estimate a linear relation of the data. The slope of the linear function was taken to be the modulus of elasticity. The intersection point of the two linear functions was considered the transition point from the initial region to the final region. The Poisson's ratio was calculated in accordance with ASTM E132. Two Poisson's ratios were found for each stress-strain curve: a Poisson's ratio for the initial region and a Poisson's ratio for the final region. The Poisson's ratio was calculated to be the ratio of the modulus of elasticity calculated using the transverse strain to the modulus of elasticity calculated using the longitudinal strain (ASTM E132, 1997). Note that the transverse strain measured was through the specimen thickness.

A typical stress-strain curve of a compression test and its modeled bilinear curve are shown in Figure 2.24. The values of the initial modulus, final modulus, Poisson's ratio, ultimate point, and transition point are indicated in Figure 2.24.

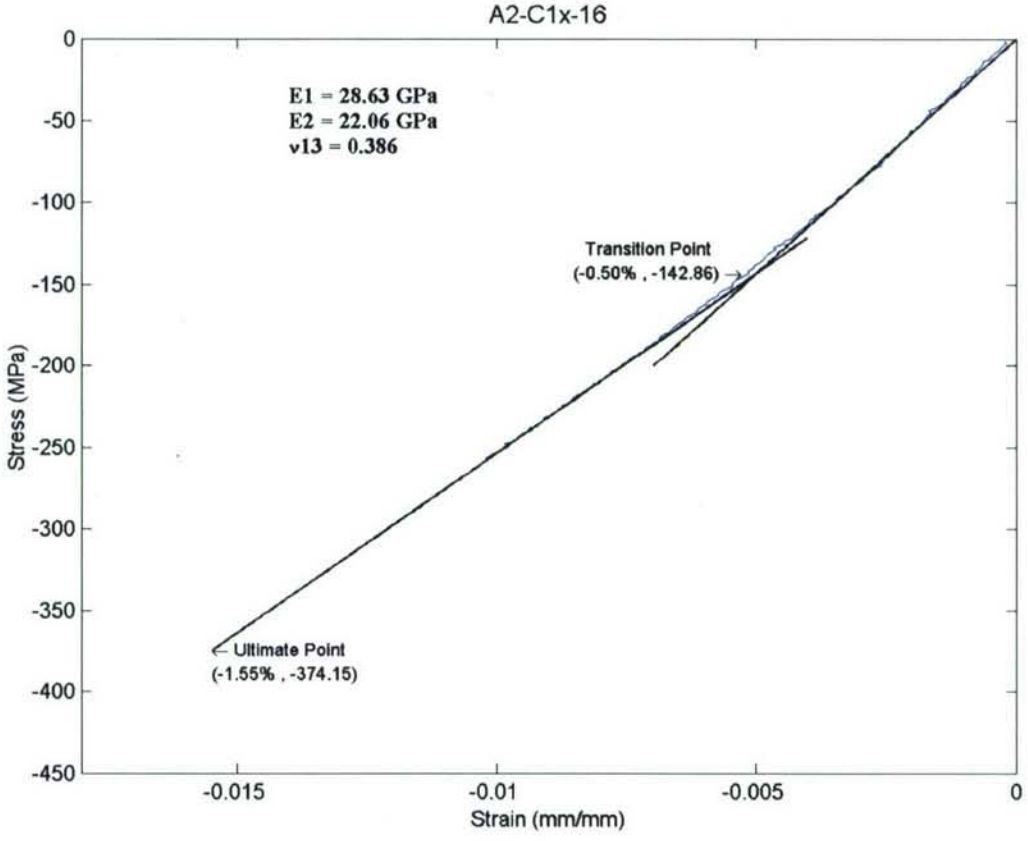

Figure 2.24: Modeled Compression Stress-Strain Curve

2.4.10. Discussion of the Experimental Results

A set of 8 specimens was tested for each direction in each panel. Having a total of 6 witness panels, 12 sets of results were computed. The following charts summarize the experimental results obtained from the compression tests conducted on the panels. Each chart has the mean, standard deviation, and coefficient of variation of the material property of the panels. Two material properties are presented: the initial modulus of elasticity and the ultimate strength. The results of each direction are presented on separate charts. The experimental results of every two witness panels with the same lay-up sequence are presented by two adjacent bars. The results are shown in Figure 2.55 through Figure 2.55 .

Each panel had two orthogonal directions: x-direction and y-direction, where the x-direction is the laminate principal axis.

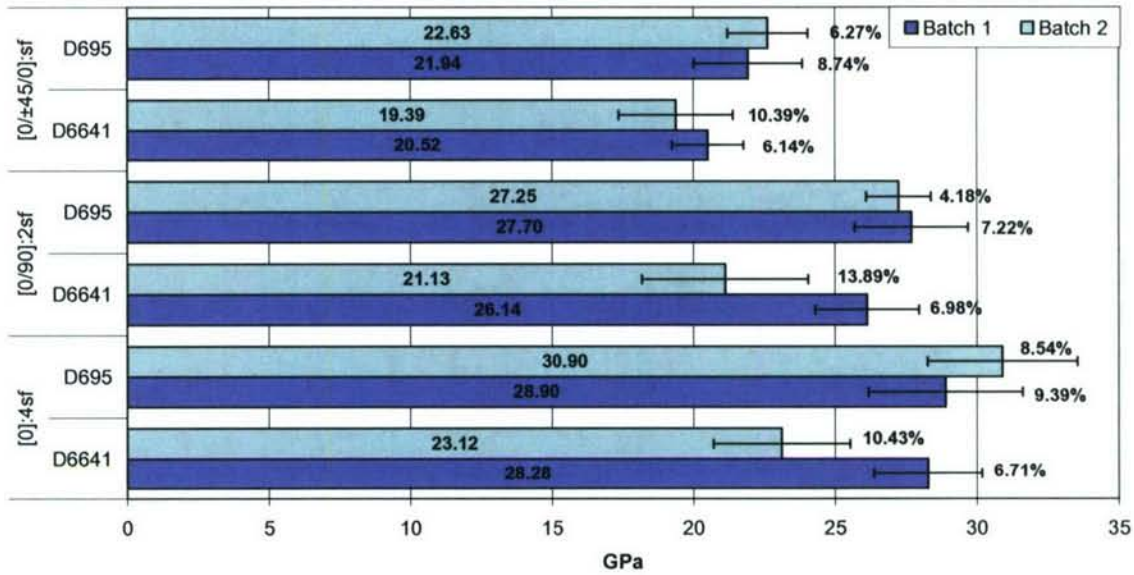

Figure 2.25: Compressive Initial Modulus of Elasticity (x-Direction)

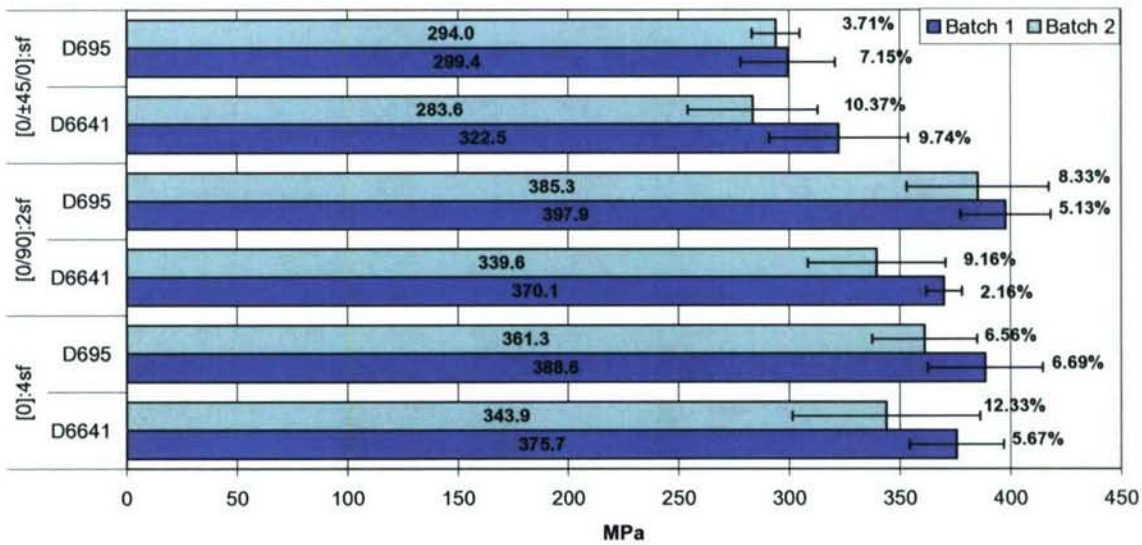

Figure 2.26: Compressive Ultimate Strength (x-Direction)

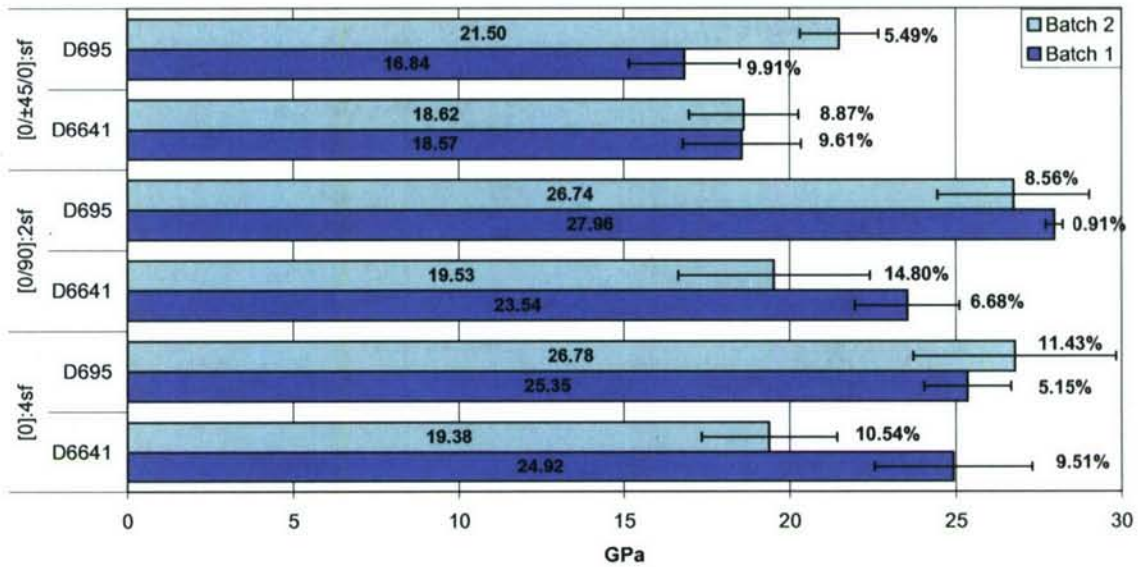

Figure 2.27: Compressive Initial Modulus of Elasticity (y-Direction)

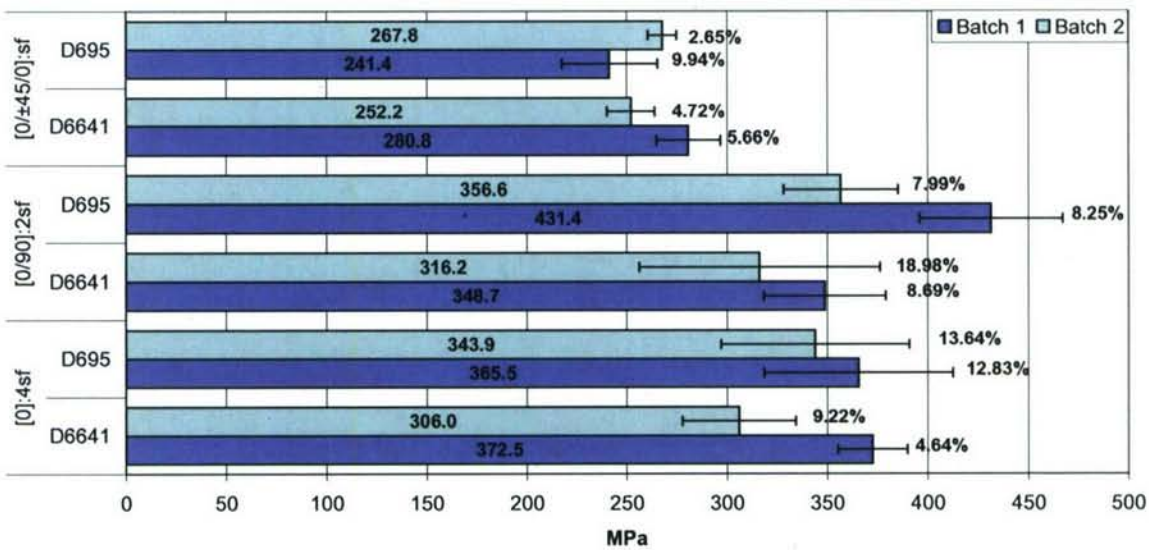

Figure 2.28: Compressive Ultimate Strength (y-Direction)

Additional analysis of the experimental results was done by normalizing the results to one thickness as part of reducing the variability caused by the thickness variation through the panel. The normalization process, normalized results and compression test method comparison are presented in section 2.4.

2.4.11. Conclusion

One of the common disadvantages for both of the test methods was the strain field viewed by the DIC cameras. As mentioned in the test setup of each test method, the cameras were able to view the edge of the specimen due to the configuration of the fixtures. Therefore, the full-field strain captured by the DIC system was through the specimen thickness and the area of the strain was confined to 5.08 mm by the specimen width and to the length of the specimen gage section. In addition, when exporting the strains from the DIC system, the areas selected did not include the whole area of the strain field. As a result, the area used to compute the material compression properties did not have a sufficient representation of the material under study.

The DIC system captured strain concentrations in the specimens of both test methods. These strain concentrations can be translated to stress concentrations. The stress concentration in a D6641 specimen is depicted in Figure 2.29, and the stress concentration in a SRM 1R specimen is depicted in Figure 2.30.

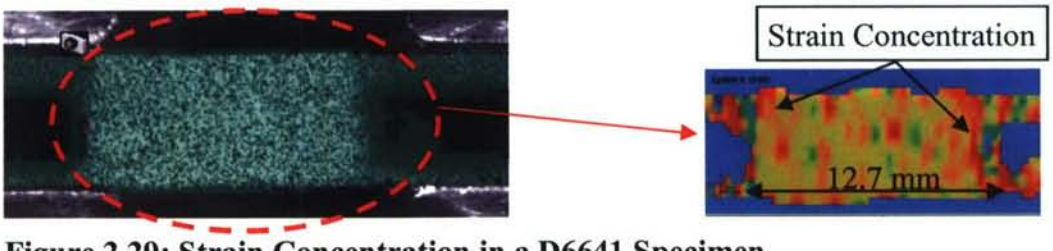

Figure 2.29: Strain Concentration in a D6641 Specimen

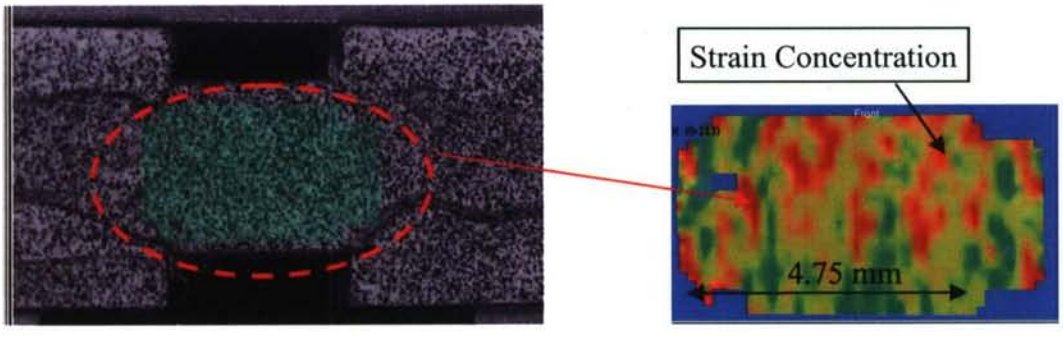

Figure 2.30: Strain Concentration in a SACMA SRM 1R Specimen

The strain concentrations are justified by the small length of the gage sections. The gage length of the D6641 specimen was 12.7 mm (0.5 in) and the gage length of the SRM 1R specimen was 4.75mm (0.188 in) due to the woven fabric used in this study.

The tow pattern of the fabric repeated every 12.7 mm (0.5 in) in the warp direction and every 10.16 mm (0.4 in) in the fill direction. Therefore, with a gage length of 12.7 mm (0.5 in), for the D6641 specimen, the gage section

contained approximately 2 or 2½ tows and in some cases the tow was under the clamping edge of the specimen, barely covering one weave pattern. The strain concentrations of the SRM 1R specimens were greater than the D6641 specimens. Since the gage length of that specimen was 4.75mm (0.188 in), the gage length contained approximately one tow or part of a tow and in some cases it contained a gap between two tows. Such small gage lengths did not properly represent the composite under study. Consequently, the small gage section could have prevented the specimen from failing properly, especially with such a small number of tows in the gage section. These failure mechanisms may over estimate the ultimate strength.

Since the SRM 1R specimen was very time consuming to prepare prior to testing, a modification for the D6641 specimen was recommended. In addition, since the fixture of the SACMA SRM 1R test method did not allow for the possibility of increasing the length of the specimen, the D6641 test method was selected for modification.

2.4.12. Modifications Recommended for the ASTM D6641 Test Method

One of the major limitations in both the test methods conducted was the specimen surface that the DIC cameras were unable to view. In both tests, the cameras viewed the specimen edge, which was relatively small compared with woven fabric reinforcement. Therefore, in the modified test method of ASTM D6641, the cameras were placed in such a way to view the front specimen surface.

The specimen width was increased from 19.05 mm (0.75 in) to 25.4 mm (1 in) to increase the area viewed by the DIC cameras and to include more of the fabric weave pattern. The increased width was the maximum possible width that can be incorporated in the D6641 CLC fixture. Increasing the specimen width enables us to increase the gage length. Increasing the gage length was desired to increase the volume of material in the gage section better representing the material under study. A proper representation of the PMC with woven fabric reinforcement is to include at lease three weave patterns in the gage section; the edge patterns are affected by the boundary conditions, thus, leaving the middle pattern unaffected by outside conditions. In order to increase the gage length, an Euler buckling check was conducted on the proposed specimen geometry for all three fiber lay-ups to prevent buckling-induced failure in the specimen while testing. Two equations were used to check for buckling (Adams and Lewis, 1990). One equation governed by the material ultimate stress is shown in equation (2.3). Another equation governed by the material ultimate strain is shown in equation (2.4).

$$L_g = t \cdot \sqrt{\left(\frac{E_{11}}{F_{1C}} - 1.2\frac{E_{11}}{G_{13}}\right) \cdot \frac{\pi^2}{12 \cdot K^2}} \tag{2.3}$$

where:

L_g = length of gage section, mm (in),

t = specimen thickness, mm (in),

E_{11} = compressive modulus of elasticity, MPa (psi),

F_{1C} = ultimate compressive strength, MPa (psi),

G_{13} = inter-laminar shear modulus, MPa (psi),

K = constant depending on the degree of constraint of the column

K = 1 when the column ends are pinned (free to rotate)

K = ½ when the column ends are clamped (restrained against rotation)

$$L_g = t \cdot \sqrt{\left(\frac{1}{\varepsilon_{1C}} - 1.2\frac{E_{11}}{G_{13}}\right) \cdot \frac{\pi^2}{12 \cdot K^2}} \tag{2.4}$$

where:

L_g = length of gage section, mm (in),

t = specimen thickness, mm (in),

E_{11} = compressive modulus of elasticity, MPa (psi),

ε_{1C} = ultimate compressive strain, mm/mm (in/in),

G_{13} = inter-laminar shear modulus, MPa (psi),

K = constant depending on the degree of constraint of the column

K = 1 when the column ends are pinned (free to rotate)

K = ½ when the column ends are clamped (restrained against rotation)

Using equation (2.3), equation (2.4), and the material properties obtained previously from the testing program, the gage lengths were calculated for each fiber lay-up. Two assumptions were made for calculating the gage lengths. The interlaminar shear modulus, G_{13}, was assumed to be equal to the in-plane shear modulus, G_{12}. This assumption was made since the interlaminar shear modulus of the material under study was not available; and assuming the latter equal to the in-plane shear modulus gave conservative results for the gage section length. In addition, the column constraints were assumed to be pinned. Such an assumption was also conservative and gave smaller values of the gage length than assuming the ends of the column clamped. The calculated lengths for the different fiber lay-ups and direction of loadings are presented in Table 2.1.

Table 2.1: Length of Gage Section of Modified D6641 Specimen

Fiber Lay-up	$[(0_w/90_f)]_{4s}$		$[(0_w/90_f)/(0_f/90_w)]_{2s}$		$[(0_w/90_f)/\pm(45_w/-45_f)/(0_w/90_f)]_s$	
Direction of Loading	x-Direction	y-Direction	x-Direction	y-Direction	x-Direction	y-Direction
Gage Length (Ultimate Stress)	36.182 mm (1.424 in)	35.292 mm (1.389 in)	34.828 mm (1.371 in)	34.806 mm (1.370 in)	37.276 mm (1.468 in)	38.857 mm (1.530 in)
Gage Length (Ultimate Strain)	34.936 mm (1.375 in)	34.094 mm (1.342 in)	33.455 mm (1.317 in)	34.006 mm (1.339 in)	35.162 mm (1.384 in)	35.899 mm (1.413 in)

Since the two assumptions used for the calculation of the gage section length were conservative, the latter was chosen to be 30.48 mm (1.2 in).

Therefore, the modification to the ASTM D6641 specimen was increasing the gage section length from 12.7 mm (0.5 in) to 30.48 mm (1.2 in) and the gage section width from 19.05 mm (0.75 in) to 25.4 mm (1 in), thus incorporating as much of fabric weave patterns as possible. The modified D6641 specimen configuration is depicted in Figure 2.31.

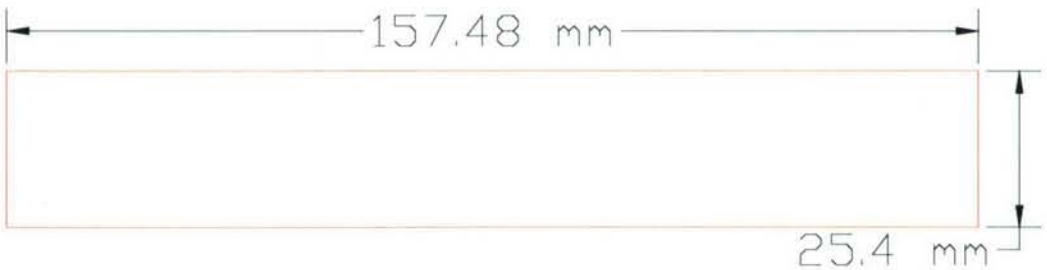

Figure 2.31: Modified D6641 Specimen Configuration

2.4.13. Discussion of the Experimental Results of the Recommended Modifications

The test was conducted similar to the ASTM D6641 test method earlier, except that the DIC cameras were facing the specimen front face as discussed in the previous section. The test was conducted on only one panel in two directions. The panel was from fabrication batch 1 and had $[0]_{4sf}$ for the fiber lay-up sequence.

A comparison of the experimental results between the specimens tested in accordance with ASTM D6641, and the modified specimens of the same test method is shown in Figure 2.32 and Figure 2.33. The charts compare the initial modulus of elasticity and ultimate strength of the two tests and present the means and coefficient of variations. In addition, the standard deviation error bars are depicted in the charts.

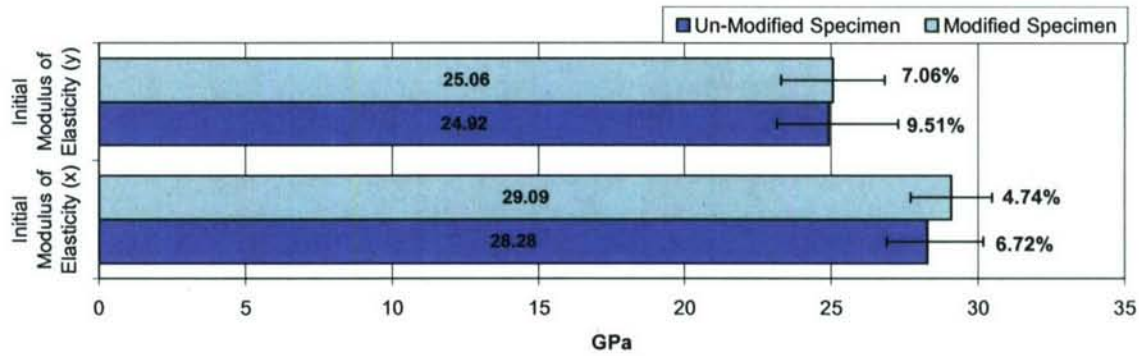

Figure 2.32: Comparison of Results for Modified and Un-Modified Specimens of ASTM D6641 (I-MOE)

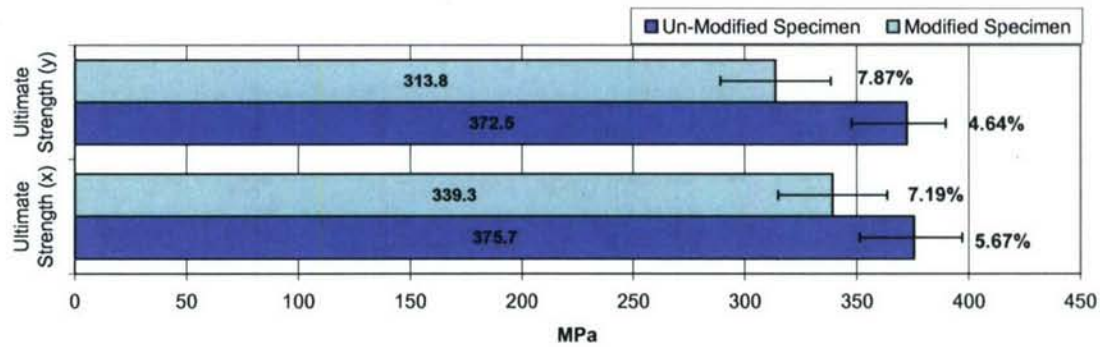

Figure 2.33: Comparison of Results for Modified and Un-Modified Specimens of ASTM D6641 (U. Strength)

As observed in the charts, the coefficient of variation has improved in the calculated results of the initial modulus of elasticity when testing the modified specimen. The improvements in the results of the initial modulus of elasticity were attributed to the change in the surface viewed by the DIC cameras. Instead of viewing the edge of the specimen, the cameras viewed the front surface of the specimen which was larger and better represents the material.

Conversely, the coefficient of variation of the ultimate strength did not improve. This can be explained by the fact that the fixture was constraining the specimen from failing normally; the fixture introduced more consistency in the ultimate strength calculated compared to having the specimen failing normally. In addition, the ultimate strength calculated for the modified specimen had lower values than the unmodified specimen. Similarly, this can be explained by the constraint the fixture introduced on the gage delaying the failure of the specimen and causing the over estimation of the ultimate strength of the material.

The modifications recommended for the compression test improved the experimental results. With the help of the DIC system these recommendation

were suggested and proven to enhance the testing method for obtaining the compressive material properties of PMC with woven fabric reinforcement. Further testing can be conducted on other lay-ups to prove the validity of the recommendations based on these lay-ups.

2.5. Tensile Testing

2.5.1. Introduction

Two tension test methods were selected for characterizing polymer matrix composites (PMC) with woven fabric reinforcement. The first test was in accordance with ASTM D3039 and is under the jurisdiction of ASTM Committee D30 on Composite Materials (ASTM D3039/D3039M, 2000); while the second test was in accordance with ASTM D638 and is under the jurisdiction of ASTM Committee D20 on Plastics (ASTM D638, 2002). The test method of the D638 standard noted that for tensile properties of resin-matrix composites reinforced with fibers of modulus greater than 20 GPa (3 x 10^6 psi) tests should be in accordance with ASTM D3039. Although the reinforcing fiber used is of modulus greater than 20 GPa (3 x 10^6 psi), the literature showed the reliability of conducting tests in accordance with ASTM D638 for such reinforcing fibers. Therefore, both tests were selected for characterizing the PMC with woven fabric reinforcement.

Each test is explained separately and any deviation from the standard is stated. In addition, the section describes the method used to cut the samples from the panels, the dimensions of the samples, and the preparation of the samples for testing. The test setup, experimental methods and instrumentation systems are briefly presented, and the different issues that arose during the experimental program discussed. The methods for synthesizing and analyzing the experimental results are explained and the findings are summarized.

The advantages and disadvantages of each test method are described and compared with recommendations from the literature. Statistical analysis of the results is presented and a set of recommendations and conclusions are provided in the section. A modified tension test method for PMC with woven fabric reinforcement, which combines the benefits of both test methods evaluated, is proposed to obtain better in-plane tensile properties of marine-grade composites.

2.5.2. Background

A number of issues have been addressed to obtain repeatable and reliable tensile properties of fiber-reinforced composites. Among these issues were the preparation of the specimen, the fiber architecture adopted in the composite, and the tabbing procedure needed for some specimens.

A study showed that the edge effects in angle ply composites greatly reduces the stiffness property of the material (Piggott and Wang, 1999). Based on this study, for improved results of modulus of elasticity, the width to length ratio should be about two. In addition, it was shown that the standard test method D3039 was not capable of giving reliable moduli except for [0/90] combinations and the modulus should be calculated from the initial slope of the stress-strain curve of the material rather than from the slope of the curve

between one quarter and one half of the ultimate strain, as recommended by that standard.

The ASTM D3039 standard test method suggests the use of tabs for gripping highly orthotropic composites to reduce stress concentration around the gripping area and induce acceptable failure in the gage area (ASTM D3039/D3039M, 2000). It was reported that this test has a better performance for cross-ply specimens, since they are less sensitive to imperfection, than for unidirectional specimens (Chaterjee, Adams et al., 1993). Additionally, the report discussed the tensile test in accordance with ASTM D638, Type I, and concluded that stresses peak in the transition region. Furthermore, the report stated that this test cannot be used for unidirectional composites due to failure in the transition region; however, it is more adequate for cross-ply reinforcement.

A detailed study on tabbing specifications of ASTM D3039 tensile specimen was conducted (Adams and Adams, 2002). This study stated that the tabs themselves can result in stress concentrations, particularly at tab terminations adjacent to the specimen gage section. More recently, a finite element analysis of the tensile test in accordance with ASTM D3039 with tabs tapered at an angle of 7^{o} showed that stress concentration is present in the region close to the termination of the tab. The ratio of the stress in the tab termination region to the stress in the gage area was found to be approximately 1.03 (Fayad, 2005).

The study presented in this work implements the new technology of digital imaging correlation and explains the different issues indicated previously for tension tests: stress concentration around the tab termination zone and stress concentration in the transition region in the dumbbell shaped specimen. Based on the experimental findings, a specimen configuration is proposed for enhanced experimental characterization of tensile properties of PMC with woven roving reinforcement. Three different fiber lay-up sequences, which are representative of marine-grade composites, were selected for this study: $[0]_{4sf}$, $[0/90]_{2sf}$, and $[0/\pm45/0]_{sf}$. The angle orientation of each layer indicates the angle between the warp direction of the weave and the reference axis, which was the laminate principal axis. The experimental results of the tension test for the different lay-up sequences were analyzed to determine if reliable and repeatable in-plane tensile properties were obtained.

2.5.3. ASTM D3039 Tension Test

The ASTM D3039 standard test method was devised for determining the in-plane tensile properties of polymer matrix composite (PMC) materials reinforced by high-modulus fibers (ASTM D3039/D3039M, 2000). The standard recommends the specimen configuration, the apparatuses needed to measure the width and thickness of the specimen, the testing fixture needed to conduct the test, and the desired strain measuring device. The following sections explain the specimen configuration, the preparation of the specimen

and the different apparatuses used to conduct the test. Any deviation from the standard is noted and explained.

2.5.4. Specimen Preparation

Referring to the standard, at least 5 specimens should be tested per testing condition. To account for specimen data that may be lost during the testing process or data analysis, 8 specimens for each direction were tested. Each panel had two orthogonal directions: x-direction and y-direction, where the x-direction was the laminate principal axis. The specimens were cut from the panels with a water-abrasive jet.

The length and width of the specimens were in accordance with Table 1 and Table 2 of the ASTM Standard D3039. The dimensions were 254 mm (10 in) by 25.4 mm (1 in). The witness panels were manufactured with 8 layers of fabric having a total thickness of approximately 5.08 mm (0.2 in), which exceeded the recommended thickness in Table 2 of the standard but abides to the requirements of Table 1 of the standard (ASTM D3039/D3039M, 2000). The surface of the panel that was not on the mold was wavy with a thickness tolerance of approximately 14%. The thickness tolerance of the specimens did not meet the requirements of the standard. The specimen dimensions are shown in a 2D-ACAD drawing in Figure 2.34.

Figure 2.34: D3039 Specimen Configuration

The specimens were conditioned in accordance with procedure C of test method D5229 (ASTM D5229/D5229M, 2002). The specimens were stored in a conditioning chamber for 3 months at a temperature of 22 ± 3°C (71.6 ± 5°F) and 50 ± 3% relative humidity. While testing the specimens, the testing room was climate controlled at room temperature (22 ± 3°C) and relative humidity of 50 ± 3%.

Although the standard states that testing multidirectional laminates can be successfully tested without tabs, the specimens in this study were tabbed since the findings in the literature recommended the use of tabs in multidirectional laminates. A set of specimens that were similar to the panels under study, were tested without tabs and a high percentage of grip failure was noticed, which reinforced the idea of tabbing the specimens under consideration in this project. The tabbing material used was a cross-ply E-glass/Epoxy composite known as G11 and used mainly for electric circuit boards. The tabs had a length of 38.1 mm (1.5 in) and the same width of the specimen with a taper

angle of 7° and a thickness of 1.575 mm (0.062 in). The tabs' material and dimensions agreed with the recommendations of the standard.

To improve the bond of the tab to the specimen, an 80 grit sandpaper was used to roughen the surface where the tabs were to bonded, and a degreaser was used to remove any residue of mold release from panel manufacturing and any dust particles. The tabs were bonded to the specimen with a structural adhesive, Plio-Grip 7770. The adhesive was mixed and applied in a climate controlled room with a temperature of 20°C and relative humidity of 50% to insure curing of the adhesive. The tabs were clamped and left overnight at the same temperature and relative humidity to cure. A tabbed D3039 tensile specimen is shown in Figure 2.35.

Figure 2.35: Tabbed D3039 Specimen

As recommended in the standard, the specimen thickness and width were measured with a 5 mm (0.19685 in) nominal diameter double-ball-interface micrometer at three random locations along the length of the specimen in the area of interest which had a length of 177.8 mm (7 in). The measurements were recorded and the average area was later used in the computation of the tensile properties of the material.

The use of a strain transducer or an extensometer was recommended by the standard to measure the strain of the specimen while loading. However, a 3-D digital image correlation (DIC) system was used to measure the strains in this study.

2.5.5. Test Setup

The two cameras of the DIC system were set in front of the specimen with the speckled pattern facing the cameras. The specimen was gripped in load heads that were rotationally self-aligning. The testing equipment was a hydraulic machine with the capability of controlling the velocity of the moving crosshead. The specifications of the testing machine were in conformance with ASTM Practices E4 (ASTM E4, 2002).

The test was conducted with a constant head speed of 1.8 mm/min (0.071 in/min) and each test elapsed between approximately two and a half minutes and three minutes. The load and strain data were collected at a rate of approximately 1 hertz. The strain data collected was a full-field strain of the area of interest of the specimen. A typical full-field strain captured by the DIC system of a D3039 tensile specimen is depicted in Figure 2.36.

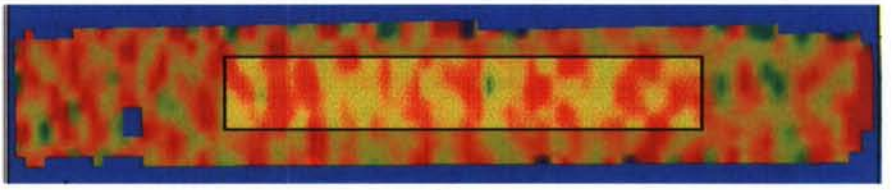

Figure 2.36: Full-Field Strain of a D3039 Specimen

An area in the middle of the specimen was used to extract the strains from the full-field strain. This area represented the gage area which is shown as a faint rectangle in the foreground in Figure 2.36. The average longitudinal and transverse strains were computed from the full-field strain in the gage area.

2.5.6. ASTM D638 Tension Test

The ASTM D638 standard test method was devised for determining the in-plane tensile properties of unreinforced and reinforced plastics in the form of standard dumbbell-shaped test specimens (ASTM D638, 2002). The standard recommends the specimen configuration, the apparatuses needed to measure the specimen width and thickness, the testing fixture needed to conduct the test, and the desired strain measuring device. The following sections explain the specimen configuration, the specimen preparation and the equipment used to conduct the test. Any deviation from the standard is noted and explained.

2.5.7. Specimen Preparation

Referring to the standard, at least 5 specimens should be tested per testing condition. To account for specimen data that may be lost during the testing process or data analysis, 8 specimens for each direction were tested. Each panel had two orthogonal directions: x-direction and y-direction, where the x-direction is the laminate principal axis. The specimens were cut from the panels with a water-abrasive jet.

The dimensions of the specimens were in accordance with Type I shown in Figure 2.37 of ASTM Standard D638. The dimensions were 165.1 mm (6.5 in) for the overall length, 19.05 mm (0.75 in) for the overall width, 57.15 mm (2.25 in) for the length of the narrow section, 12.7 mm (0.5 in) for the width of the narrow section, and 76.2 mm (3 in) for the radius of the fillet. The witness panels were manufactured with 8 layers of fabric resulting in a total thickness of approximately 5.08 mm (0.2 in), which met the recommended thickness in Figure 2.37 of the standard (ASTM D638, 2002). The surface of the panel that was not on the mold was wavy with a thickness tolerance of approximately 14%. The thickness tolerance of the specimens did not meet the requirements of the standard which was ±4% of the thickness. The specimen dimensions are shown in a 2D-ACAD drawing in Figure 2.55 .

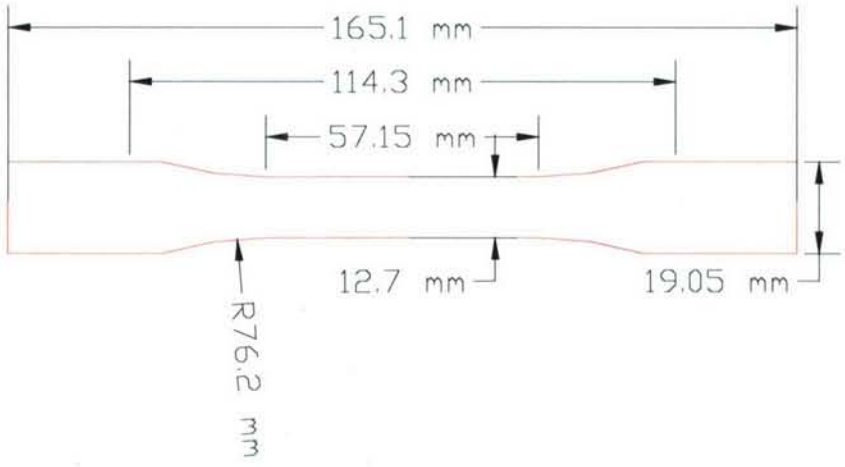

Figure 2.37: D638 Specimen Configuration

The specimens were conditioned in accordance with procedure C of test method D5229 (ASTM D5229/D5229M, 2002). The specimens were stored in a conditioning chamber for 3 months at a temperature of 22 ± 3°C (71.6 ± 5°F) and 50 ± 3% relative humidity. While testing the specimens, the testing room was climate controlled at room temperature (22 ± 3°C) and relative humidity of 50 ± 3%.

As recommended in the standard, the specimen thickness and width were measured with a 5 mm (0.19685 in) nominal diameter double-ball-interface micrometer at three random locations along the length of the specimen in the area of interest which had a length of 57.15 mm (2.25 in). The measurements were recorded and the average area was later used in the computation of the material tensile properties.

A strain transducer or an extensometer was recommended to measure the strain of the specimen while loading, but, a 3-D DIC system was used to measure the strains in this study.

2.5.8. Test Setup

The two cameras of the DIC system were set in front of the specimen with the speckled pattern facing the cameras. The specimen was gripped in the testing machine with a distance of 114.3 mm (4.5 in) between the grips and the grip heads were rotationally self-aligning. The testing machine was a servo-controlled hydraulic machine with the capability of controlling the velocity of the moving crosshead. The specifications of the testing machine were in conformance with ASTM Practices E4 (ASTM E4, 2002).

The test was conducted with a constant head speed of 1.2 mm/min (0.047 in/min) and each test elapsed between approximately two and a half minutes and three minutes. The load and strain data were collected at a rate of approximately 1 hertz. The strain data collected was a full-field strain of the

area of interest of the specimen. A typical full-field strain in the direction of the applied load captured by the DIC system of a D638 tensile specimen is depicted in Figure 2.38.

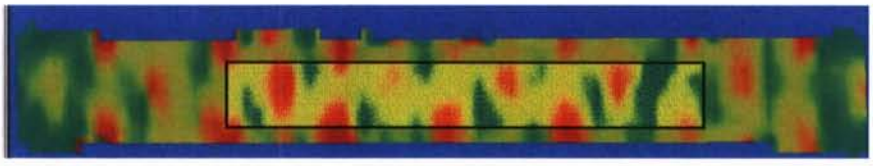

Figure 2.38: Full-Field Strain of a D638 Specimen

An area in the middle of the specimen was used to extract the strains from the full-field strain. This area represented the gage area which is shown as a faint rectangle in the foreground in Figure 2.38. The average longitudinal and transverse strains were computed from the full-field strain in the gage area.

2.5.9. Stress-Strain Representation

Using the data exported from the DIC system, measured average area of the specimen load, a stress-strain curve was formed for each specimen. Different methods for calculating the modulus of elasticity of a material from the stress-strain curve are described in ASTM E111 standard test method for Young's modulus, tangent modulus, and chord modulus. Young's modulus is a material property useful in design and is calculated for materials that follow a linear elastic stress-strain behavior. The tangent or chord modulus is calculated for materials that follow a nonlinear elastic stress-strain behavior and is useful to estimate the behavior of the material for a specified range of stress (ASTM E111, 1997). The stress-strain curves were slightly nonlinear for the tensile specimens. Therefore, a bilinear representation of the stress-strain curve was adopted. The material was then classified to have an initial modulus of elasticity and a final modulus of elasticity.

Two regions were selected from the curve: the first region lay between 5% and 20% of the ultimate strain and the second region lay between 60% and 90% of the ultimate strain. For each region, the least square error approach was used to estimate a linear relation of the data. The slope of the linear function was taken to be the modulus of elasticity. The intersection point of the two linear functions was taken to be the transition point from the initial region to the final region. The stress-strain curve representation and the two regions modeled are shown in Figure 2.39

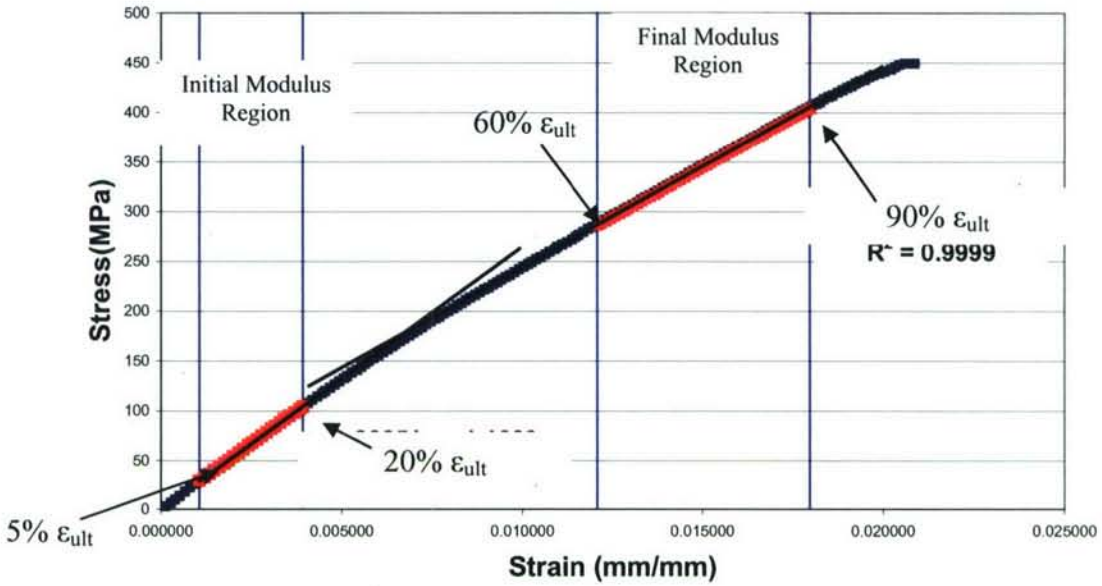

Figure 2.39: Initial and Final Regions in the Stress-Strain Curve

A typical stress-strain curve of a tensile test and its modeled bilinear curve are shown in Figure 2.40. The values of the initial modulus, final modulus, Poisson's ratio, ultimate point, and transition point are indicated in the figure.

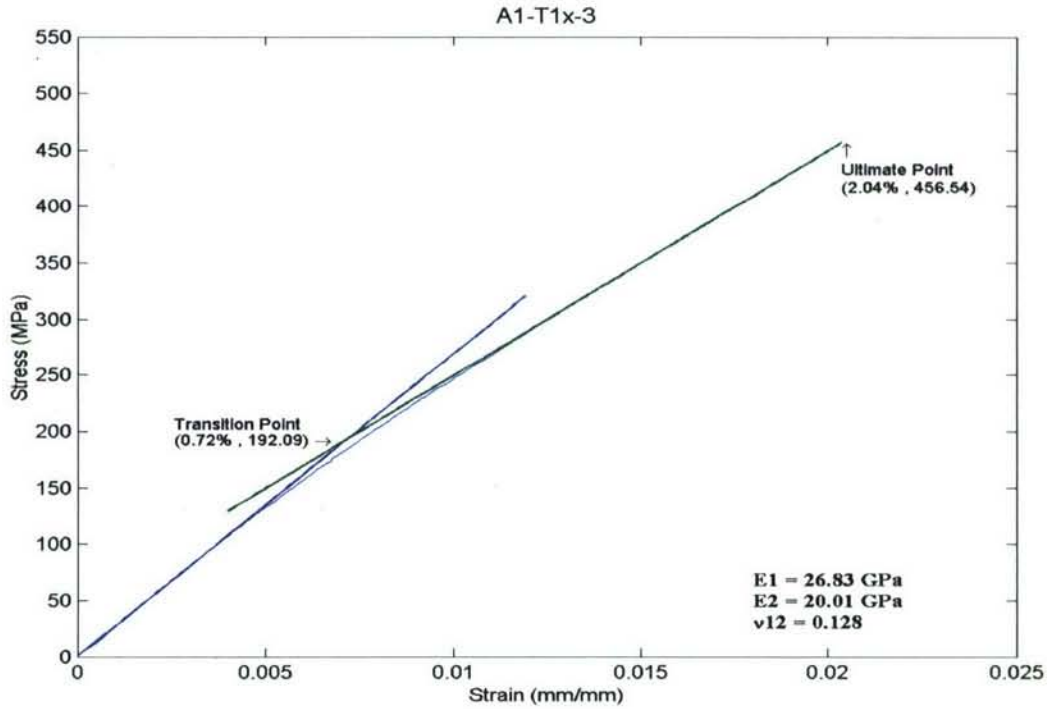

Figure 2.40: Modeled Tensile Stress-Strain Curve

2.5.10. Discussion of Results

A set of 8 specimens was tested for each direction in each panel. Having a total of 6 witness panels, 12 sets of results were computed. The following charts summarize the experimental results obtained from the tension tests conducted on the panels. Each chart has the mean, standard deviation, and coefficient of variation of the material property of the panels. Two material properties are presented: the initial modulus of elasticity and the ultimate strength. The results of each direction are presented on separate charts, Figure 2.55 through Figure 2.55 . The experimental results of the two witness panels with the same lay-up sequence from each batch are represented by two adjacent bars. Each panel had two orthogonal directions: x-direction and y-direction, where the x-direction is the laminate principal axis.

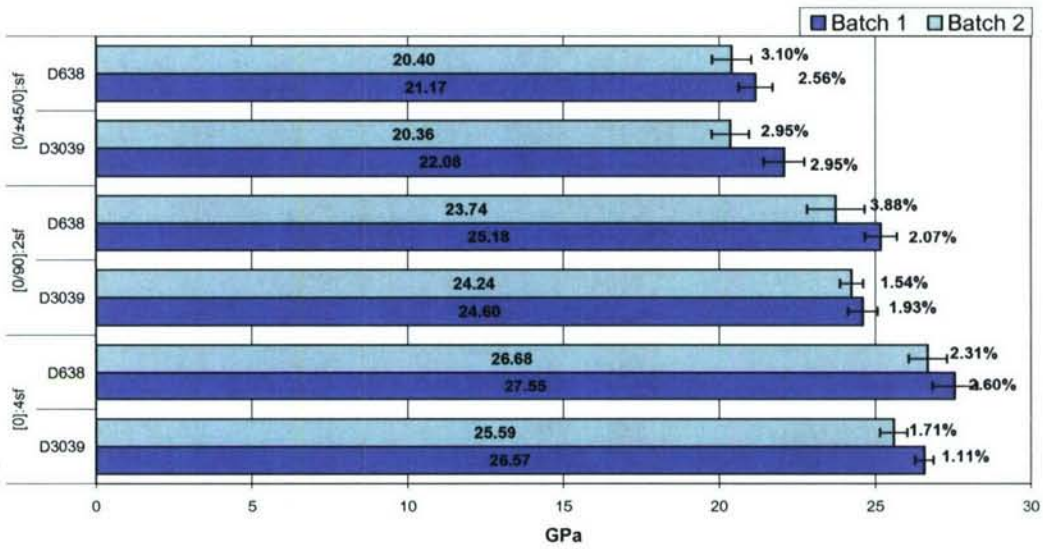

Figure 2.41: Tensile Initial Modulus of Elasticity (x-direction)

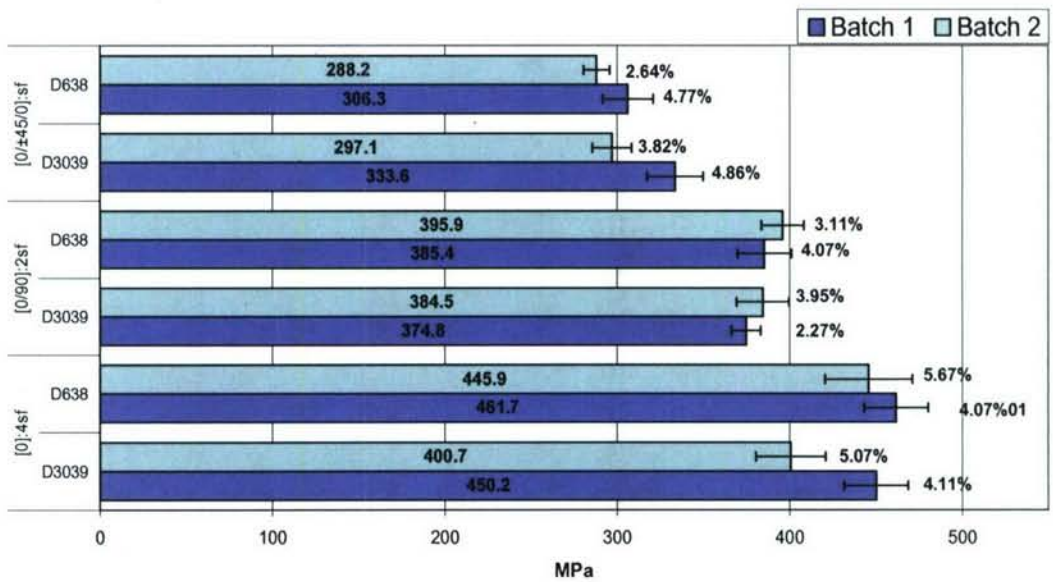

Figure 2.42: Tensile Ultimate Strength (x-direction)

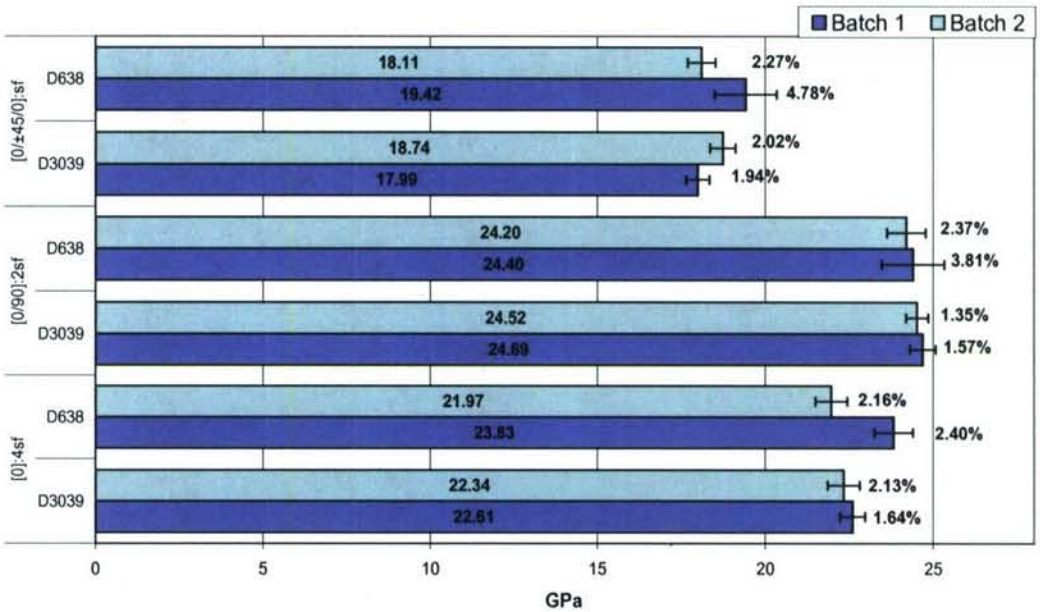

Figure 2.43: Tensile Initial Modulus of Elasticity (y-direction)

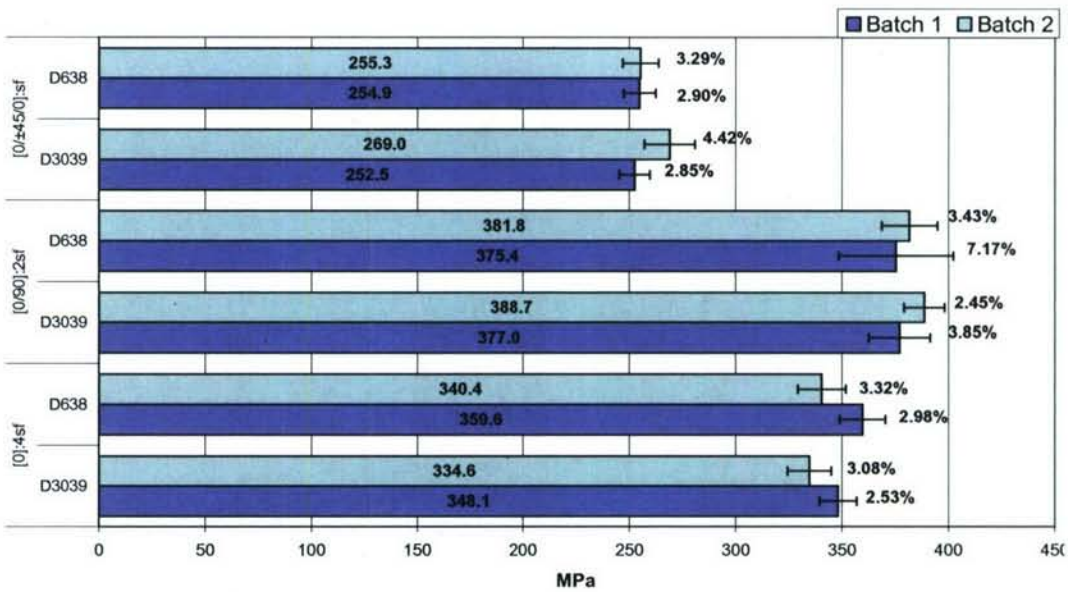

Figure 2.44: Tensile Ultimate Strength (y-direction)

Additional analysis of the experimental results was carried on by normalizing the results to one thickness as part of reducing the variability caused by the thickness variation through the panel. The normalization process, normalized results and compression test method comparison are presented in section 2.4

2.5.11. Conclusion

While testing the D3039 specimens, failure near the tabs was observed. The tabs were intended to force failure in the gage area but were not effective. The high percentage of failure around the tab region (at least 5 out of 8 specimens) can be justified by the peaking of stresses near the termination of the tab as mentioned in the previous sections. Note that the stress concentrations were not captured by the DIC system but were observed in the failure mode.

The test machine has rotational self-aligning gripping heads providing the specimen has sufficient torsional stiffness to activate the mechanism. Looking at the out-of-plane displacement field of the D638 specimens, it was observed that the specimen remained twisted after the load was applied. The specimen width and material stiffness did not provide enough torsional stiffness to induce the self-aligning mechanism of the gripping heads. The twist in the specimen was depicted in the stress-strain curve of the specimen as a toe region at the start of the curve. The toe region does not represent a property of the material and is an artifact caused by alignment of the specimen during loading (ASTM D638, 2002). The twist in the specimen affected the calculation of the modulus of elasticity of the specimen. The out-of-plane displacement field of a D638 specimen captured by the DIC system shows the twist of the specimen during testing in Figure 2.45. The D3039 specimens were wide enough to provide enough torsional stiffness for the self-aligning mechanism of the gripping heads. It should be noted that for self-aligning grip heads, the torsional stiffness of the specimen is significant, but when using prealigned grip heads, the torsional stiffness of the specimen is not as significant.

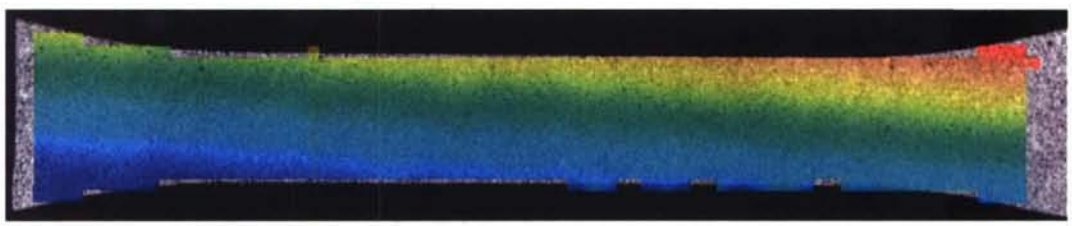

Figure 2.45: Twist captured of a D638 specimen

The D638 tensile specimen was 12.7 mm (0.5 in) wide in the gage area thus including less than two weave patterns when tested in the warp direction and only one weave pattern when tested in the fill direction. It was observed from the full field strains captured by the DIC system that the strain is larger over the tow compared to the strain over the gap between two tows. The pattern of the woven fabric is perceived when looking at the full field strain in Figure 2.38. When the strains in the gage area were averaged and exported, the value was affected by the presence of a tow in the middle of the specimen or a gap between two tows and thus misrepresenting the average strain needed to obtain in-plane tensile properties of the composite under study.

2.5.12. Modifications Recommended for the ASTM D3039 Test Method

Bonding the tabs to the D3039 specimens was time consuming and the tabs appeared to be ineffective in forcing failure into the gage area. However, the width of the specimen was adequate to produce enough torsional stiffness to rotationally align the specimen when loaded. While the dumbbell shape of the D638 specimens forced the failure into the gage area for more than half the specimens, the width caused problems aligning the specimen and including a large enough number of tows needed to properly average the strain in the gage area.

The width of the specimen should be in accordance with the pattern of the fabric used in the composite under study. The fabric is represented properly when 3 tow patterns are included in the gage section; the edge patterns are affected by the free edge boundary conditions, thus, leaving the middle pattern unaffected by outside conditions. The tow pattern of the fabric repeated every 12.7 mm (0.5 in) in the warp direction resulting in a recommended specimen width of 30.48 mm (1.2 in); similarly, the tow pattern of the fabric repeated every 10.16 mm (0.4 in) in the fill direction resulting in a recommended specimen width of 38.1 mm (1.5 in). Due to the limitation of most of the testing frames and their load cell, a specimen width of 30.48 mm (1.2 in) was considered for both directions: warp and fill. In addition, it was considered that the free edge effects of the tensile specimen are not large enough to affect the middle tow pattern of the fabric.

To simplify the specimen preparation by eliminating the tabbing process, a dumbbell shape for the specimen configuration is recommended. A finite element analysis, utilizing an optimized procedure, was used to redefine the specimen configuration. The finite element analysis was conducted using ANSYS, a commercially available finite element software with design optimization. The detailed study is presented in a report by Walls (Walls and Thompson, 2005). The optimized specimen configuration is depicted in Figure 2.46. The main significance of the optimized configuration is the smooth transition from the grip width to the gage width, fillet radius of 365 mm (14.375 in), which caused the specimen to be longer.

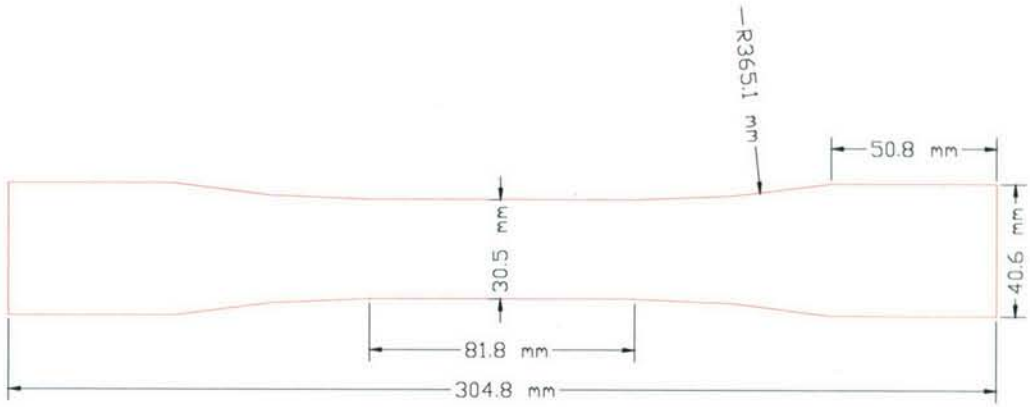

Figure 2.46: FEA Optimized Tensile Specimen

The optimized tensile specimen configuration was cut using the CNC controlled water jet system and tested following the ASTM D3039 test method previously described. The test was conducted on one panel in two directions. The panel was from batch 2 and had $[0]_{4sf}$ for fiber lay-up sequence. The percentage of failure in the gage area ranged between 60% and 50%, with 8 specimens in each direction. The optimized specimen configuration demonstrated a higher percentage of gage failure compared to the rectangular-tabbed ASTM D3039 specimen. The experimental results of the optimized specimens compared with the unmodified specimens, ASTM D3039, are depicted in Figure 2.47 and Figure 2.48. The figures represent the mean value of 8 specimens with the standard error bars and the coefficient of variation.

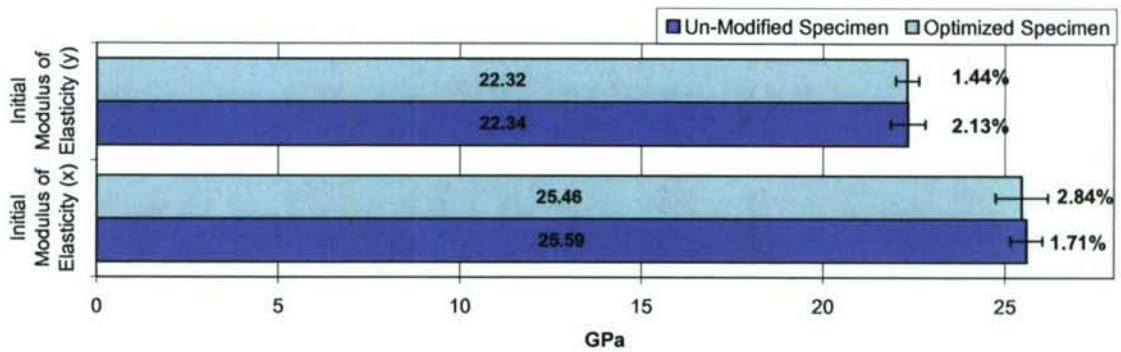

Figure 2.47: Comparison of I-MOE for Optimized and Un-Modified Specimens of ASTM D3039

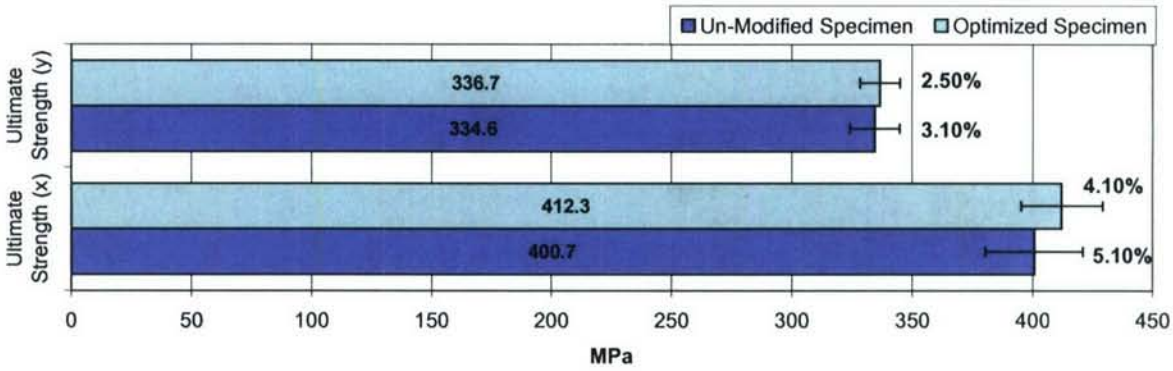

Figure 2.48: Comparison of Ultimate Strength for Optimized and Un-Modified Specimens of ASTM D3039

The results of the optimized specimens showed a high agreement with the rectangular-tabbed specimens. This fact indicated that the ultimate strength was not affected by the failure mode, due to the low factor of stress concentration observed in the tab termination region. From the total of 5 types of specimen configurations tested to calculate the in-plane tensile properties, it was recommended to use the optimized specimen configuration for the material used in the study, marine grade composites with woven fabric reinforcement. The optimized specimen configuration shown in Figure 2.46 gave repeatable test results and the ratio of failure in the gage area observed was larger than all the other types of specimen configurations tested. In addition, the gage area used in the optimized specimen was large enough to cover at least two weave patterns in the y-direction and three weave patterns in the x-direction, thus giving a good representation of the PMC under study. The dumbbell shape used in the optimized specimen configuration promoted the test to be conducted without the use of tabs in the grip area.

2.6. Evaluation of the Experimental Results and Implementation of the Classical Lamination Theory

2.6.1. Introduction

Material properties of composites were obtained from several different standard tests. The tests conducted were tension, compression, and shear. The density and fiber volume fraction of the material was obtained in accordance with ASTM standard methods. The experimental test results were used to obtain the material properties. The criteria for selecting the appropriate material properties for design purposes and comparison is stated. The selected results were then normalized to a nominal thickness value. The method behind the normalization and the selection of the nominal value is discussed. The normalized results were then presented and the different issues related to the inability to normalize some material properties are discussed. Since more than one test was conducted to obtain the same material property, a statistical analysis was used to compare the normalized results from different test methods. The statistical analysis indicated if the results were significantly the same, from the same population, or significantly different. A similar method was used to compare similar material properties obtained from different batches. Using the normalized material properties, design allowable values were derived using the standard deviation of the sample population and its distribution about the mean. The calculation of both A- and B-basis allowables is discussed and the "knockdown" factor for each material property is represented.

As part of utilizing the properties obtained from the coupon testing program, the classical lamination theory (CLT) was used to estimate material property values for different fiber lay-ups: $[0/90]_{2sf}$ and $[0/\pm45/0]_{sf}$; the estimated values were compared to the experimental values. The CLT was implemented starting with lamina material properties obtained from the experimental results conducted on the $[0]_{4sf}$ fiber lay-up panel. The association between the experimental results and the CLT calculated values is stated and discussed.

2.6.2. Background

Developing design allowables for composite materials requires extensive testing to accommodate the orthotropic nature of the material. Therefore, obtaining the design allowables for composites is more complex when compared to metallic materials (Wang, Banbury et al., 1998). Variability of the material properties of composites commonly originate from the nature of the material. To account for this variability, the assignment of the design allowables for the material should acknowledge the variability through the statistical procedure (Tomblin, Ng et al., 2001).

As part of reducing the variability in the experimental results originating from the fiber volume content of the material, the experimental data were normalized to a nominal fiber volume content value (Tomblin, Ng et al., 2001). This process reduced the variability of fiber-dominated properties and was

justified on the basis that most of the load was carried by the fibers, whether under tension or compression.

Design allowables are produced from the statistical distribution of the data. A "knock-down" factor was a calculated and multiplied by the mean of the data to give the design allowable. More data points for a material property result in a higher confidence level in the data, consequently, resulting in a higher, closer to one, "knock-down" factor. One material property might have more than one design allowable. Each design allowable has a different confidence level. Two common confidence levels used in the aerospace industry is the A-basis and the B-basis. The A-basis offers 95% confidence that 99% of the samples will exceed the allowable. The B-basis offers 95% confidence that 90% of the samples will exceed the allowable.

2.6.3. Evaluating the Experimental Results

The material properties of the polymer matrix composite (PMC) reinforced with woven fabric was evaluated by conducting a series of experimental tests in accordance with ASTM standard methods shown in Table 2.3. The tensile properties were calculated by conducting two tests ASTM standard methods: ASTM D3039 and ASTM D638. The compression properties were calculated by conducting two tests, ASTM D6641 and the other SACMA SRM 1R. Only the properties calculated from the experimental results from the ASTM D6641 test were considered, due to concerns with the SACMA SRM 1R test method. As for the shear properties, similarly, two test methods were conducted, ASTM D4255 and ASTM D5379. The shear properties for ASTM D5379 were not considered due to the high variability in the results that were due to non-uniform strain in the region of interest.

Table 2.3: Material Properties Obtained from Standard Test Methods

Test	Coupon	Standards	Properties
Tension (composites)	Tabbed Rectangular	ASTM D3039	E_1, E_2, ν_{12}, F_{1t}, F_{2t}
Tension (plastics)	Dumbbell	ASTM D638	E_1, E_2, ν_{12}, F_{1t}, F_{2t}
Compression (composites)	Rectangular	ASTM D6641	E_1, E_2, ν_{13} (ν_{12}), F_{1c}, F_{2c}
Compression (plastics)	Tabbed Rectangular	SACMA SRM 1R (ASTM D695)	E_1, E_2, ν_{13}, F_{1c}, F_{2c}
Shear (large – composites)	Three-Rail	ASTM D6641	G_{12}, F_6
Shear (small – composites)	V-Notched	ASTM D5379	G_{12}, F_6

2.6.4. Normalizing the Material Properties

Two sets of panels were tested; each set was manufactured at a different time and each is referred to as a different batch. Three fiber lay-up architectures constituted each set of panels: $[0]_{4sf}$, $[0/90]_{2sf}$, and $[0/\pm45/0]_{sf}$ – a total of 8 layers for each lay-up. Due to the fact that each batch was manufactured, infused, at a different time, the physical properties of the batches differed. The difference was mainly in the thickness of the panel and the resin properties. The thickness variation was characterized by either mean thickness variation and/or local thickness variation. The local thickness variation was measured to be approximately 0.48 mm (0.0189 in); while, the total thickness variation was measured to be approximately 0.68 mm (0.0268 in). A surface contour plot presented in Figure 2.49 shows the thickness variation of one of the panels under study; the panels were manufactured with a length of 1.83 m (6 ft) and a width of 1.22 m (4 ft).

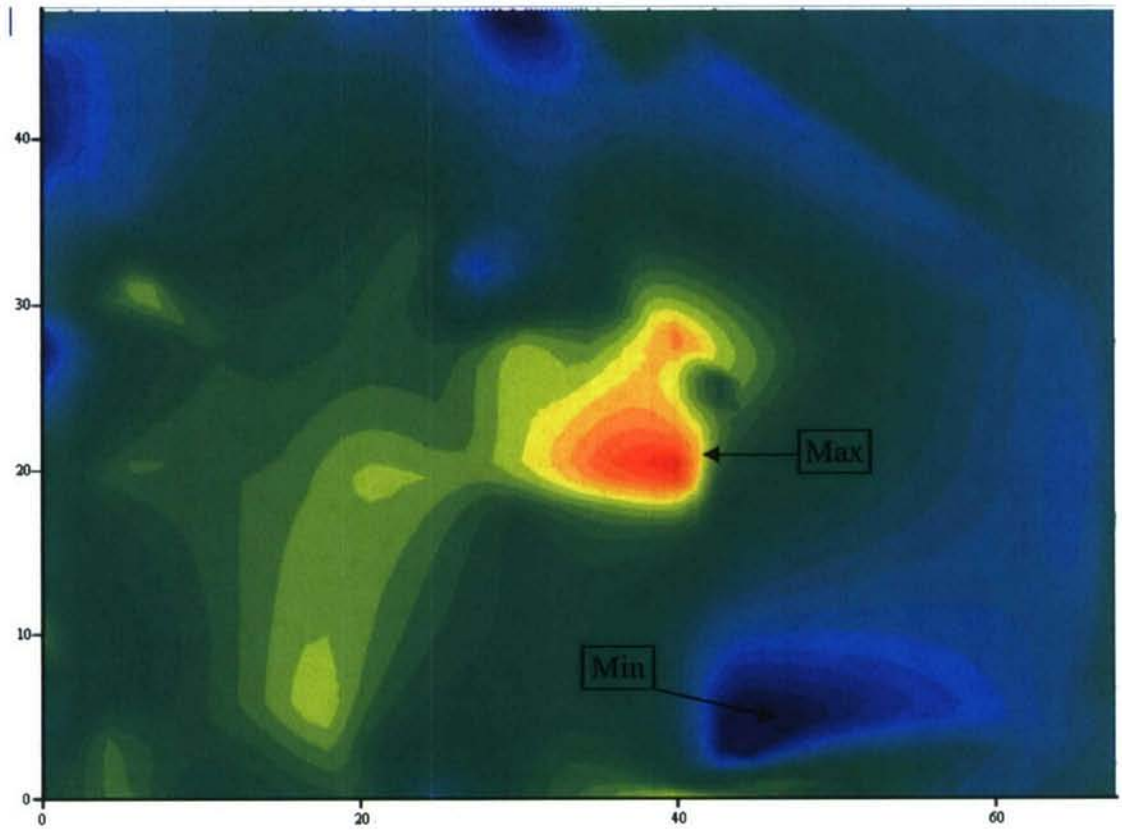

Figure 2.49: Contour Plot of the Total Thickness Variation

The thickness of the panels varied locally and across the surface of the panel, which necessitated the material properties to be normalized to a nominal thickness. The thickness variation affected fiber dominated material properties: E_1, E_2, F_{1t}, F_{1c}, F_{2t}, and F_{2c}. These properties were normalized to a nominal thickness of 5.08 mm (0.2 in). The properties were normalized based on the fiber areal weight, as given by the fabric supplier: 817.13 g/m^2 (24.1 oz/yd^2), and the E-glass fiber density: 2.54 g/cm^3 (158.57 lb/ft^3). Using these two properties, it was found that the product of the material thickness and the fiber volume fraction is constant. The constant value and the equation are given in equation (2.2).

$$V_f \cdot t = N \cdot \frac{A_w}{D_f} = 2.574\, mm \tag{2.5}$$

where:

V_f = volume fraction of the fiber,

t = thickness of the material, mm (in),

N = number of layers of the fabric, 8 layers,

A_w = aerial density weight, 817.13 g/m^2 (24.1 oz/yd^2),

D_f = density of the fiber, 2.54 g/cm^3 (158.57 lb/ft^3).

The fiber dominated properties were normalized by multiplying the experimental value by the ratio of the nominal thickness and the average thickness of the coupon. This process was carried out for every specimen tested in tension or compression from each batch and for both standard tests.

The matrix-dominated properties: G_{12}, ν_{13}, and F_6, were not normalized due to the complexity of the different parameters that control the matrix. The matrix was made of vinyl ester rubberized resin. Some of the parameters that control the properties of the matrix are: temperature and relative humidity of infusion, additives used, gel time, and vacuum applied during infusion. Such parameters are not measurable after the panels are manufactured and thus make it difficult to normalize to a nominal value.

A summary of the normalized experimental values are presented in Table 2.4. The table presents the results from batch 1 separate from batch 2 for emphasis on the difference in the results.

Table 2.4: Summary of Normalized Experimental Results

		$[0]_{4sf}$	$[0/90]_{2sf}$	$[0/\pm45/0]_{sf}$
		Experimental	Experimetal	Experimetal
Batch 1	E1t (GPa)	25.82	24.56	20.19
	E2t (GPa)	22.41	24.33	17.37
	v12	0.14	0.128	0.334
	F1t (MPa)	435	374.9	298.6
	F2t (MPa)	342.2	372.8	235.5
	E1c (GPa)	27.84	26.05	18.97
	E2c (GPa)	24.24	23.81	17.05
	v13c	0.369	0.408	0.436
	F1c (MPa)	369.88	368.7	298.15
	F2c (MPa)	362.4	352.15	257.5
	G12 (GPa)	4.71	4.53	7.72
	F6 (MPa)	35.53	32.81	33.26
Batch 2	E1t (GPa)	26.22	24.32	19.48
	E2t (GPa)	22.58	24.17	18.03
	v12	0.146	0.127	0.331
	F1t (MPa)	424.3	395.5	279.6
	F2t (MPa)	344	382.4	256.4
	E1c (GPa)	23.27	21.04	18.6
	E2c (GPa)	19.49	19.87	17.92
	v13c	0.432	0.439	0.423
	F1c (MPa)	346.42	338.31	271.7
	F2c (MPa)	307.78	321.7	242.9
	G12 (GPa)	5.25	5.08	8.33
	F6 (MPa)	19.03	17.81	43.485

The tensile properties represented in the table are the average of the normalized results of the two tensile tests conducted: ASTM D3039 and ASTM D638. The compression properties are the normalized values of the

ASTM D6641 test and the shear properties are the normalized values of the ASTM D4255 test. The values in the shaded area shown in Table 2.4 were obtained from un-normalized properties.

2.6.5. Statistical Comparison of Normalized Material Properties

Since two standard test methods were conducted to obtain the same material property, it was imperative to check if the results were from the same sample population. The comparison was conducted on all pair of combinations of four different experimental results obtained from two test standards and from two batches. In addition, all four results were compared simultaneously. Both the student t-test and the ANOVA statistical analysis were used to identify the significance of difference between each pair of results. The level of confidence was set to 95% (alpha = 0.05). Both analyses gave the same results. As for the comparison of all four experimental results, the ANOVA statistical analysis was used. The statistical comparison was conducted on normalized material properties to eliminate the effect of the thickness variation in the panel. Therefore, the statistical study was conducted on tension and compression material properties but not on shear properties. It was conducted on the modulus of elasticity obtained from the initial range and the ultimate strength, in both principal material directions. The results of the comparison are represented in Table 2.5 for tension and Table 2.6 for compression and are summarized in a matrix format in which all three lay-ups are presented. The color of the material property indicates if the statistical comparison showed that the experimental results of the compared pair come from the same population sample; the green color indicates that the experimental results come from the same population sample while the red color indicates that they are significantly different.

Table 2.5: Statistical Comparison of Tension Normalized Material Properties

Tension		Batch One								Batch Two					
		D3039				D638				D3039				D638	
Batch One	D3039														
	D638	E1	E2	F1	F2	$[0]_{4sf}$									
		E1	E2	F1	F2	$[0/90]_{2sf}$									
		E1	E2	F1	F2	$[0/\pm45/0]_{4sf}$									
Batch Two	D3039	E1	E2	F1	F2	E1	E2	F1	F2	$[0]_{4sf}$					
		E1	E2	F1	F2	E1	E2	F1	F2	$[0/90]_{2sf}$					
		E1	E2	F1	F2	E1	E2	F1	F2	$[0/\pm45/0]_{4sf}$					
	D638	E1	E2	F1	F2	E1	E2	F1	F2	E1	E2	F1	F2	$[0]_{4sf}$	
		E1	E2	F1	F2	E1	E2	F1	F2	E1	E2	F1	F2	$[0/90]_{2sf}$	
		E1	E2	F1	F2	E1	E2	F1	F2	E1	E2	F1	F2	$[0/\pm45/0]_{4sf}$	

ALL		E1	E2	F1	F2	$[0]_{4sf}$
		E1	E2	F1	F2	$[0/90]_{2sf}$
		E1	E2	F1	F2	$[0/\pm45/0]_{4sf}$

Table 2.6: Statistical Comparison of Compression Normalized Material Properties

Compression		Batch One								Batch Two					
		D6641				D695				D6641				D695	
Batch One	D6641														
	D695	E1	E2	F1	F2	$[0]_{4sf}$									
		E1	E2	F1	F2	$[0/90]_{2sf}$									
		E1	E2	F1	F2	$[0/\pm45/0]_{4sf}$									
Batch Two	D6641	E1	E2	F1	F2	E1	E2	F1	F2	$[0]_{4sf}$					
		E1	E2	F1	F2	E1	E2	F1	F2	$[0/90]_{2sf}$					
		E1	E2	F1	F2	E1	E2	F1	F2	$[0/\pm45/0]_{4sf}$					
	D695	E1	E2	F1	F2	E1	E2	F1	F2	E1	E2	F1	F2	$[0]_{4sf}$	
		E1	E2	F1	F2	E1	E2	F1	F2	E1	E2	F1	F2	$[0/90]_{2sf}$	
		E1	E2	F1	F2	E1	E2	F1	F2	E1	E2	F1	F2	$[0/\pm45/0]_{4sf}$	

ALL		E1	E2	F1	F2	$[0]_{4sf}$
		E1	E2	F1	F2	$[0/90]_{2sf}$
		E1	E2	F1	F2	$[0/\pm45/0]_{4sf}$

The latter tables were inconclusive and a definite pattern was not found in the agreement of the compared results. Therefore, the experimental results were not concluded to come from the same population sample when tested using different test methods or different panel batches.

2.6.6. Selecting the Relevant Material Properties

The results of the tests conducted showed higher variability in the compression values than in the tension values. In addition, as part of obtaining design values from the properties, the relevant material properties were selected. Therefore, the moduli of elasticity calculated by the tension tests were considered to be the moduli of the material and Table 2.7 displays the material properties selected for further evaluation. The tension properties from batch 1 and batch 2 were averaged due to the small differences between the values. The tension properties were fiber-dominated properties that did not change significantly between batch 1 and batch 2. Therefore, the compression and shear properties for each batch were not averaged due to the large difference in the values; note that the compression properties were not considered to be fiber dominated properties due to the nature of the fabric used which was woven fabric with relatively heavy tows with an areal weight of 817.13 g/m^2 (24.1 oz/yd^2). The compression ultimate strength, F_{1c} and F_{2c}, were not considered to be fiber-dominated properties since the compression failure was controlled by the local buckling of the fabric in the matrix which was governed by the resin's properties.

Table 2.7: Selected Relevant Material Properties

		$[0]_{4sf}$	$[0/90]_{2sf}$	$[0/\pm45/0]_{sf}$
		Experimental	Experimetal	Experimetal
	E1 (GPa)	26.01	24.44	19.83
	E2 (GPa)	22.51	24.25	17.7
	v12	0.143	0.127	0.332
	F1t (MPa)	429.1	385.2	289.1
	F2t (MPa)	343.2	377.6	245.96
Batch 1	F1c (MPa)	369.9	368.7	298.15
Batch 1	F2c (MPa)	362.4	352.15	257.5
Batch 1	G12 (GPa)	4.71	4.53	7.72
Batch 1	F6 (MPa)	35.5	32.81	33.26
Batch 2	F1c (MPa)	346.4	338.31	271.7
Batch 2	F2c (MPa)	307.8	321.7	242.9
Batch 2	G12 (GPa)	5.25	5.08	8.33
Batch 2	F6 (MPa)	19.0	17.81	43.485

2.6.7. Obtaining the Design Allowable Values

The experimental results obtained from the tests were useful for comparison purposes with other composite data and for preliminary design. As part of using the material properties obtained for the PMC with woven fabric reinforcement, statistical analysis was implemented to calculate the A-basis and B-basis design allowables for the material. The A-basis allowable provided 95% confidence that 99% of the material sample would exceed the allowable. This type of design allowable is typically used for critical structures. On the other hand, the B-basis allowable provided 95% confidence that 90% of

the material sample would exceed the allowable and is typically used for non-critical structures.

The methodology for obtaining design allowables for composite materials is explained in the Military Handbook 17-1E (MIL-HDBK-17-1E) section 2.4.3. The data for each material property was grouped together. Each testing environment group was pooled together; in the testing program presented in this study, one testing environment was used which was standard conditions of 22°C (71.6°F) and 50% relative humidity. The pool of sample values for one material property was normalized to a nominal thickness of 5.08 mm (0.2 in). Outliers were checked from each group by calculating the Maximum Normed Residual (MNR) according to equation (2.5). The MNR value for each sample was compared to the critical value of the sample size of the pool. The critical value was provided by the MIL-HDBK-17-1E for a wide number of sample sizes. For every sample with an MNR greater than the critical value, it was considered to be an outlier and thus removed from the pool which was carried on for analysis method.

$$MNR_i = \frac{|x_i - \bar{x}|}{s} \tag{2.5}$$

where:

MNR_i = Maximum Normed Residual of sample i,

x_i = the data value of sample i, Pa (psi),

$\bar{x}$ = the mean of the pooled samples, Pa (psi),

s = the standard deviation of the pooled samples, Pa (psi).

The pooled data was then checked for normality. This process was conducted by visual comparison of the data distribution with the best-fit normal curve. The probability of survival of each sample from the pool was calculated according to equation (2.6) and plotted against its corresponding data value.

$$\text{Probability of Survival of } x_i = 1 - \frac{i}{n+1} \tag{2.6}$$

where:

i = rank of the x_i data value in the sorted list, ascending order,

n = the total number of samples in the pool.

The generated curve was visually compared to the best-fit normal curve which was generated from the mean and standard deviation of the pooled data. A typical graph of such a comparison is depicted in Figure 2.50. The graph presented in Figure 2.50 was generated from the pooled data of F_{1t} experimental values.

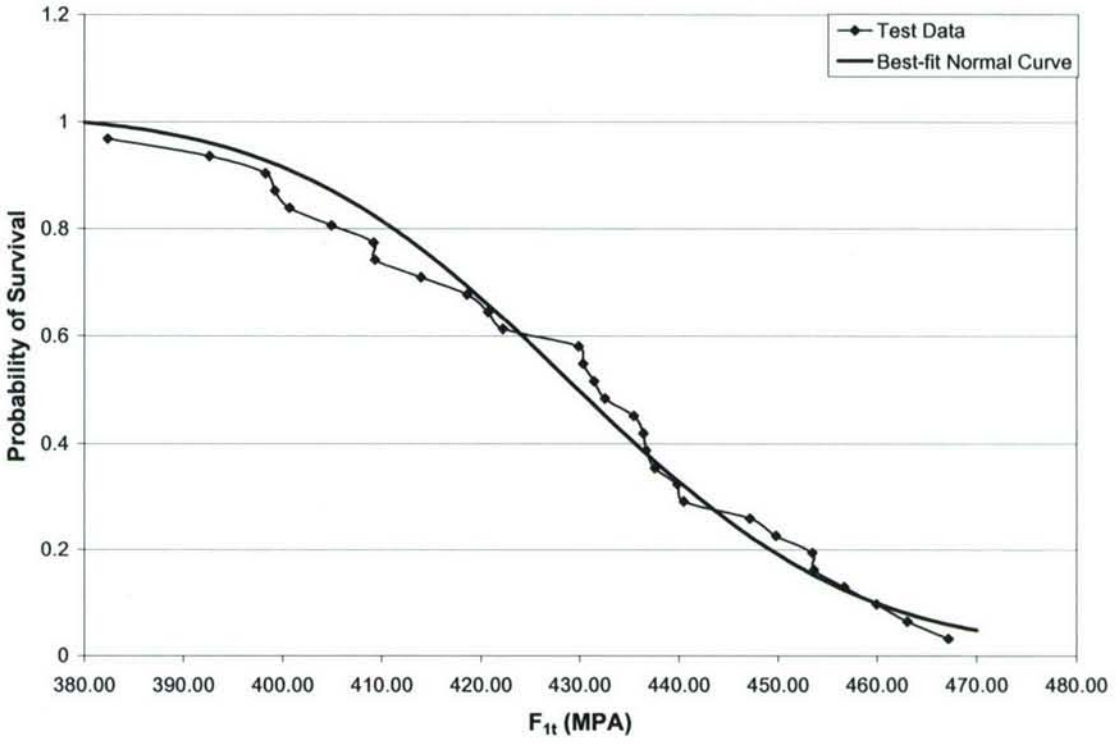

Figure 2.50: Typical Normality Check

If the assumption for normality was violated, the Weibull distribution would have been chosen for data fitting. After the normality distribution of the data was verified, the A- and B- basis "knock-down" factors were calculated. The tolerance factor was first calculated according to equations (2.5) and (2.6).

$$k_A = z_A\sqrt{\frac{f}{Q}} + \sqrt{\frac{1}{c_A \cdot n} + \left(\frac{b_A}{2c_A}\right)^2} - \frac{b_A}{2c_A} \tag{2.5}$$

where:

k_A = A-basis tolerance factor

z_A = 2.32635

f = $n-2$

n = the number of pooled samples

$$Q = f - 2.327\sqrt{f} + 1.138 + 0.6057\frac{1}{\sqrt{f}} - 0.3287\frac{1}{f}$$

$$c_A = 0.36961 + 0.0026958\frac{1}{\sqrt{f}} - 0.65201\frac{1}{f} + 0.011320\frac{1}{f\sqrt{f}}$$

$$b_A = 2.0643\frac{1}{\sqrt{f}} - 0.95145\frac{1}{f} + 0.51251\frac{1}{f\sqrt{f}}$$

$$k_B = z_B\sqrt{\frac{f}{Q}} + \sqrt{\frac{1}{c_B \cdot n} + \left(\frac{b_B}{2c_B}\right)^2} - \frac{b_B}{2c_B} \tag{2.6}$$

where:

k_B = B-basis tolerance factor

z_B = 1.28115

f = $n-2$

n = the number of pooled samples

Q = $f - 2.327\sqrt{f} + 1.138 + 0.6057\frac{1}{\sqrt{f}} - 0.3287\frac{1}{f}$

c_B = $0.36961 + 0.0040342\frac{1}{\sqrt{f}} - 0.71750\frac{1}{f} + 0.19693\frac{1}{f\sqrt{f}}$

b_B = $1.1372\frac{1}{\sqrt{f}} - 0.49162\frac{1}{f} + 0.18612\frac{1}{f\sqrt{f}}$

Once the tolerance factors were determined, the normal distribution allowables were calculated according to the equations presented in (2.7). These values are considered as "knock-down" factors less than 1.

$$\begin{aligned} A &= \bar{x} - k_A \cdot s \\ B &= \bar{x} - k_B \cdot s \end{aligned} \tag{2.7}$$

where:

A = normal distribution A-basis allowable

B = normal distribution B-basis allowable

k_A = A-basis tolerance factor

k_B = B-basis tolerance factor

$\bar{x}$ = the mean of the pooled samples, Pa (psi)

s = the standard deviation of the pooled samples, Pa (psi).

The basis values are calculated by multiplying the mean of each pooled set by the "knock-down" factors. The design allowables were calculated for one set of fiber lay-up panels, $[0]_{4sf}$. A summary of the values obtained is presented in Table 2.8, which depicts the average normalized values, the "knock-down" factors, and the basis values for both the A- and B- basis design.

Table 2.8: A- and B-basis Design Allowable Values

	$[0]_{4sf}$				
	Average Normalized Experimental	"knockdown" factor		Statistic Basis Value	
		A-basis	B-basis	A-basis	B-basis
E1 (GPa)	26.01	0.9291	0.9589	24.17	24.94
E2 (GPa)	22.51	0.9337	0.9616	21.02	21.65
F1t (MPa)	429.1	0.8383	0.9063	359.7	388.9
F2t (MPa)	343.2	0.9111	0.9485	312.7	325.5
F1c (MPa)	360.1	0.6311	0.7831	227.3	282.0
F2c (MPa)	336.9	0.6236	0.7794	210.1	262.6

Note that the values of batch 1 and batch 2 were combined to calculate the design allowables. Since there was a large variability in the ultimate compression strength values, the "knock-down" factors are relatively small compared to the "knock-down" factors of the other properties, thus, reducing the design allowables calculated.

2.6.8. Classical Lamination Theory Based Modeling Approach

A Classical Lamination Theory (CLT) based model was implemented to verify, through modeling techniques, the experimental results. The model predicts the behavior of multidirectional laminate as a function of the properties of the individual layers and the stacking sequence of the layers. The CLT takes into account basic assumptions as part of predicting the behavior of the laminate. The assumptions are the following (Daniel and Ishai, 1994):

1. Each layer of the laminate is quasi-homogenous and orthotropic.
2. The laminate and its layers are in a state of plane stress.
3. All displacements are small compared with the thickness of the laminate.
4. Displacements are continuous throughout the laminate.
5. In-plane displacements vary linearly through the thickness of the laminate.
6. Transverse shear strains γ_{xz} and γ_{yz} are negligible.
7. Strain-displacement and stress-strain relations are linear.
8. The transverse normal strain ε_z is negligible.

The properties of the lamina were obtained from the experimental results of testing the $[0]_{4sf}$ lay-up laminate. In this type of fabric lay-up sequence, the laminate properties are the same as the individual layer properties as long as all the layers are composed of the same material. By this approach, the lamina properties of the PMC reinforced with woven E-glass fabric under study were measured experimentally. Using the properties of the lamina, the different fabric lay-up sequence was predicted using the CLT-based model approach. Since two other fabric lay-up sequences were tested, $[0/90]_{2sf}$ and $[0/\pm45/0]_{sf}$,

the properties of these lay-up sequences were predicted using the model and compared with the experimental results.

To predict ultimate failure of the PMC, a damage factor was applied to the material properties. A typical damage factor is 0.25, applied to material properties governed by the matrix. Since the material's stress-strain curve of the following study was modeled with a bi-linear model, the ratio of the elastic modulus of the final region to the elastic modulus of the initial region was taken to be the degradation factor that was applied to the material's property in the CLT-based model. The degradation factors calculated for both principal material directions were: $r_1 = 0.83$ and $r_2 = 0.76$. As for the degradation factor in the shear direction, r_{12}, a different method was implemented since the shear stress strain curve was not represented by a bi-linear model but rather by a hyperbolic tangent curve fit. Therefore, an optimization technique was implemented to calculate the r_{12} degradation factor such that the $[0/\pm45/0]_{sf}$ experimental results agree with the CLT-based model predictions; and the calculated value was 0.51.

Once the degradation factors were applied to the material's elastic properties, the same process of calculating the first ply failure was repeated but matrix failure was ignored and fiber failure only detected. This approach focused on detecting fiber failure in the material which was considered the ultimate failure of the material. The safety factor calculated in this approach was considered the material ultimate failure in the direction and state of loading assumed at the beginning, tension, compression, or shear. In some cases, the first ply failure was the same as the ultimate failure and occurred when the first ply failure detected its fiber failure. The procedure of implementing the CLT-based model was taken from the following reference (Daniel and Ishai, 1994).

2.6.9. Discussion of the Comparison of Results

The material properties used in the model were the experimental values of the $[0]_{4sf}$ fiber lay-up panel. Since two batches were tested, two sets of material properties were obtained from each fabric lay-up sequence. The material properties were normalized to a nominal thickness of 0.508 mm (0.2 in). As discussed previously, the tensile properties obtained from both batches showed relatively similar values while the compression and shear properties showed large difference between the two batches. This was explained by the difference in the matrix between the two batches which introduced significant effects on the compression and shear properties obtained from the experiments and did not affect the tensile experimental values, since they were solely fiber dominated properties. The lamina properties were taken from the $[0]_{4sf}$ experimental results after normalizing the values and selecting the relevant properties; the values are presented in Table 2.7.

The lamina properties used as an input were different for batch 1 and batch 2. The values of the predicted properties compared to the experimental properties

are presented in Table 2.9. The presented comparison in Table 2.9 shows a high agreement between the experimental and CLT-based model predictions. This was due to the use of degradation factors obtained from experimental results. It was observed that the Poisson's ratio and the shear ultimate strength of the $[0/\pm45/0]_{sf}$ showed large errors in the comparison. It was explained by the inability to normalize the results and thus rendering them universal for comparison with the CLT-based model. The shaded properties in Table 2.9 are un-normalized values.

Table 2.9: CLT Predictions and Experimental Results Comparison

		Lamina Data Input $[0]_{4sf}$	$[0/90]_{2sf}$			$[0/\pm45/0]_{sf}$			
			CLT	U Maine		CLT		U Maine	
		Experimental	Pred.	Exp.	%Error	(FPF)	(FF)	Exp.	%Error
Batch 1	E1 (GPa)	25.82	24.12	24.56	1.82%	20.58		20.19	1.90%
	E2 (GPa)	22.41	24.12	24.33	0.87%	18.99		17.37	8.53%
	v12	0.140	0.13	0.128	1.54%	0.298		0.334	12.08%
	F1t (MPa)	435.0	366.9	374.9	2.19%	119.2	306.6	298.6	2.62%
	F2t (MPa)	342.2	366.9	372.8	1.62%	118.8	253.4	235.5	7.05%
	F1c (MPa)	369.9	346.8	368.7	6.33%	117.3	262.1	298.2	13.75%
	F2c (MPa)	362.4	346.8	352.2	1.56%	110.0	275.2	257.5	6.43%
	G12 (GPa)	4.71	4.71	4.53	3.82%	7.69		7.72	0.39%
	F6 (MPa)	35.53	35.53	32.81	7.66%	58.01	140.4	33.26	42.67%
Batch 2	E1 (GPa)	26.22	24.4	24.32	0.33%	21.27		19.48	8.42%
	E2 (GPa)	22.58	24.4	24.17	0.94%	19.56		18.03	7.82%
	v12	0.146	0.135	0.127	5.93%	0.288		0.331	14.93%
	F1t (MPa)	424.3	370.1	395.5	6.87%	60.41	298.3	279.6	6.28%
	F2t (MPa)	344.0	370.1	382.4	3.33%	56.58	258.0	256.4	0.63%
	F1c (MPa)	346.4	323.4	338.3	4.62%	58.92	252.1	271.7	7.77%
	F2c (MPa)	307.8	323.4	321.7	0.51%	55.12	242.3	242.9	0.26%
	G12 (GPa)	5.25	5.25	5.08	3.24%	8.00		8.33	4.13%
	F6 (MPa)	19.03	19.03	17.81	6.41%	29	139.1	43.49	49.95%

= un-normalized data

2.6.10. Conclusion and Recommendations

It was essential to normalize the composite material properties obtained from experiments for comparison of different panels. This was achieved by using a nominal thickness chosen according to the needs of the comparison. The normalization was possible only for fiber-dominated properties. Therefore, the matrix-dominated properties were not normalized and were not comparable. A statistical analysis was conducted on the normalized properties to measure the degree of significance of two sets of results that should ideally give the same values. The statistical analysis compared results from different test methods and different material batches.

Normalized properties were used to obtain the corresponding design allowables. The "knock-down" factor obtained through calculating the design allowables was based on the variation of the results and their distribution. In other words, the "knock-down" factor revealed the repeatability and reliability of properties obtained through the testing program. Due to the difficulties

faced during the compression testing, the design allowables were significantly smaller than the mean of the experimental results. Normalization of the matrix dominated properties is necessary for future work, and further understanding and improving with composite materials designs.

The CLT-based model showed accurate predictions of experimental results when the properties were normalized. The pseudo-quasi isotropic lay-up experimental results were used to calculate the degradation factor needed to predict the failure of the material in the CLT-based made. Since the matrix dominated properties were not normalized, the comparison of the CLT-based model and the experimental results did not show good agreement with the in-plane shear properties. As part of verifying the model, different fiber lay-ups can be tested and used in comparison with the CLT-based model predictions. Such further study is recommended for future work.

The results as presented here rely on a purely statistical interpretation of the data using a variety of statistical tests. Statistical significance is when it is highly unlikely that the difference is caused by sampling error or by chance. Practical or substantive significance has not been considered. Given that our data typically has very low coefficients of variation, the practical level of significance may actually govern our results as to whether the similarities between fabrication batches exist or not. Our recommendation would be to use the student t-test and a simple percent difference of the means calculation for future interpretations. Typically in engineering practice the practical significance would be between 5% and 10%.

2.7. Flexural Testing

2.7.1. Introduction

The testing study has previously investigated the variability in tension, compression, and shear testing of E-glass vinyl-ester composites. The parametric flexure study will investigate the effects of span-to-thickness, width-to-thickness, and load head size on the variability in flexural strength, flexural modulus, and failure location of 12.7 mm (0.5 in) and 25.4 mm (1.0 in) thick E-glass vinyl-ester composites. The use of a three-dimensional digital image correlation (DIC) system to record full-field strain measurements should allow the effects of shear deformations, on beam displacement and stress concentrations, at the load head contact points.

The work reported here is the first phase of the flexure study and is intended to investigate the variability in flexural strength, flexural modulus, stress distribution, failure type, and failure location due to selection of load head size. The use of a tabbing material, between the specimen and the load/support points of the flexure fixture is also investigated. The results of this phase will be used to examine the effects of span-to-thickness and width-to-thickness ratios in the next phase of the study.

2.7.2. Specimen Preparation

The test specimens were cut from the panels to a nominal dimension of 38.1 mm (1.5 in) wide by 610 mm (24 in) long, using a wet saw with a diamond coated blade. The dimensions of each specimen were then measured and recorded as per ASTM D5947. Prior to testing, all specimens were conditioned at 23 ± 2°C and 50 ± 5% relative humidity, as outlined in ASTM D5229.

The specimens were then prepared for the Digital image correlation (DIC) measurement system by applying a speckled grayscale pattern of paint to the side of the specimen as shown in Figure 2.55 . This allows full-field strain measurements to be recorded through-the-thickness of the beam during testing.

Figure 2.51 Speckled Grayscale Pattern on Face of Specimen

2.7.3. Experimental Setup

A 4-point flexural test configuration, with quarter-point loading, was used for this investigation, as shown in Figure 2.55 span-to-thickness ratio of 22 was used for all tests. While the ASTM D6272 flexural standard recommends ratios of 16, 32 or 40, the ratio of 22 was selected for two reasons. 1) The span ratio of 16 was deemed to be too short for the material system and specimen thickness under investigation; and 2) a size limitation of 610 mm (24 in) existed, because the panels had been fabricated before the flexural testing had been incorporated into the variability study.

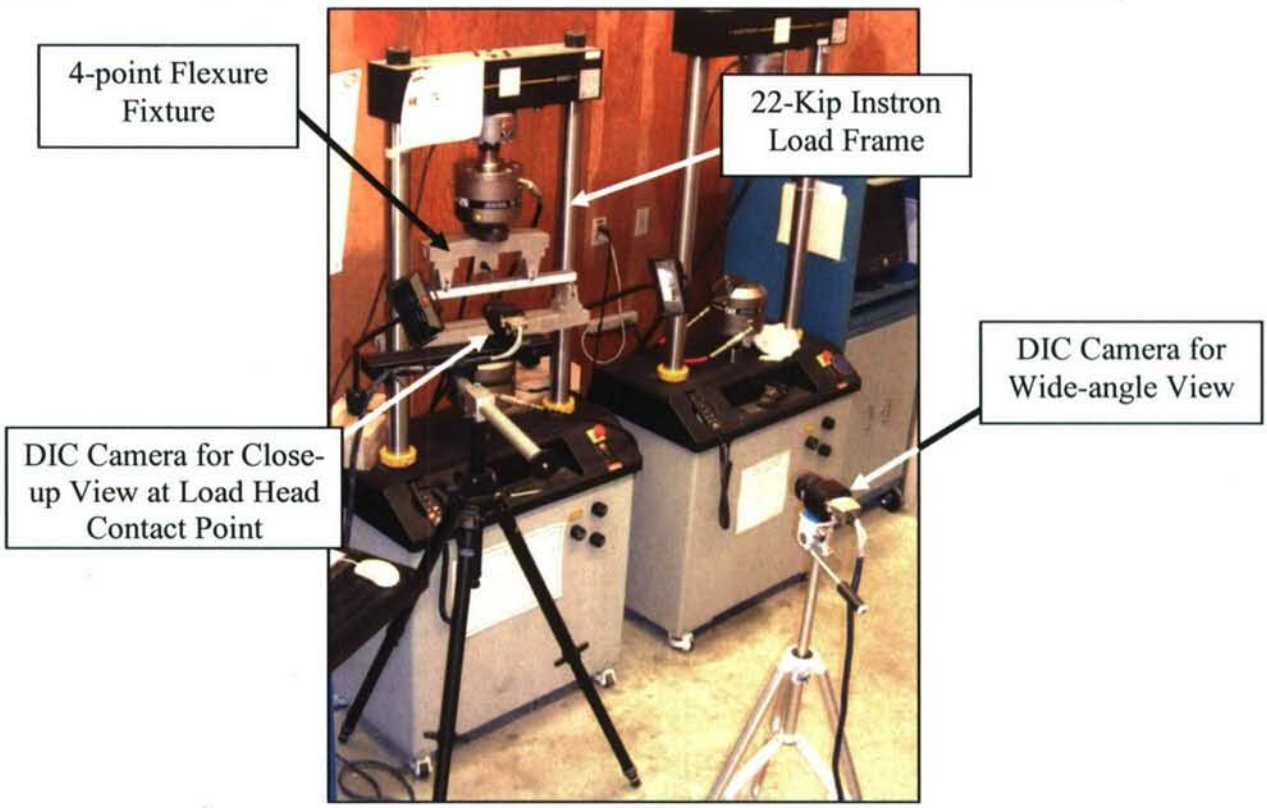

Figure 2.52 4-Point Flexure Experimental Setup

Specimen Configuration	Load Head		Number of Specimens
	Diameter	Tab Material	
	mm. (in.)		
05LH	12.7 (0.5)	None	8
05TM	12.7 (0.5)	Tabbing	8
10LH	25.4 (1.0)	None	8
10TM	25.4 (1.0)	Tabbing	8
20LH	50.8 (2.0)	None	8
20TM	50.8 (2.0)	Tabbing	8

Figure 2.53 Flexural Test Matrix

As shown in the table of Figure 2.55 **Error! No bookmark name given.**, six different load-head configurations were investigated during this study. Specifically, 12.7 mm (0.5 in), 25.4 mm (1.0 in), and 50.8 mm (2.0 in) diameter load heads, with and without tabbing material, were investigated. These three diameters correspond to diameter-to-thickness ratios of 0.5, 1.0, and 2.0 for the 25.4mm (1.0 in) thick composite specimens used in this study. Eight specimens were tested for each of the six configurations. The material used for tabs between the load-head and the specimen was 25.4 mm (1.0 in) wide by 1.6 mm (0.0625 in) thick FRP tabbing material.

The testing was performed on a 22Kip Instron load frame, in an environmentally controlled test lab, at the Advanced Engineered Wood Composites (AEWC) Center, at the University of Maine. The rate of crosshead loading was constant at 0.10 in/min. This rate was calculated based on the rate equation given in section 10.1.4 of the ASTM D 6272-02 flexural standard.

A 3-D Digital image correlation (DIC) system was used to record the mid-span deflection and the full-field strain distribution during each test. The system was used in a 2-D mode, with each of the two cameras observing a different location. The information being sought, during this testing, was restricted to in-plane movements and strains of the test specimen. The test configuration used in this study allowed for simultaneous 2-D monitoring of two locations without the loss of critical data. A wide angle view recorded the mid-span deflection and strain distributions throughout the viewing area, while the close-up view allowed for a more detailed investigation of the stress distribution under the load head.

In addition to the load and displacement data recorded during the tests, the load at which the first audible sound, or the "crack load", was recorded through operator observation. Future testing will incorporate acoustic emission sensors to properly quantify the crack load.

2.7.4. Discussion Of Results

The table in Figure 2.55 shows the test results for the six test configurations investigated in this study. The table shows the calculated values for flexural strength and flexural modulus of the six configurations. The mean and COV were calculated for the flexural strength and flexural modulus of each configuration and are plotted in Figure 2.55 and Figure 2.55 respectively.

The use of the 25.4 mm (1.0 in), versus the 12.7mm (0.5 in), load heads had virtually no effect on the mean flexural strength for the tests without tabbing material, but showed an 11% increase for the tests with tabbing material. The COV's had a 25% reduction both with and without the tabbing material for the 25.4 mm (1.0 in) load heads.

Specimen Configuration	Strength		Modulus	
	Mean	COV	Mean	COV
	MPa (ksi)	*%*	*GPa (Msi)*	*%*
05LH	379 *(54.9)*	4.1	25.6 (3.72)	2.4
05TM	356 (51.7)	3.7	25.1 (3.65)	1.4
10LH	379 (54.9)	3.1	25.4 (3.69)	1.1
10TM	396 (57.4)	2.7	25.4 (3.68)	0.8
20LH	401 (58.1)	2.2	26.4 (3.83)	1.1
20TM	391 (56.7)	3.7	26.0 (3.77)	1.0

Figure 2.54 Flexural Strength and Modulus Results

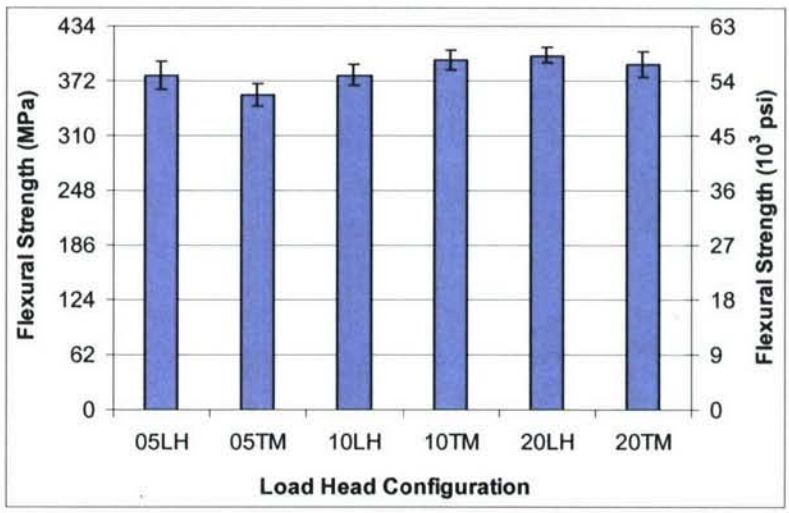

Figure 2.55 Flexural Strength Results

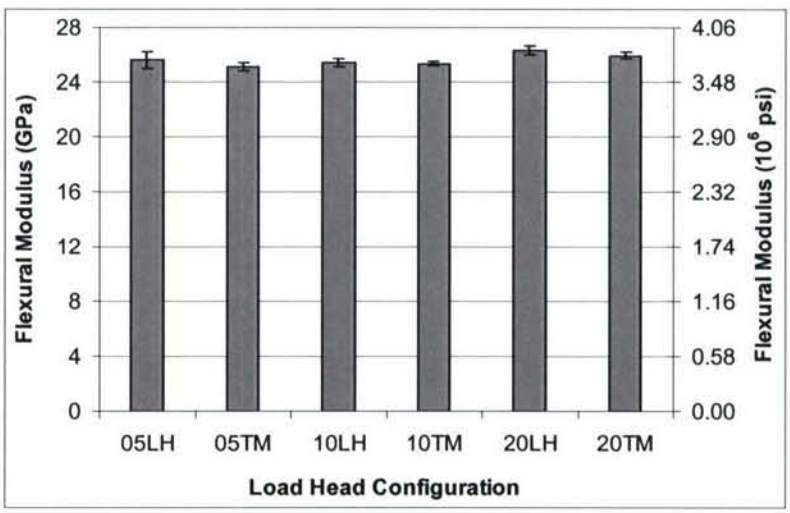

Figure 2.56 Flexural Modulus Results

The use of the 50.8 mm (2.0 in), versus the 25.4 mm (1.0 in), load heads had a 5.7% increase in the mean flexural strength for the tests without tabbing material, but showed a 1.3% reduction for the tests with tabbing material. The COV's showed a reduction of 28% without the tabbing material and an increase of 36% with the tab material for the 50.8 mm (2.0 in) load heads versus the 25.4 mm (1.0 in) load heads

The use of the tabbing material under the load heads and supports resulted in: a 5.9% decrease in the mean flexural strength with a 2.0% decrease in the mean flexural modulus for the 12.7 mm (0.5 in) load head; a 4.5% increase in the mean flexural strength with a 0.3% decrease in the mean flexural modulus for the 25.4 mm (1.0 in) load head; and a 2.5% decrease in the mean flexural strength with a 1.5% decrease in the mean flexural modulus for the 50.8 mm (2.0 in) load head. In general, the use of the tabbing material led to less surface damage occurring under the load heads, as shown in Figures 2.57 through 2.59. The use of the tabbing material to help prevent failures near the load head (within one load head diameter) was inconclusive. While the percentage of failures in the gage area increased from 25 to 87.5% for the 12.7 mm (0.5 in) load heads, it remained unchanged at 62.5% for the 50.8 mm (2.0 in) and decreased from 50 to 25% for the 25.4 mm (1.0 in) load heads.

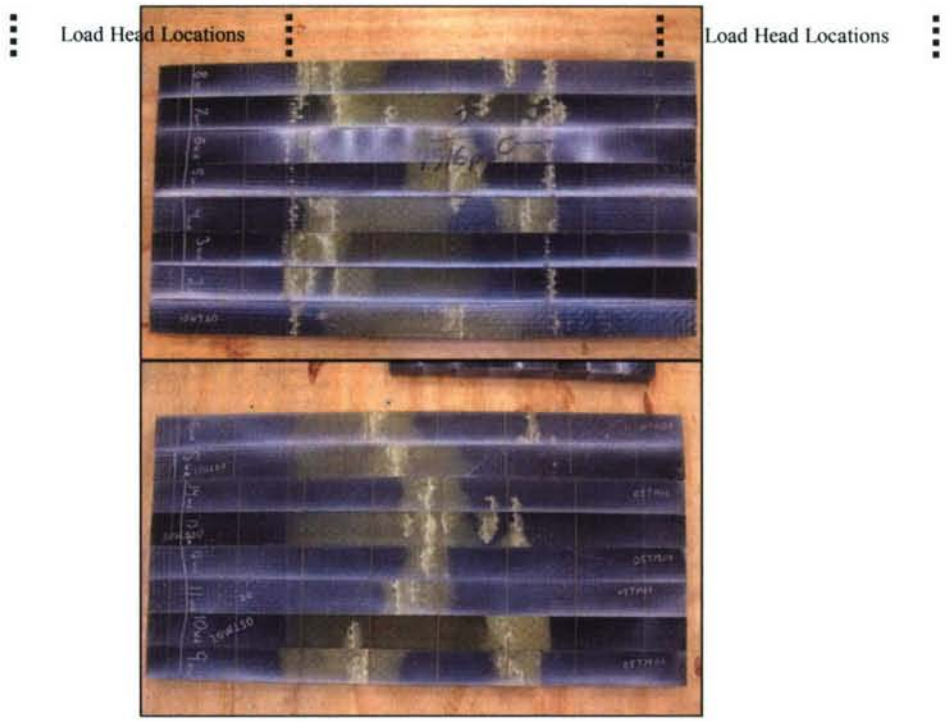

Figure 2.57 Failed Specimens - 05LH (left) and 05TM (right)

Figure 2.58 Failed Specimens - 10LH (left) and 10TM (right)

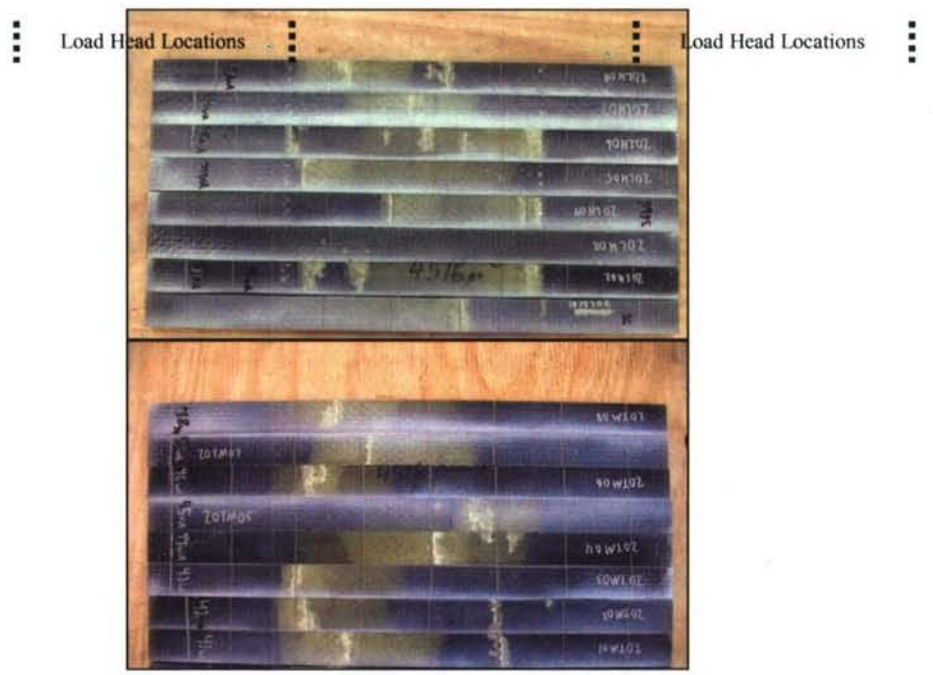

Figure 2.59 Failed Specimens. - 20LH (left) and 20TM (right)

The mean and COV's for the crack loads and failure loads are given in the table of Fig. 2.60 and plotted in Fig. 2.61. The ratio of crack load to failure load increased with increasing load head size, from 85% to 89%, for the tests without tabbing material. The same ratio for the tests with tabbing material was larger, but showed slightly less variation at 94% to 96%.

Specimen Configuration	Crack Load		Failure Load	
	Mean	COV	Mean	COV
	kN (lb)	*%*	*kN (lb)*	*%*
05LH	18.2 (4084)	5.3	21.4 (4807)	4.4
05TM	19.0 (4280)	2.7	19.8 (4447)	4.1
10LH	18.9 (4256)	5.4	21.5 (4839)	2.5
10TM	21.1 (4750)	6.4	22.5 (5064)	3.7
20LH	19.5 (4378)	3.8	21.8 (4896)	2.5
20TM	20.9 (4701)	6.0	21.6 (4863)	4.1

Figure 2.60 Crack & Failure Load Results

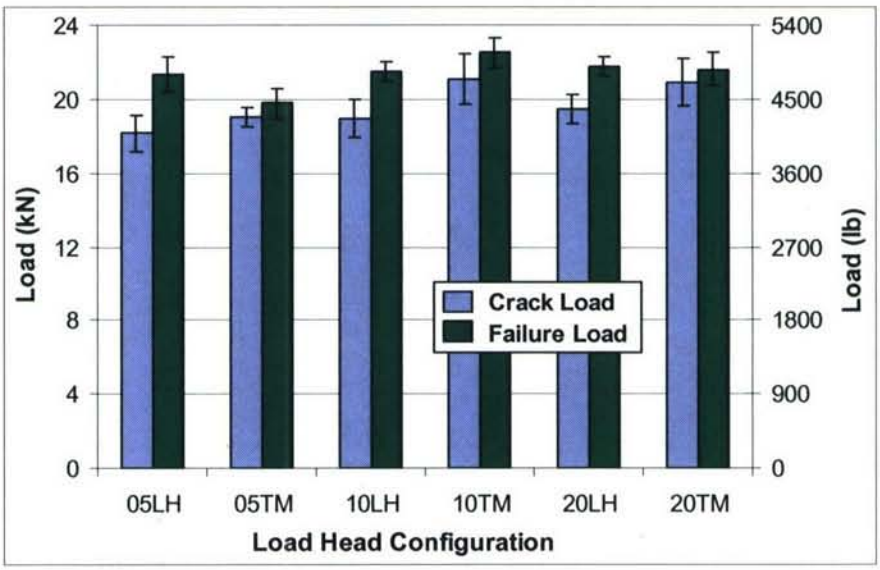

Figure 2.61 Plot of Crack & Failure Loads

Figures. 2.62 through 2.64 show close-up views of specimen failures, with the specimens placed in the orientation that they were cut from the original panels. As seen in these photos, cracks and failures occurred at the same locations in adjacent specimens indicating a possible flaw location in the original panels at these locations. Without pretest nondestructive evaluation data it is not possible to say with certainty that the common failure locations were a result of panel flaws, but it is the author's opinion that failures occurring at the same location through three specimens (as seen in Figures 2.62 and 2.63) minimizes the possibility of the damage occurring during specimen preparation.

Figure 2.62 Possible Specimen Flaw in 05LH Series

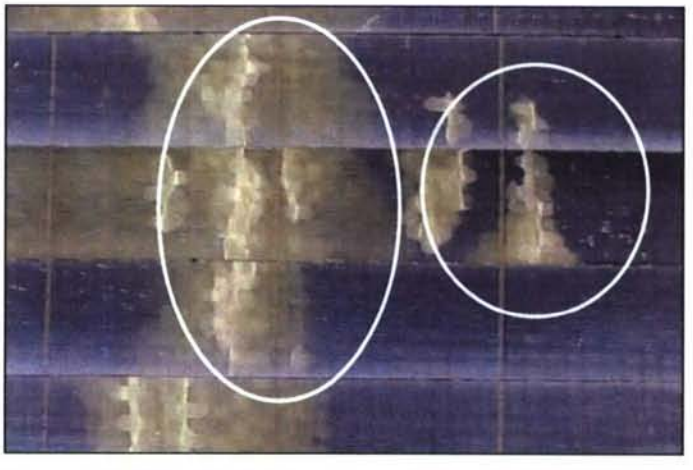

Figure 2.63 Possible Specimen Flaw in 05TM Series

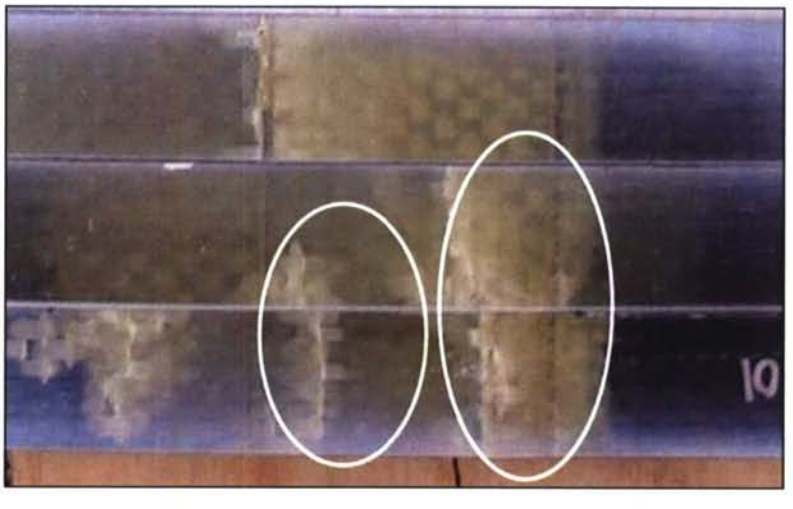

Figure 2.64 Possible Specimen Flaw in 10TM Series

The majority of the specimens failed in compression of the top surface followed by a delamination, as shown in Figure 2.65. The remainder of the specimens failed in compression either near the center of the beam or at the load head. 90% of the ultimate failures were preceded by localized failures without a drop in the applied load leading to an eventual progressive failure with a drop in load. The remaining 10% were of a more catastrophic nature not preceded by a drop in load.

Figure 2.65 Typical Failures of the Flexure Test Specimens

The stress distribution through-the-thickness of a typical beam can be seen in Figure 2.66. As shown in the series of pictures, the top of the beam goes into compression while the bottom of the beam experiences a tensile strain equal in magnitude to the compressive side.

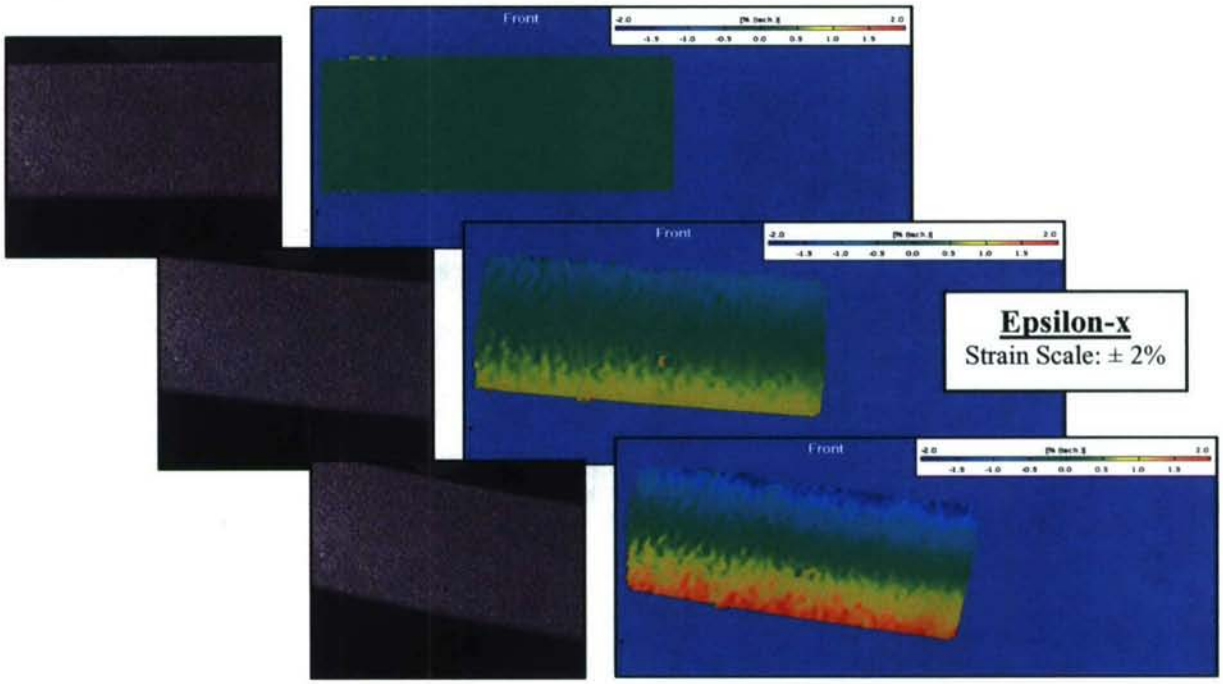

Figure 2.66 Flexural Strain Distribution Progression during Testing

2.7.5. Conclusions and Recommendations

A load head size of 50.8mm (2.0 in), without tabbing material, resulted in the highest mean and lowest COV for the flexural strength for the six test configurations investigated. This configuration also resulted in 62.5% of the failures occurring near the load heads.

The tabbing material helped reduce the surface damage to the specimens but showed less benefit at reducing failures near the load heads for larger diameter load heads.

The DIC system was successful at recording the mid span deflections and photo documenting the tests. The system also gave a detailed visualization of, and quantified, the stress distribution through the thickness of the specimen. Further processing and analysis of the data is necessary to distinguish the stress concentrations at the load head contact point. This is an area of ongoing work on the project.

The load head size of 50.8mm (2.0 in), without tabbing material, will be used in the next phase of the study to examine the effects of different span-to-thickness ratios and width-to-thickness ratios on the flexural response of 25.4mm (1.0 in) thick E-glass vinyl-ester specimens.

2.8. Probabilistic FEA

2.8.1. Introduction

The use of polymer matrix composite (PMC) materials fabricated by Vacuum Assisted Resin Transfer Molding (VARTM) in marine applications has been increasing. At the same time, the variability of composite mechanical properties produced using the VARTM process is not well understood. This affects the ability to produce reliable designs.

During the last decade, several researchers applied reliability techniques to PMC materials (Engelstad et al. 1993; Kam et al. 1993; Jeong et al. 2000; Jeong et al. 2000; Liu et al. 2000; Wu et al. 2000; Frangopol et al. 2003; Camata et al. 2004). The uncertainties associated with constituent material properties, variability in processing parameters and precision of experimental methods affect the mechanical properties measured in a standard tension test of a polymer matrix composite. Because of the complexity of the problem, most researchers evaluated sources of variability due to material properties, geometric dimensions and loads. Some researchers considered that most variability is due to material properties and to some geometric dimensions (i.e. ply thickness and ply angle) (Engelstad et al. 1993; Jeong et al. 2000; Jeong et al. 2000; Liu et al. 2000). Also, because of numerical complexity, only a few researchers considered the spatial variation of the material properties (random field) in their analysis. Engelstad et al. (Engelstad et al. 1993) considered random fields in the study of spherical shells under uniform external pressure and in the postbuckling of a flat panel under axial compression. However, "The random fields were assumed to be fully correlated" for the flat panel because the computational expense was too high. Outside PMC materials, Bazant et al. (Bazant et al. 1991) studied the effect of spatial variability of material properties on deflections of prestressed concrete segmental box-girders and concluded that the spatial variability effect is only minor and negligible from the practical viewpoint. Most researchers have assumed that the material property random variables are normally distributed, whereas, Jeong et al. (Jeong et al. 2000) used both normal and two-parameter Weibull distribution for the ultimate strength parameters and showed that considering Weibull distribution for the ultimate strength does not affect the results if a normal distribution was assumed instead. Camata et al. (Camata et al. 2004) also assumed that the strength of a single fiber follows a Weibull distribution. In terms of loads, in a study of laminated composite plates, Frangopol et al. (Frangopol et al. 2003) considered the random load to have a lognormal distribution since there was no available information on the type of distribution. Even though there are many failure theories available, Tsai-Wu, maximum stress and maximum strain were the most commonly used in probabilistic analyses of composites materials (Engelstad et al. 1993; Kam et al. 1993; Jeong et al. 2000; Jeong et al. 2000; Frangopol et al. 2003).

In this section, both experimental and finite element analyses are used to evaluate the impact of property variability on a multidirectional composite material tensile response.

In the experimental work, a three-dimensional digital image correlation (DIC) photogrammetry system capable of non-contact full field measurements of strains and displacements during composite material tests was implemented. The 3-D DIC system was used in a testing environment for generating composite material mechanical properties using robust techniques (Lopez-Anido et al. 2004).

2.8.2. Objectives and Significance

The objectives of this study are: 1) model the variability of PMC materials subjected to unidirectional tension; 2) identify key parameters that affect tensile coupon property variability; 3) study the convergence of a probabilistic FEA model of a tension coupon; and, as a result 4) provide a better understanding on how to assign property variability in FEA models of marine grade composites which will lead to a better design with realistic safety factors.

2.8.3. Approach

The work consisted of both experimental testing and probabilistic FEA modeling.

The experimental work consisted of fabricating four (1.2 m x 1.8 m x 4.9 mm) composite plates made of E-glass / vinyl ester using the Seemann Composites Resin Infusion Molding (SCRIMP) technology under an industrial setting. The plate lay-ups were as follows: $[0]_{4sf}$ and $[0/90]_{2sf}$. The materials and quality control were representative of marine grade composites typically used by the US Navy. Eight tension specimens were extracted from the plates for each lay-up and tested following ASTM D3039. To reduce machining variability and edge effects, the standard tensile test coupons were cut from the 1.2 m x 1.8 m plates using automated CAD-driven water jet machining. In addition, to reduce experimental variability, a three-dimensional digital image correlation (DIC) photogrammetry system capable of non-contact full field measurements of strains and displacements during composite material tests was used.

The numerical work consisted of developing a 3D probabilistic finite element analysis (FEA) using ANSYS 8.0 and comparing numerical with experimental results. In the probabilistic FEA model, mechanical, strength and geometric properties ($E_{11}, E_{22}, G_{12}, \nu_{12}$, $F_{1t}, F_{1c}, F_{2t}, F_{2c}, F_{12}$, $\varepsilon_{1t}, \varepsilon_{1c}, \varepsilon_{2t}, \varepsilon_{2c}, \varepsilon_{12}$) of the woven fabric E-glass / vinyl ester coupons were considered as random fields and generated using Monte Carlo simulations. These material properties were obtained from laboratory test data of $[0]_{4sf}$ lay-up, and in turn used to predict the properties of the $[0/90]_{2sf}$ lay-up. The FEA study evaluated the effects of spatial correlation, probability distribution functions (PDF), finite element size

and failure criteria on the predicted statistical strength properties of the $[0/90]_{2sf}$ tension coupons.

Property variability and failure locations predicted using the FEA model were compared with those obtained in the laboratory tests. This allowed evaluation of how uncertainties propagate within an FEA model and how to properly assign mean, COV and PDF of material properties to individual finite elements within a mesh.
This section is focused on the modeling effort and a detailed description of the laboratory work is provided elsewhere (Lopez-Anido et al. 2004).

2.8.4. Description of Tension Test

The geometry of the standard tension coupons used in both the experimental and numerical evaluations were in accordance with ASTM Standard D3039 (ASTM 2000). The standard specimen was 254 mm (10 in) long, 25.4 mm (1 in) wide and 4.9 mm (1.93 in) thick with a gage length of 177.8 mm (7 in) as shown in Figure 2.67. The tabs were 38.1 mm (1.5 in) long, 25.4 mm wide, 1.575 mm (0.062 in) thick with a taper angle of 7°. The tabbing material used was a cross-ply E-glass/Epoxy composite known as G11 (Dess Machine, Dover, DE). The tabs were bonded to the specimen using a structural adhesive Plio-Grip7770 (Ashland 2004). The adhesive layer mean thickness was 0.12 mm and measured using a binocular optical microscope; the adhesive layer thickness variability was not included in the model.

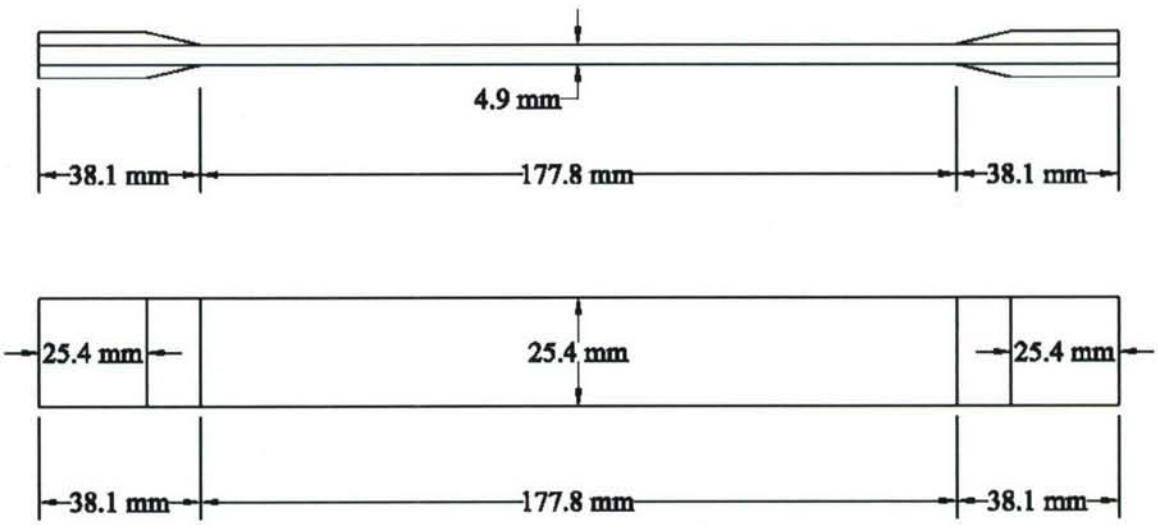

Figure 2.67 The modeled specimen

2.8.5. Model Overview

A 3-D solid model of the actual test specimen was built using ANSYS 8.0 software package (ANSYS 2003) using the SOLID191 element. SOLID191 is a layered 20-node structural solid element designed to model layered thick shells or solids (Zienkiewicz 1977). The element allows up to 100 different material layers. If more than 100 layers are required, the elements may be stacked. The element is defined by 20 nodes having three degrees of freedom per node: translations in the nodal x, y, and z directions. The y-direction corresponds to the longitudinal direction of the test specimen and the loading direction. The x-direction corresponds to the lateral direction of the test specimen. The z-direction corresponds to the thickness direction. Since the tensile specimen is placed in a servo hydraulic testing frame in the vertical position, directions x and y will be referred to herein as the horizontal and vertical directions, respectively. In this study, one SOLID191 finite element is used through the thickness of the specimen, each with eight layers. Convergence studies were conducted to evaluate the proper mesh size for the problem at hand. It was determined that 400 SOLID191 elements (5.08x8.89x4.9 mm (0.2x0.35x0.19 in)) were required as shown in Figure 2.68.

2.8.6. Model Restraints and Load Application

The outer surface nodes on the lower tabs in contact with the grips were restrained in the y-direction (Uy = 0), whereas the outer surface nodes in contact with the grips on the upper tabs were subjected to a uniform displacement of 10 mm (Uy = 10 mm) applied to the outer flat area. A uniform pressure of 130 kPa was applied perpendicular to the outer surface of the tabs to simulate the experimental grip pressure. The model along with its restraints, load application and mesh are shown in Figure 2.68.

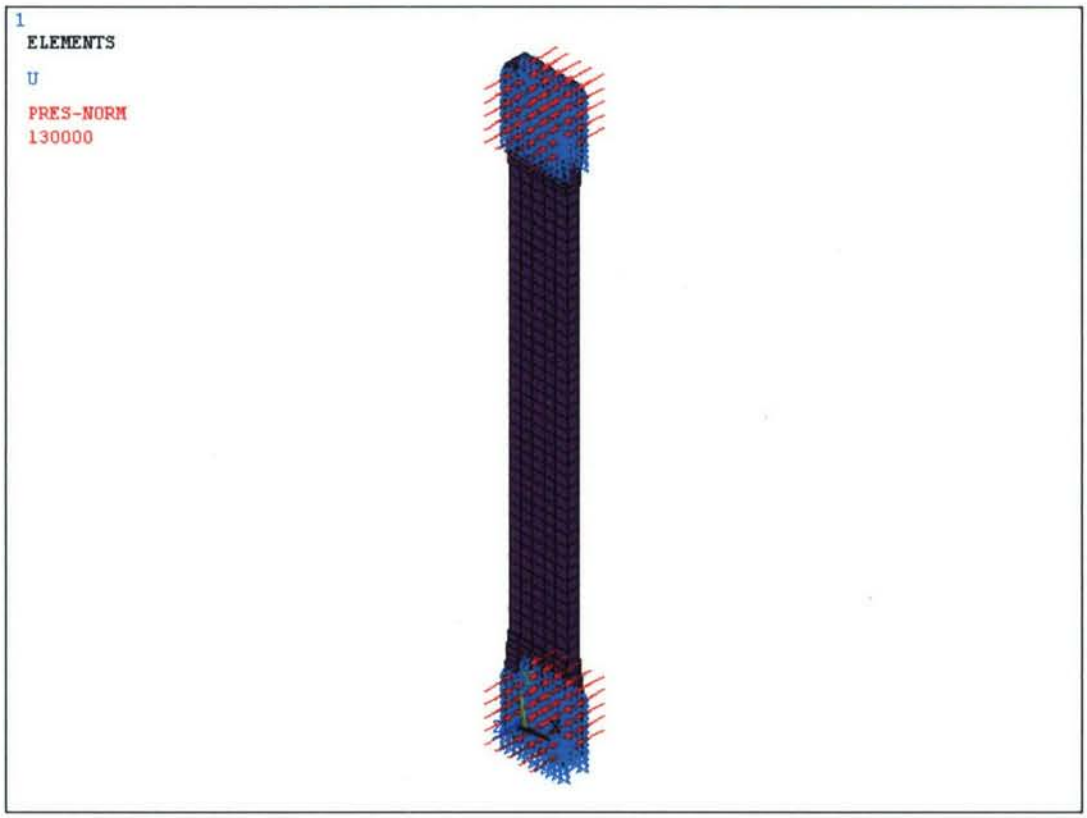

Figure 2.68 Finite element model of tension specimen with tabs

2.8.7. Model Components

The model is composed of three different components: tabs, adhesive and the PMC material. The mesh through the thickness of the tab area is shown in Figure 2.69. A single SOLID191 finite element consisting of eight layers was used to model the entire thickness of the specimen. In the tab region, three SOLID191 finite elements were stacked to model two elements were used to model the tabbing material and the adhesive layer on both sides and a single element for all eight PMC layers.

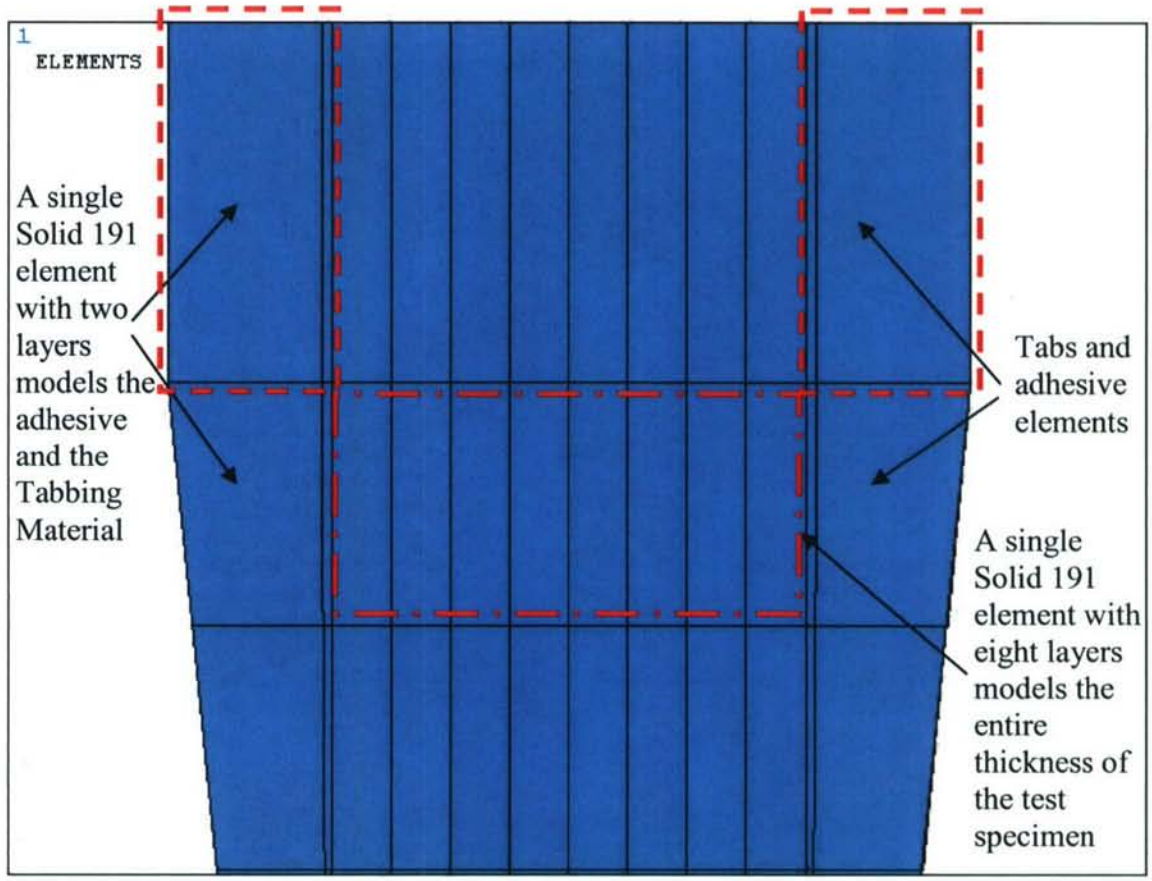

Figure 2.69 Vertical through the thickness section of the mesh within the tab area

2.8.8. Failure Criteria

In this study the following tow failure theories are considered: maximum stress theory and maximum strain theory (Daniel 1994; Barbero 1998). The strength ratio for maximum stress failure criterion is defined by equation (2.8) (ANSYS 2003):

$$\xi_1 = \text{maximum of} \begin{cases} \dfrac{\sigma_{xt}}{F_{1t}} \text{ or } \dfrac{\sigma_{xc}}{F_{1c}} \text{ whichever is applicable} \\ \dfrac{\sigma_{yt}}{F_{2t}} \text{ or } \dfrac{\sigma_{yc}}{F_{2c}} \text{ whichever is applicable} \\ \dfrac{\sigma_{zt}}{F_{3t}} \text{ or } \dfrac{\sigma_{zc}}{F_{3c}} \text{ whichever is applicable} \\ \dfrac{|\sigma_{xy}|}{F_{12}} \\ \dfrac{|\sigma_{yz}|}{F_{23}} \\ \dfrac{|\sigma_{xz}|}{F_{13}} \end{cases} \quad \textbf{(2.8)}$$

where

ξ_1 = value of maximum stress failure criterion

$\sigma_{xt} = \begin{cases} 0 \\ \sigma_x \end{cases}$ whichever is greater

σ_x = stress in layer x-direction

$\sigma_{xc} = \begin{cases} \sigma_x \\ 0 \end{cases}$ whichever is lesser

F_{1t} = failure stress in layer x-direction

The strength ratio for maximum strain failure criterion is defined by equation (2.9) (ANSYS 2003):

$$\xi_2 = \text{maximum of} \begin{cases} \dfrac{\varepsilon_{xt}}{\varepsilon_{1t}} \text{ or } \dfrac{\varepsilon_{xc}}{\varepsilon_{1c}} \text{ whichever is applicable} \\ \dfrac{\varepsilon_{yt}}{\varepsilon_{2t}} \text{ or } \dfrac{\varepsilon_{yc}}{\varepsilon_{2c}} \text{ whichever is applicable} \\ \dfrac{\varepsilon_{zt}}{\varepsilon_{3t}} \text{ or } \dfrac{\varepsilon_{zc}}{\varepsilon_{3c}} \text{ whichever is applicable} \\ \dfrac{|\varepsilon_{xy}|}{\varepsilon_{12}} \\ \dfrac{|\varepsilon_{yz}|}{\varepsilon_{23}} \\ \dfrac{|\varepsilon_{xz}|}{\varepsilon_{13}} \end{cases} \quad (2.9)$$

where

ξ_2 = value of maximum strain failure criterion

$\varepsilon_{xt} = \begin{cases} 0 \\ \varepsilon_x \end{cases}$ whichever is greater

ε_x = strain in layer x-direction

$\varepsilon_{xc} = \begin{cases} \varepsilon_x \\ 0 \end{cases}$ whichever is lesser

ε_{1t} = failure stress in layer x-direction

2.8.9. Probabilistic FEA Model using Monte Carlo Simulations

The Monte Carlo numerical simulation is a powerful tool for analyzing structures with property uncertainty (Ayyub et al. 1984; Mansour 1990; Di Sciuva et al. 2003). This method predicts the response of a structure subjected to variable design parameters of known or pre-described probability distributions. Using statistical sampling techniques, a set of values of the basic random variables are generated according to their corresponding probability distributions. The generated basic random variables are used in the finite element model to compute the structure response. The sampling procedure is repeated to obtain a multitude of simulated solutions. In addition to mesh convergence studies for the deterministic model, additional convergence studies were conducted to evaluate the number of simulations required to properly characterize the output property of interest in terms of its mean value and its coefficient of variation (COV). It was determined that 500 simulations as shown in Figure 2.73 were adequate to achieve convergence for both the mean and the COV of the tensile strength and the modulus of elasticity of the tensile coupon x. Figure 2.70 provides a simplified flowchart of the probabilistic FEA model used in this study.

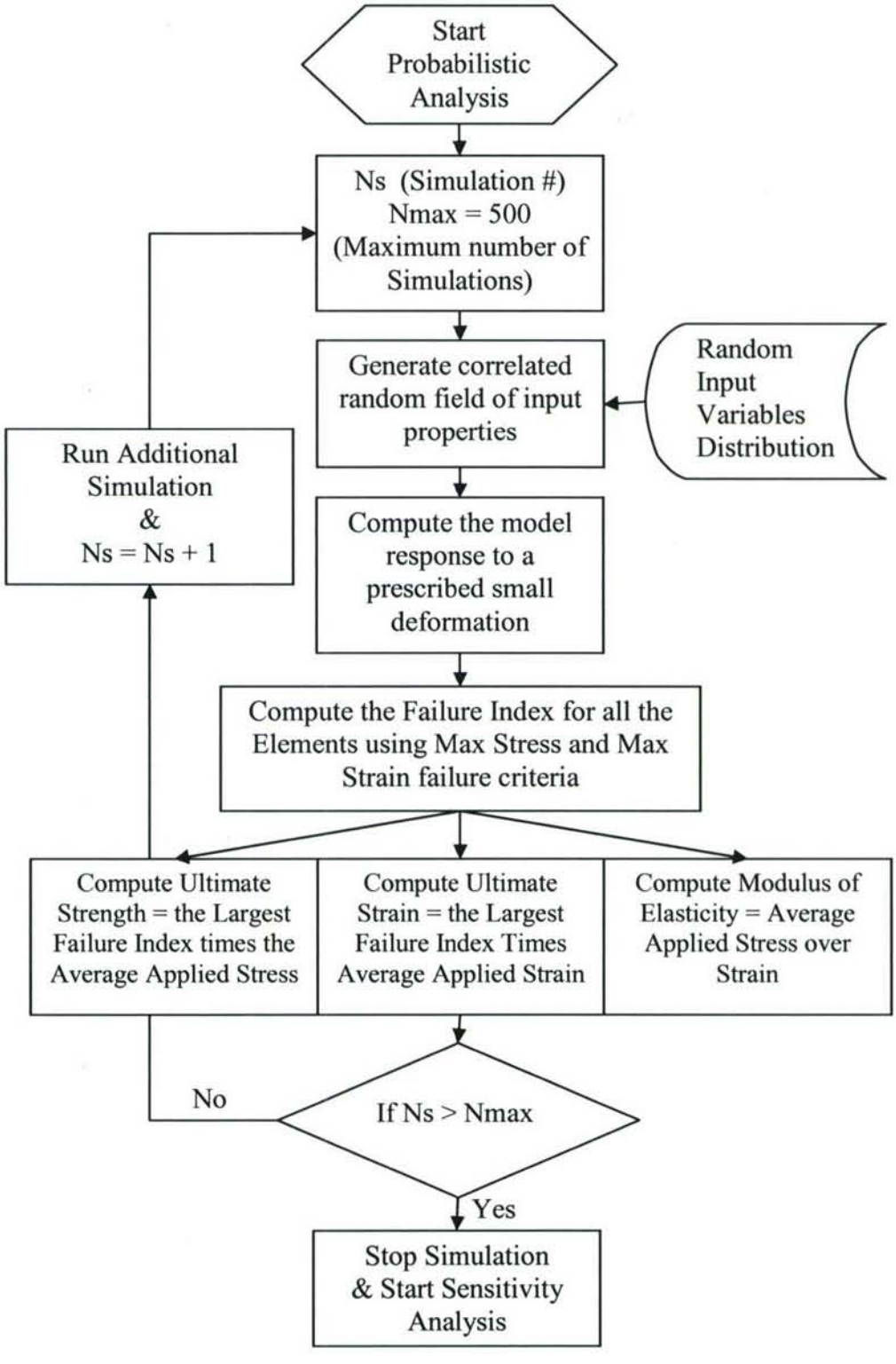

Figure 2.70 Flowchart for the probabilistic strength analysis of tension test

2.8.10. Statistical Properties of the Basic Random Variables Used in the FEA Model

The PMC panels used in this study were composed of woven fabric reinforcement and a vinyl ester resin. Composite panels with a thickness of 4.9 mm (0.193 in) were fabricated using the Vacuum Assisted Resin Transfer Molding (VARTM) process with the proprietary SCRIMP technology. The fiber reinforcement was woven fabric with a weight per unit area of 817.13 g/m^2 (24.1 oz/yd^2) and the style was Saint Gobain Vetrotex 324. The warp and fill directions have 55% and 45% respectively of the total fiber weight. In the warp direction tows are spaced 5.1 mm (5 tows per inch) and in the fill direction 6.4 mm (4 tows per inch). The polymer resin selected was Derakane 8084 (Ashland 2004), which is an elastomer-modified epoxy vinyl ester resin. The material system selection is consistent with the materials used in other Navy composite programs. The input material properties used in the FEA model to predict the $[0/90]_{2sf}$ properties were determined by conducting a series of material property tests on the $[0]_{4sf}$ materials in a climate controlled room with a temperature of (22°C) and a relative humidity of 50%. The experimental test methods used are listed in Table 2., even though only tension is relevant in this context. Eight specimens were tested to obtain each of the tension, compression and shear properties, from which the mean values and COV used in the FEA model

Table 2.10 Material test methods used to obtain the FEA model input data

Tests	Test Methods
Tension	ASTM D3039
Compression	ASTM D6641
Shear	ASTM D4255

The $[0]_{4sf}$ lay-up PMC material has a slightly nonlinear response in tension that may be represented using a bi-linear model as shown in Figure 2.71. The change in slope of the stress-strain curve, which corresponds to a reduction in longitudinal elastic modulus, is an indicator of the onset of damage.

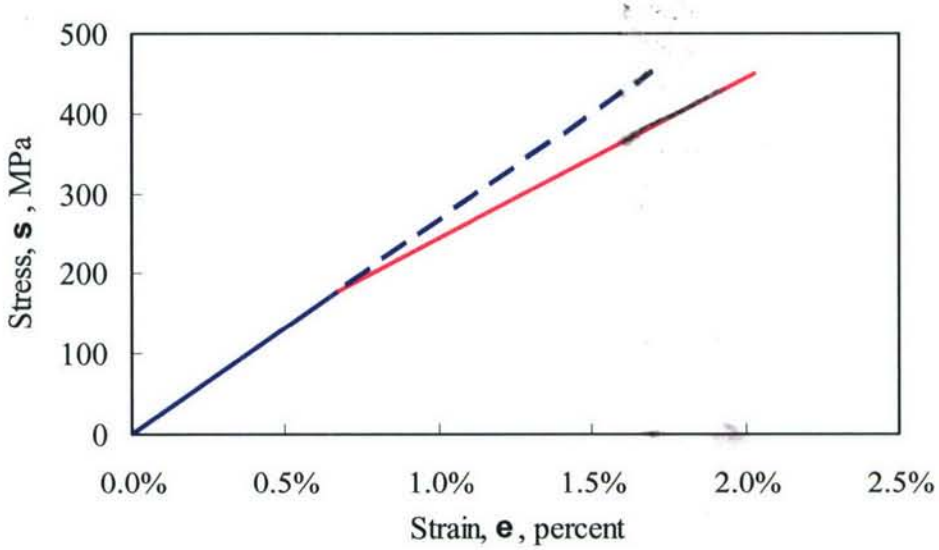

Figure 2.71 Linear and Bi-linear model of PMC material (Lopez-Anido et al. 2004)

Because of the computational effort required in a nonlinear probabilistic FEA model, in this work, the stress-strain relationship was approximated as linear-elastic to failure as represented by the dashed line in Figure 2.71. Therefore, the failure prediction corresponds to ultimate failure (UF). When a stress-based failure criterion is used (Maximum Stress) this approximation results in a good estimation of tensile strength corresponding to UF; however, ultimate strain predictions will be considerably smaller than actual experimental values. Conversely, when a strain-based failure criterion is used (Maximum Strain), ultimate tensile strength predictions are considerably higher than actual experimental values.

Sources of variability of the material coupon test results include overall specimen dimensions, inherent material property variability of both the resin and fibers, manufacturing process variables including fiber alignment, degree of cure and post-cure related to the environment in which the specimens were stored, and laboratory testing variability. In this probabilistic FEA study, elastic properties ($E_{11}, E_{22}, G_{12}, \nu_{12}$), strength parameters ($F_{1t}, F_{1c}, F_{2t}, F_{2c}, F_6$, $\varepsilon_{1t}, \varepsilon_{1c}, \varepsilon_{2t}, \varepsilon_{2c}, \varepsilon_{12}$) and geometric properties (thickness, fiber misalignment) of woven fabric E-glass / vinyl ester coupons in the warp and fill directions were considered as random fields, and were generated using Monte Carlo simulations. The basic material properties were obtained from laboratory test data of $[0]_{4sf}$ lay-ups, and in turn used to predict the properties of the $[0/90]_{2sf}$ lay-ups. Table 2.1 summarizes the woven fabric E-glass / vinyl ester material properties used as input to the FEA model in this study. Elastic moduli of the PMC material were considered to follow normal distributions. The ultimate

strength properties of the laminates were considered to follow both normal and lognormal distributions.

Table 2.11 Woven fabric E-glass / vinyl ester material properties

Random Variable	Mean Values	COV	Distribution Type
E_{11}	26.6 GPa	1.11%	Normal
E_{22}	22.6 GPa	1.64%	Normal
ν_{12}	0.136	8.78%	Normal
G_{12}	4.86 GPa	3.50%	Normal
ε_{1t}	0.0203	4.18%	Normal/Lognormal
ε_{1c}	0.0142	9.37%	Normal/Lognormal
ε_{2t}	0.0199	2.79%	Normal/Lognormal
ε_{2c}	0.0164	9.76%	Normal/Lognormal
ε_{12}	0.00245	5.00%	Normal/Lognormal
F_{1t}	450 MPa	4.10%	Normal/Lognormal
F_{1c}	376 MPa	5.70%	Normal/Lognormal
F_{2t}	348 MPa	2.50%	Normal/Lognormal
F_{2c}	373 MPa	4.60%	Normal/Lognormal
F_{12}	182 MPa	1.79%	Normal/Lognormal

The probabilistic model developed herein assumes a linear exponential decay autocorrelation function of the material properties defined by equation (2.10) (ANSYS 2003):

$$\rho_{ij} = \exp\left(-\left(\frac{D(\{x_i\},\{x_j\})}{C_L}\right)\right) \qquad \textbf{(2.10)}$$

where $D(\{x_i\},\{x_j\})$ is the distance between the elements centroids in the finite element mesh and C_L is the correlation length. As the distance between the elements increases the autocorrelation of the properties decreases as shown in Figure 2.72. Conversely, as the correlation length increases the autocorrelation between the elements properties increases.

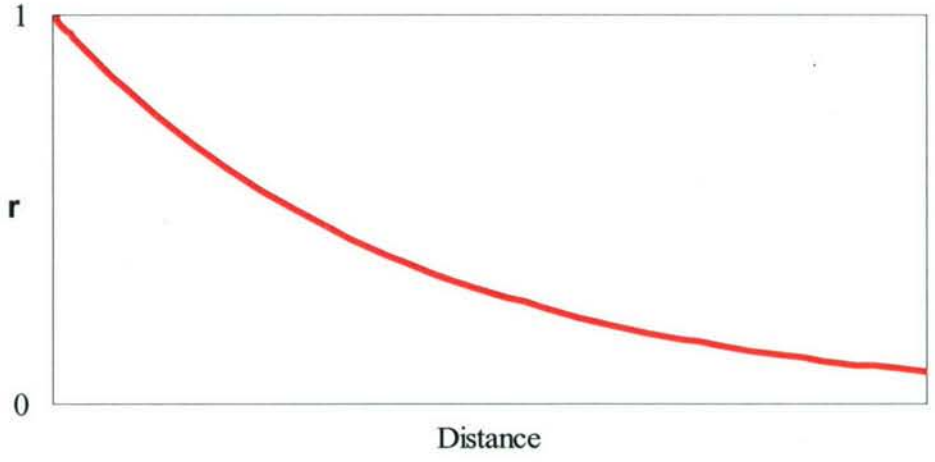

Figure 2.72 Linear exponential decay autocorrelation function

2.8.11. Numerical Results and Discussion

The observations given below relate to the specific tension coupon problem at hand and may change for different material types, material tests, and failure modes. In the figures that follow, the experimental minimum and maximum values from the material tension tests are plotted as dotted horizontal lines, allowing a comparison between the probabilistic FEA results and the laboratory test results.

In the following discussion, we seek to gain a better understanding of how to assign property variability to individual finite elements in order to properly predict the variability of the tension coupon properties. As we do so, it is important to note that the input properties' correlation lengths have not been obtained experimentally, so an effort is also made in the discussion below to "back out" the PMC correlation lengths by comparing the probabilistic FEA model predictions with the experimental results.

2.8.12. Convergence of Monte Carlo Simulation

The statistical accuracy of the ultimate strength, ultimate strain and effective modulus of elasticity's mean and standard deviation predictions in the y-direction increased as the number of simulation cycles increased. The probabilistic analysis convergence for 500 simulations of the mean and standard deviation of the ultimate strength as predicted using maximum stress failure criterion are shown in Figure 2.73 (a) and (b), respectively.

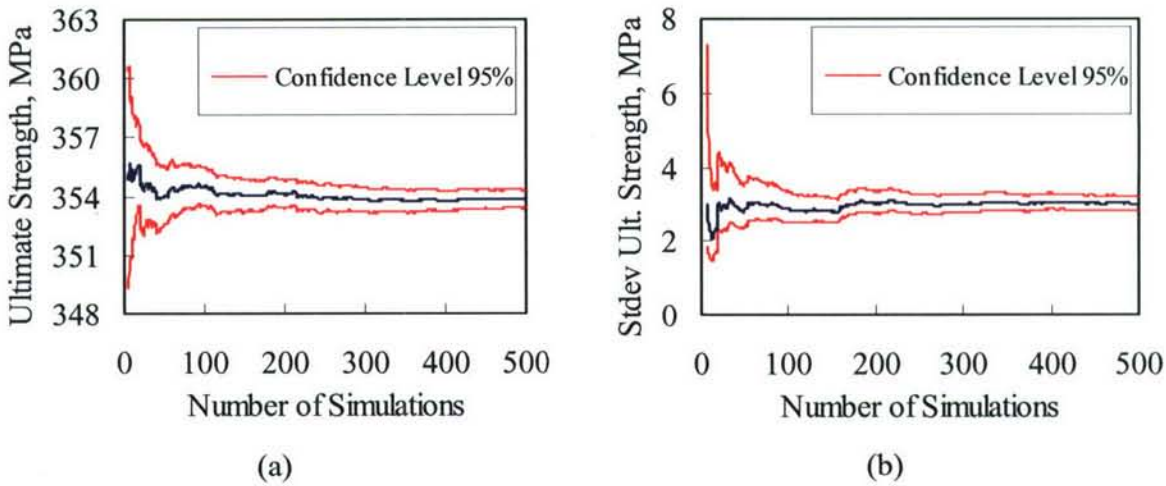

Figure 2.73 Convergence of the mean value (a) and standard deviation (b) of the ultimate strength using maximum stress failure criterion for 500 simulations

In addition to verifying convergence of the results with respect to both the number of elements and the number of simulations, the accuracy of the generated property probability density functions (PDF) was verified for each of the basic input random variables, as shown for example for the elastic property E_{11} in Figure 2.74.

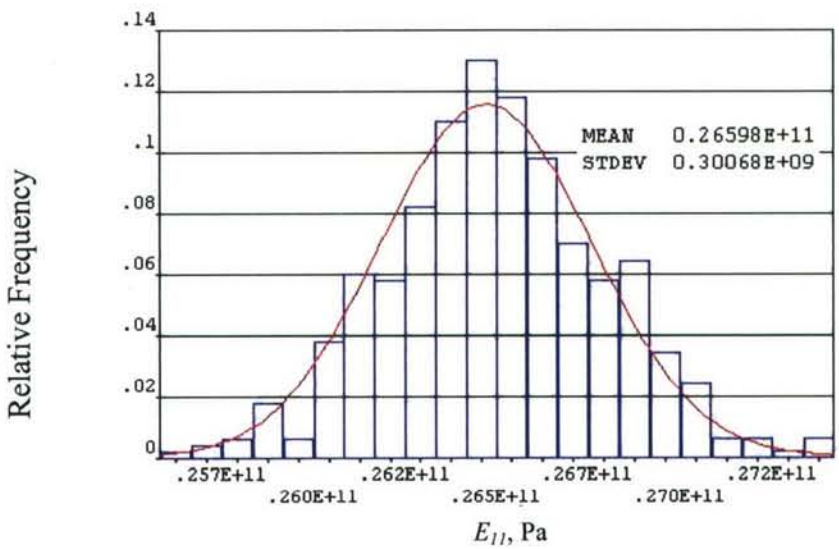

Figure 2.74 Modulus of elasticity E_{11} samples follow the pre-assigned normal distribution with the input mean and COV

2.8.13. Effect of Type of PDF

Both the lognormal and normal distribution assumptions for the basic input variables produced similar results for the coupon ultimate strength's mean and COV, as shown in Figure 2.75 (a) and (b).

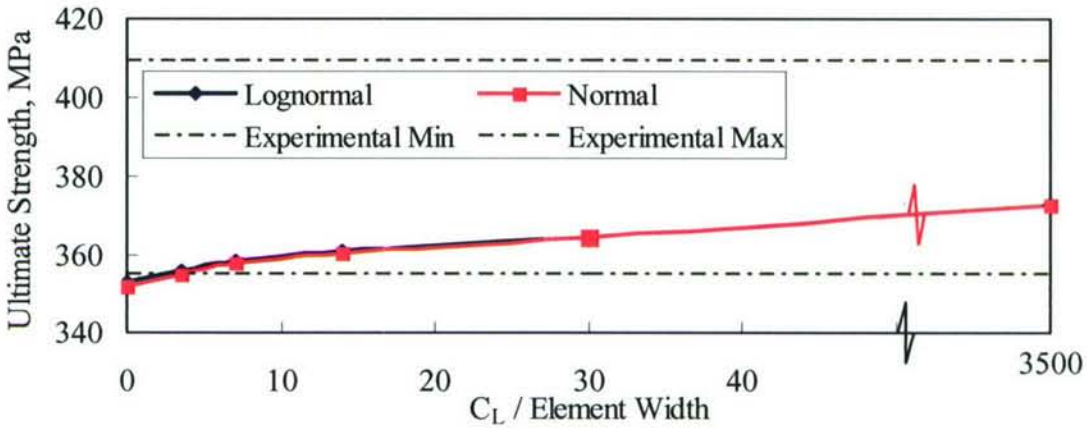

(a)

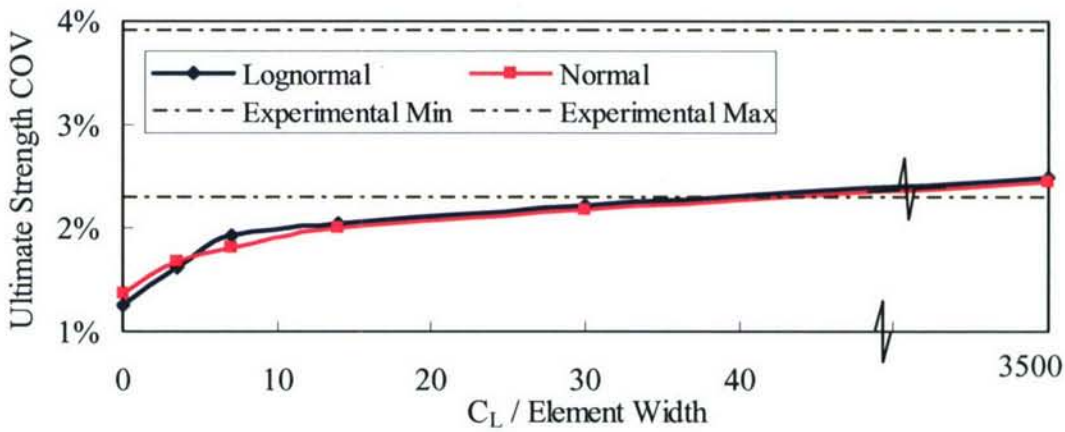

(b)

Figure 2.75 Effect of normal vs. normal/lognormal distribution on ultimate strength mean (a) and COV (b) using maximum stress failure criterion

2.8.14. Effect of Failure Criteria

Maximum stress failure criteria produced very good predictions for the ultimate strength as shown in Figure 2.76. However, as previously mentioned maximum strain failure criteria over predicts the ultimate strength and this is due to the linear elastic material model used in this study for a bilinear material in tension as shown in Figure 2.71.

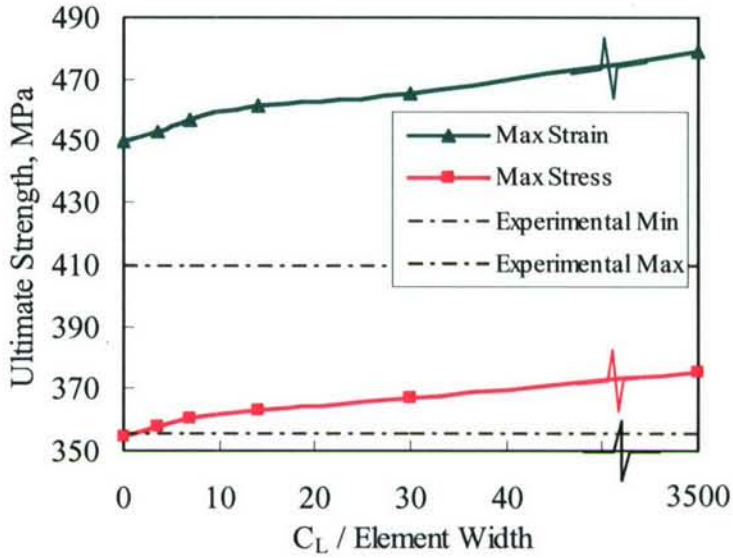

Figure 2.76 Effect of failure criteria on the ultimate strength

2.8.15. Effect of Spatial Correlation

The effect of spatial correlation is tied to the magnitude of the basic input properties COV. To evaluate this effect, the experimentally determined input material properties COV given in Table 2.1 were multiplied by the following factors: 0.5, 2 and 4 and the probabilistic FEA analyses were conducted for each case. The results are given in Figure 2.77 through Figure 2.80, in which the horizontal axis gives a dimensionless correlation length: (correlation length)/(width of finite element in the x-direction).

Figure 2.77 (a) shows that the mean effective modulus of elasticity Eyy is not significantly affected by the correlation length, material variability, nor by the mesh refinement. On the other hand, Figure 2.77 (b) shows that the COV effective modulus of elasticity Eyy increases as the correlation length increases and that assigning the experimental material property COV to all individual finite elements will underestimate the predicted COV of the effective modulus of elasticity. For this problem, assigning 1.5 to 2 times the material experimental COV to individual finite elements and a correlation length over element width ranging between 10 and infinity will lead to a better prediction of the effective Eyy COV.

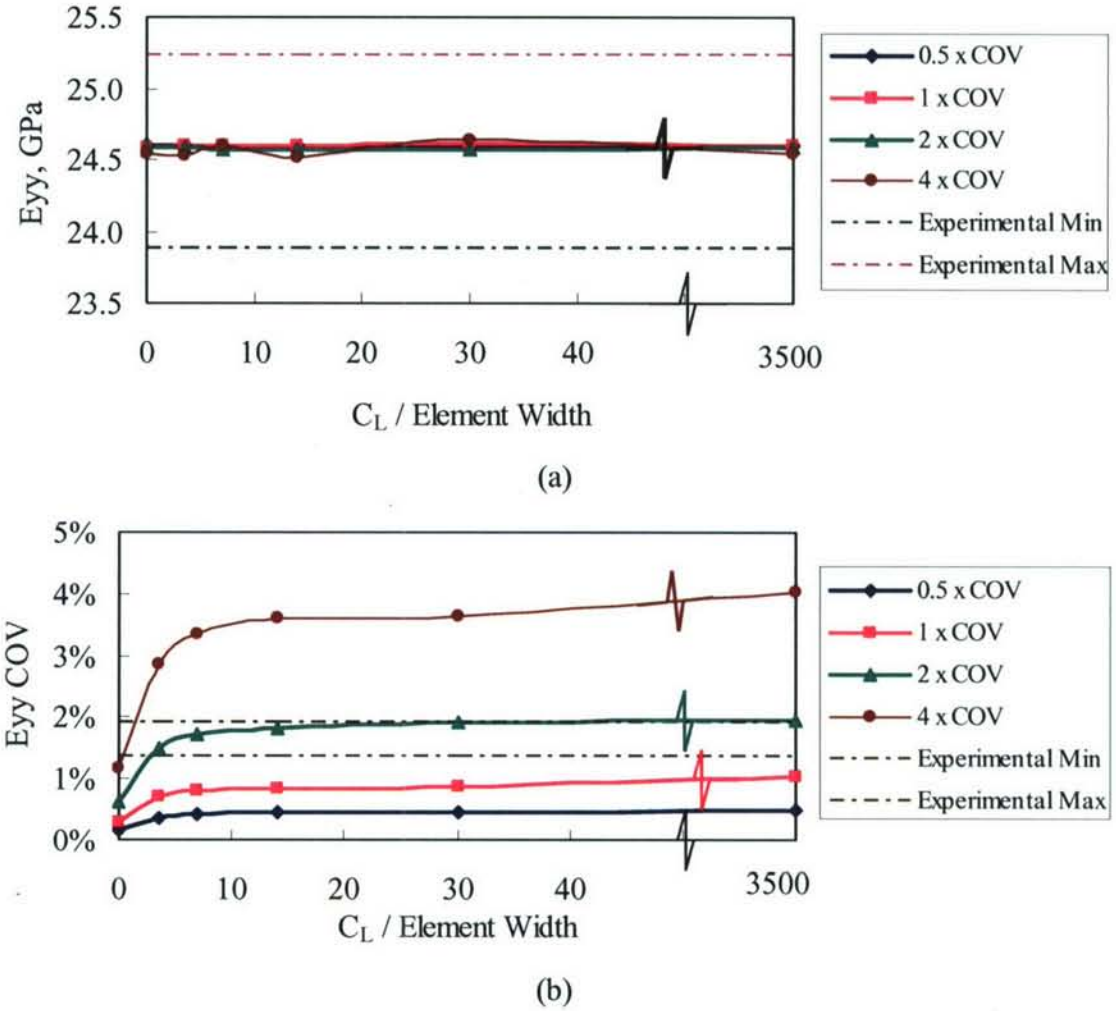

Figure 2.77 Effective modulus of elasticity: (a) mean value, (b) coefficient of variation

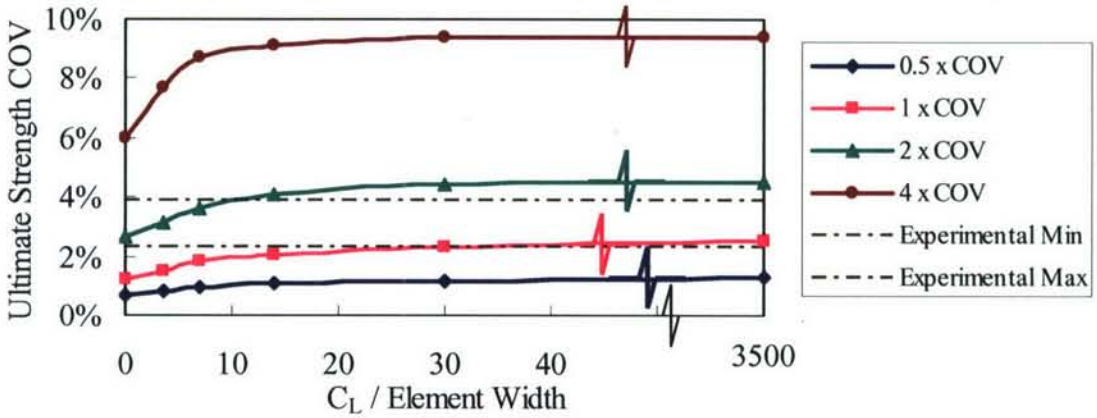

Figure 2.78 Correlation length and material variability effect on the ultimate strength variability using maximum stress failure criterion

The predicted ultimate strength COV is a function of the correlation length, as shown in Figure 2.78. In this case, assigning one to two times the material experimental COV to individual finite elements with a correlation length over element width ranging between 10 and infinity will lead to a better estimation of the ultimate strength variability, as predicted by maximum stress failure criterion.

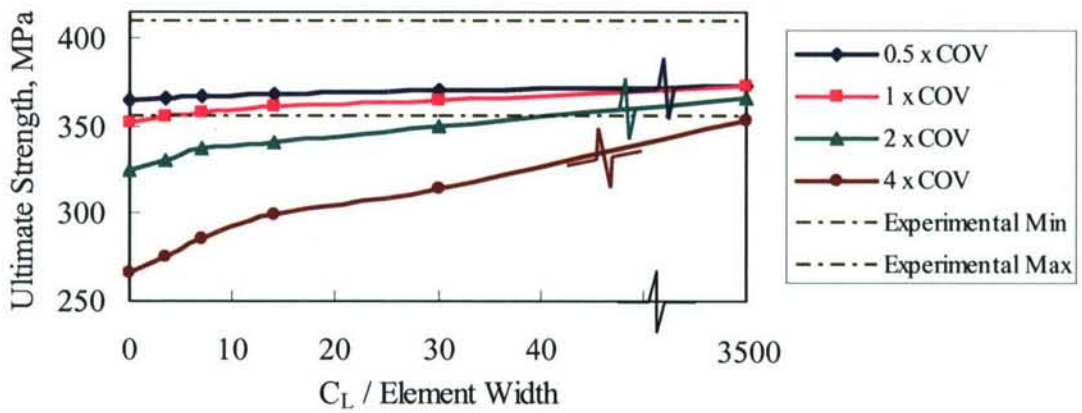

Figure 2.79 Ultimate strength vs. correlation length for various material COVs

Other studies (Kural et al. 1983; Adams et al. 2002) have evaluated the effects of stress concentrations in the tab region of the PMC tension test. This stress concentration in the vicinity of the tabs is due to the geometric discontinuity at the tab termination and the difference of material properties among the adhesive, the tabs and the PMC material. It was previously shown (Adams et al. 2002) that the stress concentration in the tab region might vary between 1.02 and 1.07 depending on several factors. The stress concentration is dependent on the adhesive thickness, tab geometry (thickness, length, taper

angle) and material properties of the tab, the adhesive properties and the properties of the composite material being tested. Using the FEA model and mesh described here, the tab stress concentration factor ranged between 1.007 and 1.036, which falls within the limits of previous studies (Adams et al. 2002).

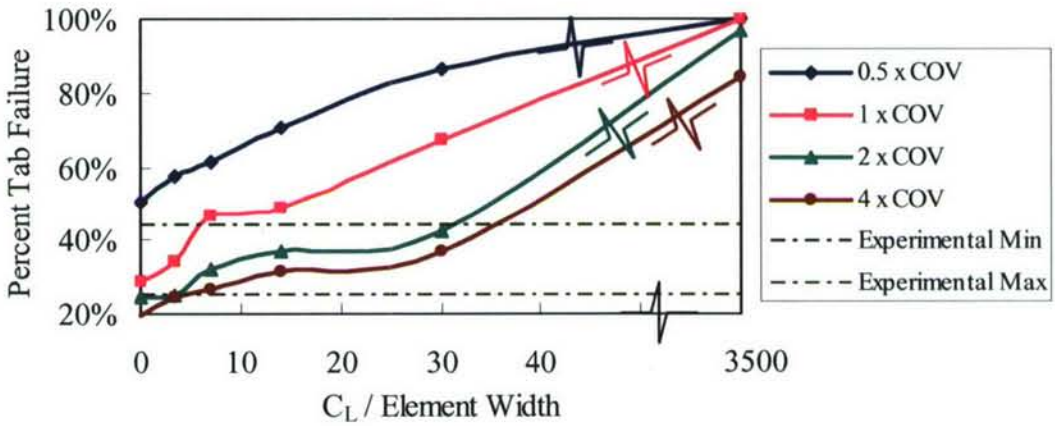

Figure 2.80 Correlation length effect on percent tab failure

It is useful to compare the frequency of tab failures as predicted by the probabilistic FEA model with the frequency of tab failure observed in the laboratory tension test. Assuming one considers a specimen to have a tab failure if failure occurs within a distance of three times the specimen thickness from the tab ending. With this definition, Figure 2.80 shows both the experimental and the predicted tab failure as one changes the correlation length and the COV of the input material properties. This figure shows that assigning one to two times the material experimental COV with a correlation length over element width ranging between 5 and 30 leads to a good prediction of the percent of experimental tab failures using the maximum stress failure criterion.

2.8.16. Effect of Mesh Refinement

When running Monte Carlo simulations, refining the FEA mesh for the tension coupon will lead to a larger number of elements generated, with a larger probability of generating an element with weak properties, leading to a lower tensile strength, using the weak-link chain model. As shown in Figure 2.81, refining the mesh in such a manner does lead to a significant decrease ~7% in the predicted ultimate strength if the basic material COV is in the range of 10% or more, and if the correlation length is small.

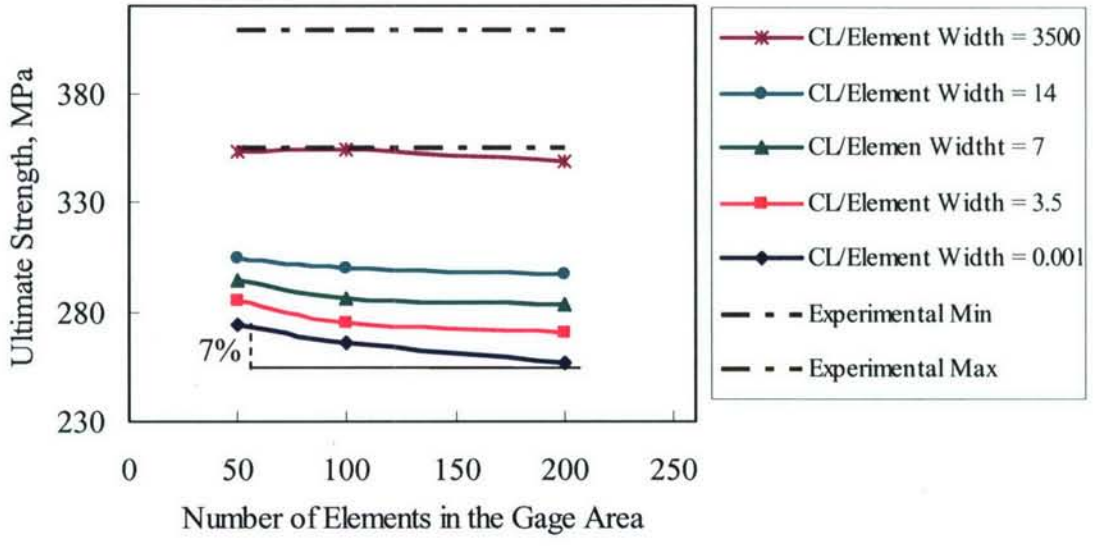

Figure 2.81 Effect of mesh refinement on the Ultimate Strength for four times experimental COV

2.8.17. Sensitivity Analysis

The probabilistic sensitivity was based on the correlation coefficients between all random input variables and the random output parameters. There is a difference between probabilistic sensitivities and deterministic sensitivities. Deterministic sensitivities are mostly only local gradient information. To evaluate a deterministic sensitivity, one would vary each input parameter by a certain percentage while keeping the remaining input parameters constant. Then, by computing the change in the output parameter one would know the sensitivity of the former input parameter on the output parameter. These deterministic sensitivities are not as accurate as the probabilistic sensitivities.

A deterministic sensitivity does not take into account the physical range of variability into account. For example having an input parameter varied by ±10% to compute the deterministic sensitivity is not accurate enough because it does take into account the actual physical variability and randomness. Whereas, the probabilistic sensitivity is influenced by the actual random input variables scatter. Therefore, two effects influence the probabilistic sensitivity: the slope of the gradient and the physical variability and randomness of the random input variables. If an input variable has a certain scatter, then the output parameter scatter is affected by the slope of the output parameter as shown in Figure 2.82 (a). However if an output parameter has a moderate variation with respect an input parameter it still can have a significant scatter if the random input variable has a wider range as show in Figure 2.82 (b).

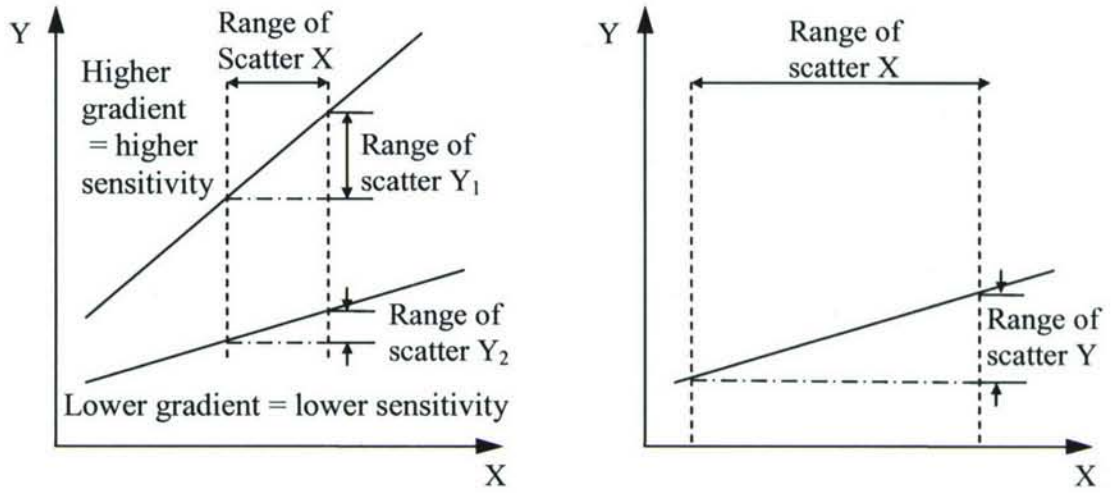

Figure 2.82 Slope and scatter range influence on the sensitivity

One should note that the deterministic gradient information does not account for possible interaction with other input parameters. On the other hand, a probabilistic sensitivity accounts for any possible interaction with other random input parameters since Monte Carlo simulations always vary all random input variables at the same time.

As expected the effective modulus of elasticity is mainly affected by the laminate extensional modulus of elasticity in both directions since the lay-up is warps alternating, see Figure 2.83. The ratio of the correlation sensitivity affecting the effective modulus of elasticity between E_{22} and E_{11} is 1.23 which nothing but 55/45 since the warp and fill directions have 55% and 45% respectively of the total fiber weight.

If a stress-based failure criteria was used, the strength is mainly affected by F_{2t}. However, if a strain based failure criteria was used then ε_2 is mainly the dominant factor as shown in Figure 2.83.

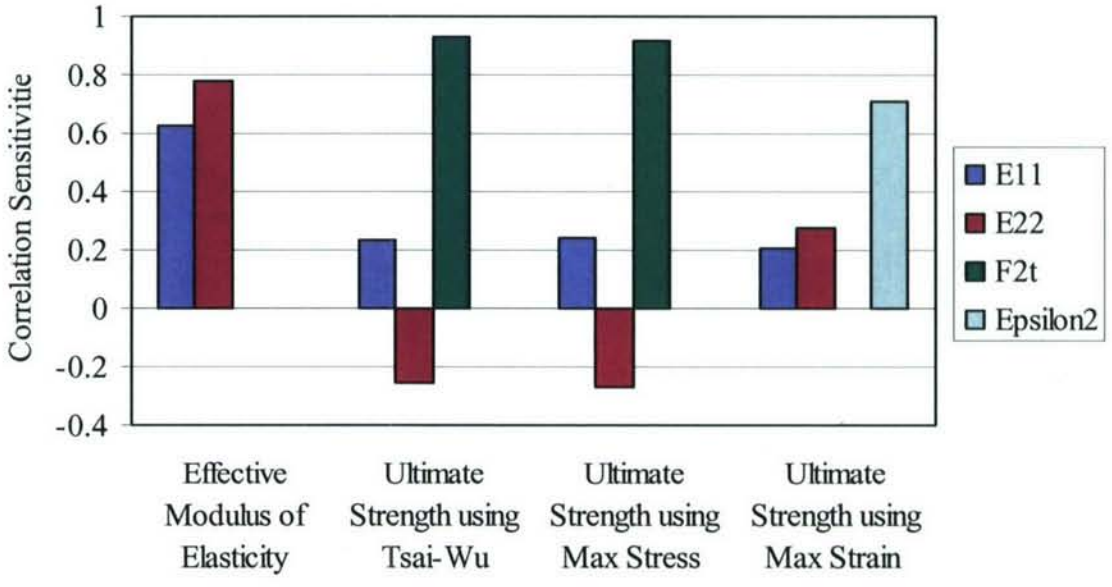

Figure 2.83 Sensitivity analysis for all output parameters

Finally, it is important to note that a positive sensitivity indicates that increasing the value of the random input variable increases the value of the random output parameter. Similarly, a negative sensitivity indicates that increasing the random input variable value decreases the random output parameter value. For example, in Figure 2.83 E_{22} have a negative sensitivity for the ultimate strength and the reason is that since E_{22} is the stiffness of the PMC material in the fill direction; as E_{22} increases more load is attracted in the fill direction and since the fill direction is weaker than the warp direction this will lead to a lower failure load.

Summarizing the observations in this section, we sought to determine how to assign individual finite elements properties in the probabilistic FEA model in order to properly predict the mean and COV of the tension coupon strength and modulus of elasticity, as well as the observed frequency of tab failures. It appears that a correlation length over element width of 15 to 30 (correlation length of 76 mm to 152 mm) with an individual finite element property COV of one to two times the experimental values will lead to good predictions of the observed coupon properties. These observations apply to the specific properties of the tension coupon used in this study.

2.8.18. Concluding Remarks

Probabilistic finite element analysis procedures based on Monte Carlo simulation techniques have been developed for the ASTM D3039 standard tension test. The study evaluated the effects of spatial correlation, finite element size, probability distribution functions and failure criteria on statistical strength properties of tension test coupons. Useful observations were given on

how to assign mean and COV of material properties to individual finite elements within a mesh, which allowed reconciliation experimental values with the probabilistic FEA model predictions. Numerical results showed the importance of correlation length, assignment of property COV to individual finite elements, and mesh refinement in a probabilistic finite element analysis

3. Recommendations

The following is a summary of the significant recommendations developed in this project that will be incorporated in future works pertaining to marine grade woven roving e-glass vinyl ester material systems.

- Use strain measuring devices capable of capturing a representative size (typically 3 weave patterns) of the reinforcing fabric. This program utilized a digital image correlation system.
- In plane shear material testing, the three rail shear test is recommended for measuring in plane shear material properties. The gage area of the specimen is sufficiently large enough to capture a representative sample of the material.
- Compression testing, ASTM 6641 with modifications to specimen geometry is recommended. Minimum specimen geometries should be set by the weave pattern of the reinforcing fibers. In this program the overall specimen length was increased to 6.2 inches and the specimen width was increased to 0.75 inches.
- Tension test, ASTM 3039 with modifications to specimen geometry is recommended. Minimum specimen geometries should be set by the weave pattern of the reinforcing fibers. A dumbbell shape was adopted and optimized to simplify material testing
- Flexure test, ASTM 7264 is recommended. This standard was adopted by the governing ASTM committee largely based on efforts of this program.
- Use probabilistic finite element methods that account for the spatial variability of the material system to predict a range of structural responses (deflections, 1st ply-failure,... etc.)
- Use appropriate statistical tests and a simple percent difference of the means calculation to establish a practical significance for future interpretations of the data. Typically in engineering practice the practical level of significance would be between 5% and 10%.

4. Future Work

The effort contained in this report is the first phase of a two-phase program to determine the variabilities of fiber-reinforced plastics particularly heavy weight e-glass vinyl ester woven roving laminates. The recommendations outlined in the previous section will be followed during the second phase of this program. Highlights for the phase two efforts are a follows

- Conduct a vendor study(five vendors have been selected) to fabricate test panels similar to the panels utilized in this body of work
    - Test coupon, component (beam in 4 point bending) and structural (panel in 4 point bending) level tests
- Continue to develop probabilistic finite element models that are capable of propagating error from material coupon level test data through component testing then finally to large structural elements.
- Conduct a laboratory study that considers the effects of fiber storage, fabric consolidation, and resin recipe on strength, stiffness and toughness of the laminate

The acoustic emission (AE) monitoring work conducted under Phase I showed a consistent response for tension testing. The AE energy distribution showed three distinct phases under uniaxial tension: little AE activity, rapid release of AE energy, and slower steady state release of AE energy up to rupture of the specimen. These three phases are consistent with microcracking behavior related to, respectively: purely elastic behavior, damage initiation and distributed cracking, and localization of damage into a failure zone. The important thing to note is that these three distinct phases do not manifest themselves in the specimen load-deformation curve, which tends to show a smooth monotonically increasing relationship. Thus, the load-deformation curves do not reflect the occurrence of damage in the same way that a yield point reflects formation of a plastic zone, for example. This lack of a clear transition in the load deformation behavior makes a definition of failure much more difficult. In Phase II of the project we will focus on this localization of damage phenomenon, and its corresponding change in AE energy distribution. Once refined it can provide the basis for a more rational definition of failure.

5. Phase I: Theses & Publications

The following is a list of published works related to the Phase I program, other internal reports and subcontractor reports are not listed but referenced where appropriate.

- Fadi El-Chiti, M.S. Thesis (in Mechanical Engineering)
  Title: *Experimental Variability of E-Glass Reinforced Vinyl Ester Composites Fabricated by VARTM/SCRIMP*
- Ghassan Fayad, M.S. Thesis (dual degree in Civil and Mechanical Engineering)
  Title: *Probabilistic Finite Element Analysis of Marine Grade Composite*
- *Composite Material Testing Using a 3-D Digital Image Correlation System,* by R. Lopez-Anido, F. El-Chiti, L. Muszynski, H. Dagher, L. Thompson, and P. Hess. COMPOSITES 2004 Convention and Trade Show, Tampa, FL, October 2004.
- *Probabilistic Finite Element Analysis of ASTM D3039 Tension Test for Marine Composites,* by G. Fayad, H. Dagher, R. Lopez-Anido, L. Thompson, and P. Hess. SAMPE 2005 Symposium & Exhibition (50th ISSE), Long Beach, CA, May 2005.
- *Experimental Approach for Characterizing VARTM Composites using a 3-D Digital Image Correlation System*, by F. El-Chiti, R. Lopez-Anido, H. Dagher, L. Thompson, L. Muszynski, and P. Hess. SAMPE 2005 Conference and Exposition, Portland, OR, June 2005.
- *Variability in Flexural Response of E-Glass/Vinyl Ester Composites Fabricated using the VARTM Process,* by K. Berube, R. Lopez-Anido, V. Caccese, and P. Hess. SAMPE 2006, Long Beach, CA, April 2006.

6. References

AASHTO, *LRFD Bridge Design Specifications*. 1998, Washington, D.C.: American Association of State Highway and Transportation Officials.

Adams, D. F. and E. Q. Lewis (1990). "Influence of Specimen Gage Length and Loading Method on the Axial Compressive Strength of a Unidirectional Composite Material." Experimental Mechanics (March 1991).

Adams, D. F. and E. Q. Lewis (1991). "Influence of Specimen Gage Length and Loading Method on the Axial Compressive Strength of a Unidirectional Composite Material." Experimental Mechanics 31 (2): 14-20.

Adams, D. F. and E. Q. Lewis (1997). "Experimental Assessment of Four Composite Material Shear Test Methods." Journal of Testing and Evaluation Vol. 25 (March 1997).

Adams, D. O. and D. F. Adams 2002. Tabbing Guide for Composite Test Specimens. U.S. Department of Transportation, Washington DC. Report#: DOT/FAA/AR-02/106.

AF&PA, *Load and Resistance Factor Design (LRFD), Manual for Engineered Wood Construction*. 1996, Washington, DC: American Forest and Paper Association & American Wood Council. 250.

ANSYS (2003). ANSYS 8.0 University high option, [CD-ROM] SAS IP, Inc. Available: ANSYS, Inc.

Ashland (2004). Derakane 8084 Epoxy Vinyl Ester Resins. Composite Polymers. Columbus, OH, Ashland Inc.: 3 Pages.

ASTM D638, (2002). Standard Test Method for Tensile Properties of Plastics. Annual Book of ASTM Standards, American Society of Testing Materials. Vol 08.01.

ASTM D695, (1996). Standard Test Method for Compressive Properties of Rigid Plastics. Annual Book of ASTM Standards. West Conshohocken, American Society of Testing Materials. Vol 08.01.

ASTM D3039/D3039M, (2000). Standard Test Method for Tensile Properties of Polymer Matrix Composite Materials. Annual Book of ASTM Standards. West Conshohocken, American Society of Testing Materials. Vol 15.03.

ASTM D3410/D3410M, (2003). Standard Test Method for Compressive Properties of Polymer Matrix Composite Materials with Unsupported Gage Section by Shear Loading. Annual Book of ASTM Standards. West Conshohocken, American Society of Testing Materials. Vol 15.03.

ASTM D3518/D3518M, (2001). Standard Test Method for In-Plane Shear Response of Polymer Matrix Composite Materials by a Tensile Test of a ±45 laminate. Annual Book of ASTM Standards. West Conshohocken, American Society of Testing Materials. Vol 15.03.

ASTM D4255/D4255M, (2002). Standard Test Method for In-Plane Shear Properties of Polymer Matrix Composite Materials by the Rail Shear Method. Annual Book of ASTM Standards. West Conshohocken, American Society of Testing Materials. Vol 15.03.

ASTM D4762, (2004). Standard Guide for Testing Polymer Matrix Composite Materials. Annual Book of ASTM Standards. West Conshohocken, American Society of Testing Materials. Vol 08.04.

ASTM D5229/D5229M, (2002). Test Method for Moisture Absorption Properties and Equilibrium Conditioning of Polymer Matrix Composite Materials. Annual Book of ASTM Standards. West Conshohocken, American Society of Testing Materials. Vol 15.03.

ASTM D5379/D5379M, (1999). Standard Test Method for Shear Properties of Composite Materials by the V-Notched Beam Method. Annual Book of ASTM Standards. West Conshohocken, American Society of Testing Materials. Vol 15.03.

ASTM D5467/D5467M, (2004). Standard Test Method for Compressive Properties of Unidirectional Polymer Matrix Composites Using a Sandwich Beam. Annual Book of ASTM Standards. West Conshohocken, American Society of Testing Materials. Vol 15.03.

ASTM D5947-03, Standard Test Methods for Physical Dimensions of Solid Plastics Specimens, ASTM International, service@astm.org.

ASTM D6272-02, Standard Test Method for Flexural Properties of Unreinforced and Reinforced Plastics and Electrical Insulating Materials by Four-Point Bending, ASTM International, service@astm.org.

ASTM D6641/D6641M, (2001). Standard Test Method for Determining the Compressive Properties of Polymer Matrix Composite Laminates Using a Combined Loading Compression (CLC) Test Fixture. Annual Book of ASTM Standards. West Conshohocken, American Society of Testing Materials. Vol 15.03.

ASTM E4, (2002). Practices for Force Verification of Testing Machines. Annual Book of ASTM Standards. West Conshohocken, American Society of Testing Materials. Vol 03.01.

ASTM E111, (1997). Standard Test Method for Young's Modulus, Tangent Modulus, and Chord Modulus. Annual Book of ASTM Standards. West Conshohocken, American Society of Testing Materials. Vol 03.01.

ASTM E132, (1997). Standard Test Method for Poisson's Ratio at Room Temperature. Annual Book of ASTM Standards. West Conshohocken, American Society of Testing Materials. Vol 03.01.

Ayyub, B. M. and A. Haldar (1984). "Practical structural reliability techniques." Journal of Structural Engineering 110(8): 1707-1724.

Ayyub, B., J. Beach, and T. Packard, *Methodology for the Development of Reliability-based Design Criteria for Surface Ship Structures.* Naval Engineers Journal, ASNE, 1995. 107(1): p. 45-62.

Barbero, E. J. (1998). Introduction to Composite Materials Design. Philadelphia, Taylor & Francis, Inc.

Barbero, E. J. (1999). Introduction to composite materials design. Philadelphia, PA : Taylor and Francis, c1998.

Bausano, J.V. and J.J. Lesko. *Designing for FRP Composites' Durability through a Modified LRFD Approach.* In Proceedings of *10th US- Japan Conference on Composite Materials*. 2002: DEStech Publications, Lancaster, PA, 301-319

Bazant, Z. P. and J.-K. Kim (1991). "Segmental box girder. Effect of spatial random variability of material on deflections." Journal of Structural Engineering 117(8): 2542-2547.
Camata, G., R. Corotis, et al. (2004). "Simplified stochastic modeling and simulation of unidirectional fiber reinforced composites." Probabilistic Engineering Mechanics 19(1): 33-40.

Bruchman, D., and B.M. Ayyub, *Uncertainties in Mechanical Strength Properties of Ship Grade Steel.* Report No. NSWCCD-TR-65-96/17. 1995: Naval Surface Warfare Center, Carderock Division.

Chaterjee, S., D. Adams, et al. 1993. Test Methods for Composites a Status Report Volume I: Tension Test Methods. U.S. Department of Transportation, Washington DC. Report#: DOT/FAA/CT-93/17.

Dagher, H.J., S. Kulendran, A.H. Peyrot, M. Maamouri, Q. Lu., *System Reliability Concepts in the Design of Transmission Lines.* Journal of Structural Engineering, ASCE, 1993. 119(1).

Daniel, I. M. (1994). Engineering mechanics of composite materials. Oxford, [England] ; New York : Oxford University Press, c1994.

Di Sciuva, M. and D. Lomario (2003). "A comparison between Monte Carlo and FORMs in calculating the reliability of a composite structure." Composite Structures 59(1): 155-162.

Engelstad, S. P. and J. N. Reddy (1993). "Probabilistic nonlinear finite element analysis of composite structures." AIAA Journal 31(2): 362-369.

Fayad, G. (2005). Probabilistic Finite Element Modeling of Marine Grade Composites. Civil and Enviromental Engineering Department. Orono, University of Maine.

Frangopol, D. M. and S. Recek (2003). "Reliability of fiber-reinforced composite laminate plates." Probabilistic Engineering Mechanics 18(2): 119-137.

He, J., M. Y. M. Chiang, et al. (2002). "Application of the V-Notch Shear Test for Unidirectional Hybrid Composites." Composite Materials 36 (23): 2653-2666.

Hess, P.E., D. Bruchman, and B.M. Ayyub, *Uncertainties in Material and Geometric Strength Variables in Marine Structures*, in *Uncertainty Modeling and Analysis in Civil Engineering*, B.M. Ayyub, Editor. 1998, CRC Press: New York, NY.

Hess, P.E., and J.E. Beach. *On Acquisition Reform, Risk, and Structural Reliability*. In Proceedings of *American Society of Engineers Conference, ASE2000*. 2000. Arlington, VA,

Hess, P., *Reliability-Based, Operational Performance Metrics for Ship Structures (Ph.D. Dissertation)*, in *Department of Civil and Environmental Engineering*. 2002, University of Maryland.

Ifju, P. G. (1994). "The Shear Gage: For Reliable Shear Modulus Measurements of Composite Materials." Experimental Mechanics 34: 369-378.

Jeong, H. K. and R. A. Shenoi (2000). "Probabilistic strength analysis of rectangular FRP plates using Monte Carlo simulation." Computers and Structures 76(1-3): 219-235.

Jeong, H. K., R. A. Shenoi, et al. (2000). "Structural reliability of thick FRP plates subjected to lateral pressure loads." Journal of Ship & Ocean Technology (SOTECH) 4(2): 38-57.

Kam, T. Y., S. C. Lin, et al. (1993). "Reliability analysis of nonlinear laminated composite plate structures." Composite Structures Proceedings of the 7th International Conference on Composite Structures, Aug 1993 25(1-4): 503-510.

Karbhari, V.M. and Y. Li. *A Review of Durability Based Safety Factors for the Use of FRP Composites in Civil Infrastructure*. In Proceedings of *10th US- Japan Conference on Composite Materials*. 2002: DEStech Publications, Lancaster, PA, 291-300.

Kural, M. H. and D. L. Flaggs (1983). "Finite element analysis of composite tension specimens." Composites Technology Review 5(1): 11-17.

Liu, X. and S. Mahadevan (2000). "Ultimate strength failure probability estimation of composite structures." Journal of Reinforced Plastics and Composites 19(5): 403-426.

Lopez-Anido, R., H.V.S. GangaRao, and R. Luciano. *Damage Mechanics Model for Evaluation of Bridge Deterioration*. In Proceedings of *7th. ASCE EMD/STD Joint Specialty Conference on Probabilistic Mechanics and Structural Reliability*. 1996. Worcester, MA: ASCE, 458-461.

Lopez-Anido, R., E. Falker, B. Mittelstadt, and D. Troutman. *Shear Tests of FRP Pultruded Beam-to-Column Connection with Clip Angles*. In Proceedings of *Materials and Construction: Exploring the Connection*. 1999. Reston, VA: ASCE, 92-99.

Lopez-Anido, R., and Karbhari, V.M., *Chapter 2: Fiber Reinforced Composites in Civil Infrastructure*, in *Emerging Materials for Civil Engineering Infrastructure - State of the Art*, R. Lopez-Anido, and Naik, T.R., Editor. 2000, ASCE Press: Reston, VA. p. 41-78.

Lopez-Anido, R., F. W. El-Chiti, et al. (2004). Composite Material Testing Using a 3-D Digital Image Correlation System. Composites 2004, American Composites Manufacturers Association, Tampa, Florida.

Mansour, A. (1990). "An introduction to structural reliability theory." SSC-351,Ship Structure Committee.

Muszynski, L., R. Lopez-Anido, and S.M. Shaler. *Image correlation analysis applied to measurement of shear strains in laminated composites*. In Proceedings of *SEM IX. International Congress and Exposition on Experimental Mechanics*. 2000. Orlando, FL: Society for Experimental Mechanics, 163-166.

Piggott, M. R. and J. Wang (1999). Basic Errors Appear to be Hampering Composite Aircraft Improvements. 44th International SAMPE Symposium, Long Beach, CA.

SACMA SRM 1R-94, (1994). Recommended Test Method for Compressive Properties of Oriented Fiber-Resin Composites. Washington DC, Suppliers of Advanced Composites Materials Association.

Tomblin, J. S., Y. C. Ng, et al. 2001. Material Qualification and Equivalency for Polymer Matrix Composite Material Systems. U.S. Department of Transportation, Washington DC. Report#: DOT/FAA/AR-00/47.

U.S. Army Research Laboratory, *Composite Materials Handbook MIL-17*. Vol. 1-3. 1998, Fort Washington, PA: Technomic Publishing Co. & Materials Science Corp.

Whitney, J. M., D. L. Stansbarger, et al. (1971). "Analysis of the Rail Shear Test-Applications and Limitations." Composite Materials 5: 24-34.

Wolfe, A. R. and M. Weiner (2004). Compression Testing - Comparison of Various Test Methods. Composites 2004 Convention and Trade Show, Florida, American Composites Manufacturers Association.

Wu, W.-F., H.-C. Cheng, et al. (2000). "Random field formulation of composite laminates." Composite Structures 49(1): 87-93.

Zienkiewicz, O. C. (1977). The finite element method. London, McGraw-Hill.

REPORT DOCUMENTATION PAGE	Form Approved OMB No. 0704-0188

1. REPORT DATE *(DD-MM-YYYY)*	2. REPORT TYPE	3. DATES COVERED *(From - To)*
1-07-2007	Final Report	March 2003 - December 2006

4. TITLE AND SUBTITLE

Effect of Processing Parameters
on Reliability of VARTM/SCRIMP
Composite Panels – Phase I

5a. CONTRACT NUMBER

n/a

5b. GRANT NUMBER

N00014-03-1-0542

5c. PROGRAM ELEMENT NUMBER

n/a

6. AUTHOR(S)

Dr. Habib J. Dagher, P.E. Director AEWC
Dr. Roberto Lopez-Anido, P.E.
Dr. Larry Thompson, P.E.
Fadi El-Chiti
Ghassan Fayad
Keith Berube

5d. PROJECT NUMBER

n/a

5e. TASK NUMBER

n/a

5f. WORK UNIT NUMBER

n/a

7. PERFORMING ORGANIZATION NAME(S) AND ADDRESS(ES)

The AEWC Center
University of Maine
Orono, Maine 04469

8. PERFORMING ORGANIZATION REPORT NUMBER

Report 08-01 Project 206

9. SPONSORING/MONITORING AGENCY NAME(S) AND ADDRESS(ES)

Dr. Roshdy Barsoum
Office of Naval Research
Ballston Centre Tower ONE
800 North Quincy Street
Arlington, Virginia 22217-5560

10. SPONSOR/MONITOR'S ACRONYM(S)

n/a

11. SPONSOR/MONITOR'S REPORT NUMBER(S)

n/a

12. DISTRIBUTION/AVAILABILITY STATEMENT

APPROVED FOR PUBLIC RELEASE

13. SUPPLEMENTARY NOTES

n/a

14. ABSTRACT

Reliability based design and acceptance criteria are currently being developed by the U.S. Navy using Navy load and strength prediction methodologies. However, this work considers only traditional structural materials and systems and a limited range of structural-failure modes. Though limited, this effort represents a significant shift in composite design methodology and assessment of design acceptance and provides a framework used in this program. The structural risks associated with new FRP composite ship structures can be mitigated by characterizing the variability of composite material properties thus ensuring acceptable levels of safety. The objectives for work outlined in this report are as follows: 1) Identify apparent material variability resulting from ASTM test procedures; 2)Modify/recommend a series of coupon level test procedures that minimizes testing variability; 3) Develop a probabilistic finite element tool to predict material variability. Recommendations for material testing of marine grade woven roving fiberglass reinforced plastic materials have been presented.

15. SUBJECT TERMS

reliability based design, composites, material testing, Fiberglass reinforced plastics

16. SECURITY CLASSIFICATION OF:			17. LIMITATION OF ABSTRACT	18. NUMBER OF PAGES	19a. NAME OF RESPONSIBLE PERSON
a. REPORT	b. ABSTRACT	c. THIS PAGE			Dr. Habib Dagher
U	U	U	UU	122	19b. TELEPHONE NUMBER *(Include area code)* 207-581-2138